This is to certify that the

dissertation entitled

PART I: THE DEVELOPMENT OF A PHOTODIODE ARRAY STOPPED-FLOW SYSTEM AND ITS APPLICATION TO CLINICAL ANALYSIS

PART II: THE DEVELOPMENT OF A NEW CHEMOMETRIC APPROACH FOR COMPUTERIZED COMPOUND IDENTIFICATION USING IR SPECTRAL DATA

presented by

Amidollah Salari

has been accepted towards fulfillment
of the requirements for

Ph.D. degree in Chemistry

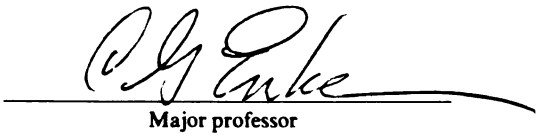

Major professor

Date 7-26-90

Part I :

THE DEVELOPMENT OF A PHOTODIODE ARRAY STOPPED-FLOW SYSTEM AND ITS APPLICATION TO CLINICAL ANALYSIS

Part II :

THE DEVELOPMENT OF A NEW CHEMOMETRIC APPROACH FOR COMPUTERIZED COMPOUND IDENTIFICATION USING IR SPECTRAL DATA

By

Amid Salari

A DISSERTATION

Submitted to
Michigan State University
In partial fulfillment of the requirements
For the degree of

DOCTOR OF PHILOSOPHY

Department of Chemistry

1990

Part I

ABSTRACT

THE DEVELOPMENT OF A PHOTODIODE ARRAY STOPPED FLOW SYSTEM AND ITS APPLICATION TO CLINICAL ANALYSIS

By

Amid Salari

A rapid scanning photodiode array stopped-flow spectrometer has been developed. The diode array allows for rapid simultaneous detection of all wavelengths over a given spectral region. A Reticon "S" series type R1-512s diode array which was specifically designed for spectroscopic applications has been used. This device consists of 512 sensor elements in a length of 12.8 mm with a 25 μm diode spacing which corresponds to 40 diodes/mm. Each diode has a height of 2.5 mm providing a slit-like geometry to each element with an aspect ratio of 100 : 1.

A polychromator equipped with a holographic grating has been employed to produce a flat field image across the detector elements with minimum stray light. The speed of data acquisition with the diode array makes it a very suitable detector for dynamic systems such as stopped-flow kinetic measurements. The stopped-flow apparatus used in conjunction with the diode array allows for rapid mixing of reagents in times as short as a few ms. The stopped-flow mixing time and dead time have been determined to be on the order of 2.048 and 7.9 ms, respectively.

A control interface has been built to allow for variable integration and delay time, and to provide proper signals for running the stopped flow system and synchronization of the data acquisition with. The system developed has

many desirable features for rapid kinetic measurements, particularly where spectral information is required. The system provides multiwavelength absorbance information for rapid changes in absorbance. The type of data generated by the diode array stopped-flow system allows for a significant degree of flexibility and convenience for performing complex analyses.

The photodiode array stopped-flow instrument has been applied to both single and multicomponent clinical analyses using a fixed-time, reaction rate approach. The kinetic analysis of total serum protein has been carried out as an example of an analysis of a single component in a sample, while the simultaneous kinetic determinations of glucose and ethanol in blood serum has been performed to demonstrate the system capabilities for multicomponent analysis.

The accuracy and precision obtained for protein determination are in good agreement with the results reported by other established methods, and those obtained for the simultaneous analyses of glucose and ethanol in blood serum are also well within the acceptable range. These results indicate that the diode array stopped-flow spectrometer in a suitable instrument for simple as well as complex fast clinical analyses.

Part II

ABSTRACT

THE DEVELOPMENT OF A NEW CHEMOMETRIC APPROACH FOR COMPUTERIZED COMPOUND IDENTIFICATION USING IR SPECTRAL DATA

By

Amid Salari

A new chemometric procedure has been developed for automated infrared spectroscopic compound identification. Availability of data bases plus more powerful laboratory computers makes computerized spectroscopic compound identification an attractive possibility. However, direct digital comparison of reference and sample spectra has some serious disadvantages. For instance, most conventional library search routines are designed to operate only with pure samples. The increasing size of spectral reference libraries, however, necessitates that we adopt new approaches to accomplish efficient searching.

The proposed method allows for direct spectroscopic analysis of pure samples as well as mixtures. A multidimensional vector approach is used which allows the application of Gram-Schmidt's orthonormalization procedure to form an orthonormalized vector space from a library of reference spectra. Computing the projection of an unknown spectrum into the space spanned by the orthonormal library yields qualitative and quantitative information.

The use of an orthonormal reference library results in a computational efficiency that could not otherwise be realized. In fact, after completion of the one time orthonormalization procedure, the qualitative and quantitative analysis of a mixture can be done in about the same amount of computer time as is required to identify a pure compound from its stored spectrum. The required computer time has been evaluated on a 108-member library of primary mass spectra acquired on a triple quadruple mass spectrometer using VAX-station 3200 computer system. The amount of time required for a typical analysis based on this library has been determined to be about 7.7 seconds.

The performance of the new procedure has been compared to that of the two most popular library search routines, namely, the methods of absolute differences and dot product matrices. compared to these two matrices,the orthonormal procedure has shown equal performance for pure samples and superior performance for mixtures. Also, the method has been found to be faster than the conventional approaches to mixture analysis as well as to provide a more efficient screening analysis of a specific target compound. Additionally, the orthonormal algorithm can be directly applied to any kind of spectroscopy; similar performance was obtained for both IR and mass spectral data.

Finally, the orthonormal procedure has also been applied to the resolution of fused chromatographic peaks. In this regard, the orthonormal method has been capable of successful qualitative and quantitative resolution of severely overlapping peaks.

To :

my dear wife Nayereh
my three lovely children Kataneh, Keyan and Autoosa
and the memory of my father

ACKNOWLEDGMENTS

I would like to extend my most sincere appreciation to my research advisor Professor Chris Enke, for his guidance, support and encouragements throughout the course of my research. I am very grateful to Chris for leading me into the fascinating field of analytical chemistry, showing me the way to independent thinking and research, and for the patience he offered me to overcome many obstacles in my life. His insight, vision and stimulating discussions were truly invaluable in helping me shape my scientific skills and standards. I do take a great deal of pride to have been associated with a man of such superb scientific stature and such great level of human decency.

Many thanks go to Professor Stan Crouch for serving as second reader for this thesis and for his valuable comments and discussions during many of our joint spectroscopy meetings. I would like to thank the members of my guidance committee for their valuable time and comments. I wish to express gratitude to the faculty and staff of the MSU chemistry department for the tremendous support they offered. I am very thankful for the financial support received from the MSU chemistry department and for the scholarship received from the ministry of higher education of Iran. I wish to thank all the members of Enke's research group whom I have learned a lot from and have become like a large family to me. I will always treasure their friendship. The generous help and support offered by Dr. Tom Atkinson is greatly appreciated.

I wish to acknowledge the collaborative effort offered by my former colleague and friend Dr. Marc Nyden at the University of Michigan-Flint for the work presented in the second part of this thesis.

I am especially grateful to my parents for their unconditional love and support. In particular my father, a lifetime educator who always placed a high priority on higher education for his children, and we all answered his dream.

Most of all, I wish to thank someone very special who is an equal partner in this journey, my dearest friend and lovely wife Nayereh. Her constant love, understanding and support made it all possible. I thank her for the greatest faith she had in me and feel lucky to be with her. Finally I would like to thank my three lovely children Kataneh, Keyan and Autoosa for their most honest love and beautiful laughs which gave Daddy a lot of strength and motivation, and made the whole thing a lot easier. Wait a minute! Did I thank myself at all?

TABLE OF CONTENT

PART II

LIST OF FIGURES

Part II

LIST OF TABLES

Tables Page

Part I

Part II

PART I

THE DEVELOPMENT OF A PHOTODIODE ARRAY STOPPED-FLOW SYSTEM AND ITS APPLICATION TO CLINICAL ANALYSIS

CHAPTER 1

Introduction

Generally in all spectroscopic systems, spectrometric information is obtained by the measurement of some characteristic of electromagnetic radiation versus either wavelength or frequency. Devices have been developed to accomplish wavelength separation for all regions of the electromagnetic spectrum.

Analytical spectroscopists, however, had a particular interest in the measurement of light in the UV-VIS region. For a long time, a variety of combinations of filters has been used to cut the light down to narrow bands of wavelength. The very poor resolution obtained by this method has been an obstacle in the way of development of higher quality systems. The introduction of dispersive elements such as the prism and grating has been a great step forward in overcoming such problems. Nowadays almost all spectrometers in use are equipped with a prism or grating, usually the latter. The typical dispersive system employed in these instruments, the monochromator, decodes the incident frequency information into an optical spatial array on the focal plane of the instrument. A photomultiplier tube in conjunction with an exit assembly is then used to monitor the light intensity in a given wavelength resolution element. Inherent to these conventional kinds of spectrometers, there exists a contradiction. The contradiction is precisely between the static nature of the measurement

system (one wavelength at a time) and the potentially dynamic nature of the matter under study. A mixture undergoing a chemical reaction, for example, could undergo substantial change in composition before or while it is being monitored. These changes could be manifest as wavelength shifts in the peak absorbance maxima, abrupt changes in the absorbances of other wavelengths, transient peaks, many of which, when a narrow wavelength range is monitored, are never detected.

It is to remove exactly these limitations that the field of analytical rapid scanning spectroscopy was developed. In this approach the spectrometric information can be obtained by rapidly scanning across the spectral region of interest. therefore, those phenomena occurring within the scan time frame can be studied. however, rapid scanning should not be percieved as simultaneous multiwavelength detection because different wavelengths are monitored at different times. Traditionally, the detection system for the simultaneous monitoring of the entire spectrum has been the photographic emulsion plate. The photographic plates, however, have poor sensitivity, marginal accuracy and precision, tedious and time consuming calibration and data retrieval procedures.

In recent years optoelectronic image devices have become the detector of choice for accomplishing such tasks. These devices actually combine the multiwavelength capability of photographic plate with a real time electronic readout and the wide dynamic range and sensitivity of photomultiplier tubes. Substantial research has been devoted to exploring the capabilities of such devices as parallel detectors in analytical rapid scanning spectroscopy. Part I of this dissertation describes the development of a

rapid scan linear diode array spectrometer in conjunction with stopped-flow mixing system and its application to clinical analysis.

Chapter 2 offers a historical review of the variety of approaches utilized in analytical rapid scan spectroscopy. The most popular and widely used techniques, from conventional scanning systems up to the recent optoelectronic image devices are explained in fairly detailed fashion. the advantages and disadvantages associated with each system are described. Chapter 3 presents a thorough discussion of the linear diode array as well as the stopped-flow mixing system. A description of the electronic interface which controls the overall operation of the system is also illustrated here.

Chapter 4 describes the application of the linear diode array stopped-flow spectrometer to the area of clinical analysis. Specifically, the kinetic determination of the serum total protein by Biuret method is studied as an example of a single component system. The multicomponent capability of the system is demonstrated by the simultaneous kinetic determination of glucose and alcohol in blood serum using the alcohol dehydrogenase and glucose oxidase enzymes.

CHAPTER 2

HISTORICAL OVERVIEW OF IMAGING DEVICES IN ANALYTICAL RAPID SCANNING SPECTROSCOPY

Introduction

Rapid scanning spectroscopy (RSS) is a technique in which a selected region of the electromagnetic spectrum is scanned on a time scale ranging from several seconds down to a few microseconds. Scanning is accomplished by mechanical or electronic means. The technique has been developed primarily for the study of chemical reactions or processes which involve short-lived intermediates with spectral properties which differ significantly from the reactants or products. Repetitive scans of the appropriate spectral region can provide information on the number and types of species present as well as the kinetics of the formation and decay of intermediates. From these data, one can drive explicit mechanistic information which could only be inferred from measurements made at a single wavelength.

The application of rapid-scan spectrometry includes both absorption and emission studies. In most cases the time resolution aspect is the important one, but the simple convenience of being able to see a large spectral region, essentially continuously, has some advantages even in systems that do not evolve in time or which change only slowly. The RSS techniques have a S/N ratio disadvantage relative to a single wavelength normal spectrometer. This arises from the fact that in a normal spectrometer the wavelength of interest is continuously monitored, whereas in RSS techniques each

wavelength increment rapidly passes by an entrance slit. Thus the detector spends only a small fraction of the time monitoring the photons of any given wavelength increment which reduces the S/N ratio by $\sqrt{n}$ where n in the number of wavelength increment monitored. The scanning speed and S/N ratio thus actually work against each other. It should be clearified at this point that the term RSS is used in a general sense here to also include optoelectronic image devices. The integrating optoelectronic image devices, however, do not suffer from the S/N ratio disadvantage mentioned above and the discussion only applies to mechanically scanned spectrometers.

A most interesting application of RSS is in molecular luminescence (1). When molecules are excited with light, they may relax to the ground state by emitting radiation in the form of fluorescence (short-lived), phosphorescence (long-lived) or both. The study of molecular luminescence has value in investigating molecular structure and chemical properties of molecules as well as in quantitative analysis. The RSS methods offer advantages to both of these fields.

The molecular electronic spectroscopist considers the the fluorescence and phosphorescence of molecules and chemical systems as probes into the structure of the molecules and the chemical interaction between molecules. The photochemist uses molecular luminescence to follow the paths for relaxation of electronically excited molecules in order to gain knowledge about photochemical reactions. The properties of molecular luminescence of greatest interest to the spectroscopist and photochemist are: emission and spectral location, shape, vibrational structure, intensity, polarization, and life time of decay. Rapid scanning spectroscopy can give all of this

information very quickly, and in the case of life times has an advantage over other methods. Some RSS techniques have calibrated scan times as fast as a few msec, and therefore, can be used to follow phosphorescent decays for many wavelength elements simultaneously. If one is doing a phosphorescence experiment with a mixture of phosphorescencing molecules, RSS can time-resolve spectra of individual molecules by taking advantage of their differing lifetimes. A molecule with a long phosphorescence decay lifetime (exponential decay) usually has a comparably long rise time during excitation. Thus, by adjusting the duration of excitation and the time interval between the end of excitation and observation, one can enhance the observation of either the long- or the short-lived molecular phosphorescence. These types of studies require rapid data acquisition speed which has only become possible after the introduction of RSS techniques.

The RSS methods can also be used to monitor molecular luminescence while changing temperature or excitation wavelength, or during a chemical perturbation. For example, one can obtain total luminescence information by simultaneously scanning both excitation and emission monochomators or, with a fixed wavelength interval ($\Delta\lambda$) between them (sychronous excitation flourometry). Also, time dependent changes as a result of any perturbation can be monitored by means of rapid and repetitive spectral acquisition.

The RSS techniques are most useful when observing spectra that evolve in time. An excellent application is stopped-flow kinetics which will be discussed in greater detail in the next chapter. The information gained

about a reaction while observing the entire spectrum (or a substantial portion of it) is powerful indeed. Chemical kinetics, when followed by spectrometry, is subject to several pitfalls. The usual approach is to monitor the radiant power transmitted by reaction mixture at a fixed wavelength as a function of time. Such a measurement, while quite precise, often will give erroneous information if spectral peaks shift, or if there are transient absorptions at the monitoring wavelength during the reaction. If one could observe the individual variations in each element of a rather large spectral region during the reaction, all of the kinetic data could be extracted while observing any spectral shifts or intermediate absorptions that could interfere with the measurement.

The RSS techniques allow one to observe a large spectral range in one scan (of a few msec duration). This makes them ideally suited for the stopped-flow kinetics scheme. Another application of RSS is in combination with liquid chromatography where the ability to identify the individual components in overlapping peaks is most helpful (2-3). Other typical examples which lend themselves to this type of study include enzyme-substrate complexes (3), mixed complexes in ligand exchange reactions (4), and products of electrochemical (5) and flash photolysis experiments.

As one can see the activity in the field of RSS is extensive and has already been fruitful. The spectral regions under consideration extend from the UV to the far IR, and the scan time sought causes some workers to begin speaking in units of nanoseconds. A variety of interesting problems are now under study that were quite out of reach only a few years ago.

The preceding examples give some indication of the kinds of interesting spectroscopy possible with RSS. There are, of course, many more specialized uses, such as: flame emission, arc emission, plasma emission, atomic absorption and fluorescence and others. Actually one of the most striking features of the literature on this topic is that it involves a series of specialized instrument systems applied to equally specialized problems, but they all share one important disadvantage "being mechanically scanned" and therefore, limited to its associated problems and pitfalls.

The evolution of "photoelectronic imaging devices", however, has opened a whole new era to the field of rapid scanning spectroscopy. Since the introduction of imaging devices, there has been a slowly growing attraction toward array detection. Within the past decade there has been an almost complete shift toward the application of imaging devices rather than rapid mechanical scanners for solving complex analytical problems. With the advancement of television technology and the development of commercially available image devices, the practical optical multichannel detector has become a reality. These devices, often referred to as optoelectronic image devices (OID), are typically constructed on a single monolithic silicon crystal wafer, using well established LSI manufacturing techniques. Linear detectors (25 nm long) with up to 2000 discrete light sensors and two dimensional image devices with a few hundred thousands sensors are now commercially available.

State-of-the-art optical parallel detectors confirm very well to most criteria of "ideal" detectors. They are reliably manufactured at a reasonable cost. They can be made immune to sudden "light-shocks". They are

mechanically rugged, compact and easily cooled, and consume little electrical power. They can be constructed with exceptionally high geometric accuracy (wavelength-to-sensor position registration across the focal plane of the spectrometer). Some of these detectors provide high flexibility in addressing the sensor elements, including individual and random access reading. The silicon type detectors, particularly self-scanned photodiode arrays, have a remarkably high sensitivity with relatively uniform characteristics across a very wide spectral range (190-1100 nm). Most significantly, their dynamic range (real-time) can be as high as 10^5:1 with highly linear transfer characteristic (gamma of 1).

The present technology of optoelectronic imaging devices favored by the advancement of minicomputers and microprocessors allows that, for almost all problems, the manual and/or conventional mechanical designs can be replaced by versatile electronically controlled systems. The time and effort required to obtain one or several scans of a spectrum covering several hundred nanometers should be little more than that now required to obtain measurements at one wavelength by use of conventional instrumentation.

The purpose of this chapter is to review the course of development of RSS according to the following two rather wide categories:

(1) Conventional (mechanical) RSS; and

(2) Optoelectronic image devices RSS.

This chapter will not cover the detailed design of the several RSS's designed in the first category, but rather will develop a perspective of the different

general approaches which have been developed for RSS. More emphasis is placed on the second category. Of course, those particular image devices that have found considerable application in analytical chemistry will be discussed in detail and the discussion about the rest will be brief.

Conventional (Mechanical) RSS

In terms of mechanism of scanning, rapid scanning spectroscopic techniques can be classified into two rather large groups: Those which employ mechanical means of scanning, also referred to as conventional RSS, and those which utilize electronically scanned array detectors, also called optoelectronic image devices (OID). This section will only deal with mechanical systems; optoelectronic image devices will be the subject of the next section.

Regardless of the scanning mechanism, most scanning spectrometers can be grouped under one or two major classifications which may be labeled as **dispersion** and **multiplex** spectrometers. Most common instruments employ the dispersion mode in which a prism or grating separates the spectrum into narrow bands of energy (resolution elements) which can be monitored independently. Spectrometers operating in the multiplex mode utilize a single detector to monitor the total beam which is modulated in a manner so that the intensity for each resolution element can be extracted from the composite signal by use of mathematical methods.

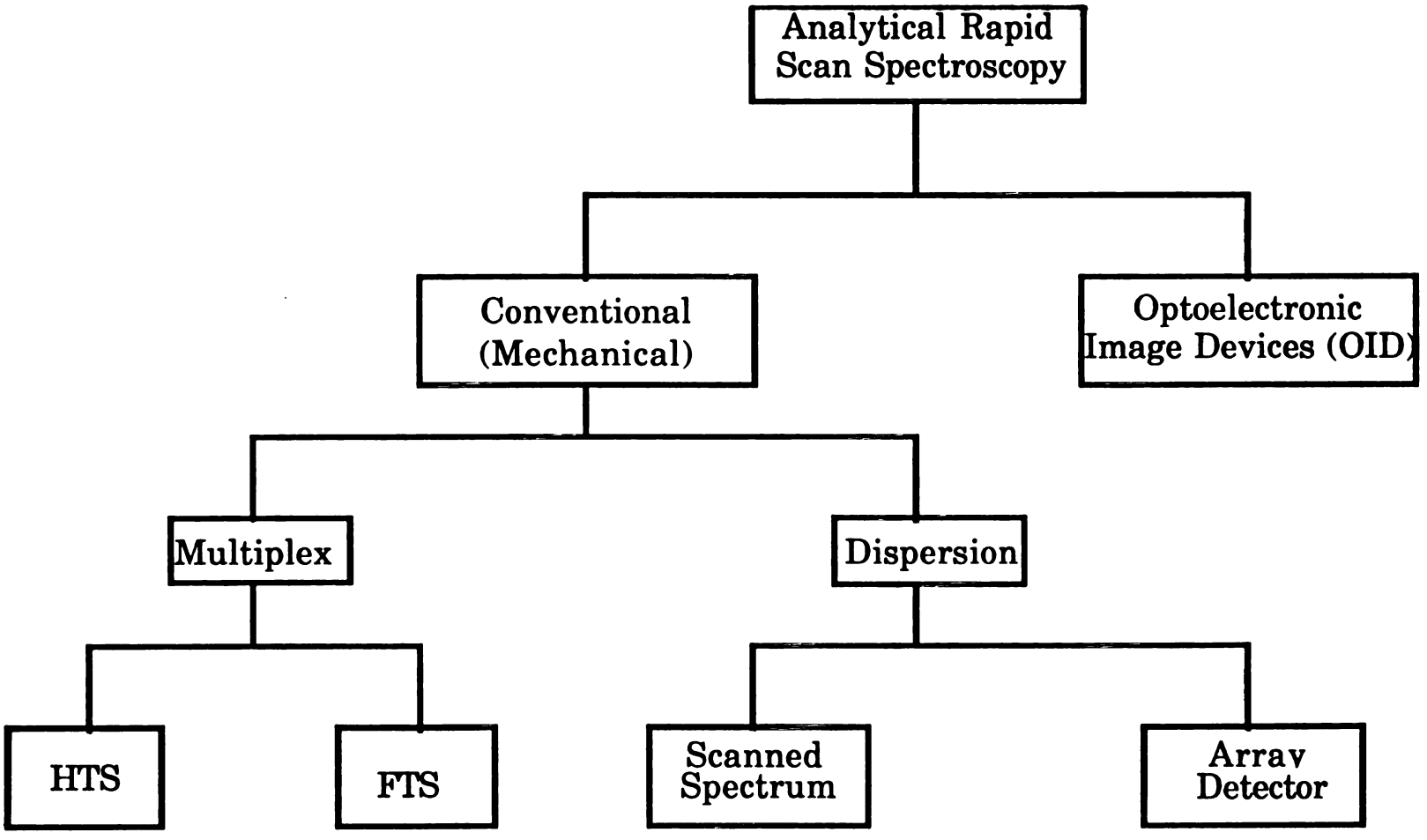

Figure 2.1 Family tree of analytical rapid scan spectroscopy

Each of these major categories can be divided into at least two significantly different subgroups. In the dispersion method the two subgroups are: **scanned spectrum methods** in which a single detector is used and **array detector methods** which uses a multichannel detector.

The two subgroups of the multiplex methods are Fourier Transform Spectroscopy (FTS) and Hadamard Transform Spectroscopy (HTS), each of which operates on a different principle. Figure 2.1 represents the family tree of rapid scan spectrometers.

Dispersion Techniques

Dispersion can be defined as breaking apart or separating a mixture of wavelengths into its component wavelength. This can be accomplished with a Prism using the phenomenon of refraction or with a Grating using the phenomenon of diffraction. Dispersion is the mechanism on which the most common spectrometers are based.

A spectrometer must eventually produce as the end result a **spectrum**, which is a plot of intensity versus frequency. Therefore, in conventional spectrometers, the polychromatic radiation must be fanned out or separated into bundles of (almost) monochromatic radiation. Then by some suitable mechanical arrangement the fanned out radiation is slowly swept past a suitable detector. Each independently identifiable set of frequencies can be termed a resolution element. The detector of the dispersion instrument then produces a simple electrical signal which is

proportional to the intensity of the radiation in the resolution element striking it. The spectrum produced in this fashion is thus the result of a series of radiometric measurements.

As previously mentioned the dispersion method is subdivided into scanned spectrum and array detector methods. Figure 2.2 represents the two subgroups. In one approach (2a), the dispersed spectrum is scanned across an exit slit and onto a single detector, the instantaneous response of which is dependent upon the wavelength and the intensity of the band of energy being passed by the slit. In another approach (2b), the dispersed spectrum falls on an array detector, and the array is interrogated to generate spectral information.

In order to discuss each of the above basic approaches of dispersion scanning spectrometers it will be helpful to take the dispersion portion of the RSS family tree and expand it further to the variety of RSS techniques developed and then briefly explain each of them. Figure 2.3 shows just that.

Scanned Spectrum Methods, Mechanical Design

Figure 2.4 shows two basic ways of using any conventional two-slit optical system in rapid scan mode. In method 1, the image of the entrance slit is swept, after dispersion, across the exit slit with mirror M_1, or an optical equivalent. This takes advantage of the fact that a range of frequencies strike M_1, and the corresponding portion of the spectrum is displayed on the exit slit jaws. Oscillation or rotation of M_1 sweeps this spectral region

A : Scanned Spectrum

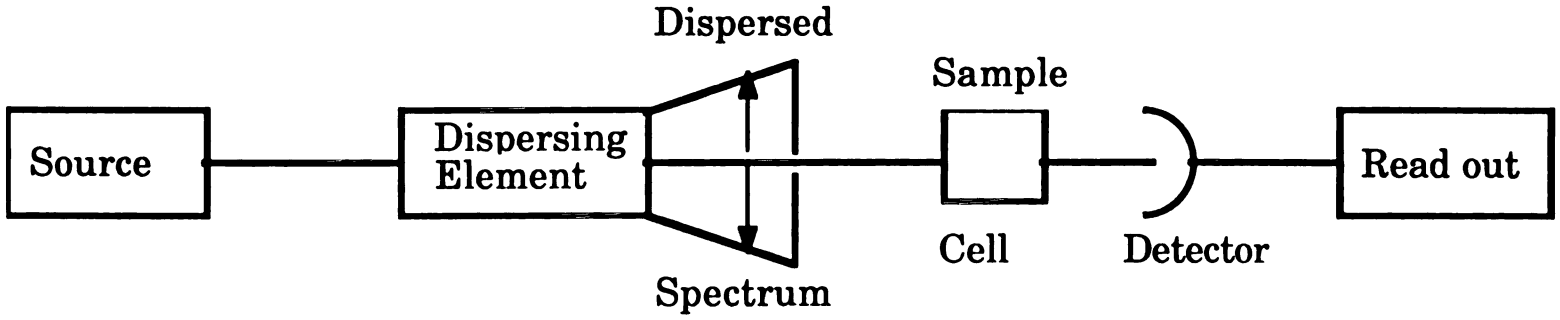

B : Array Detector

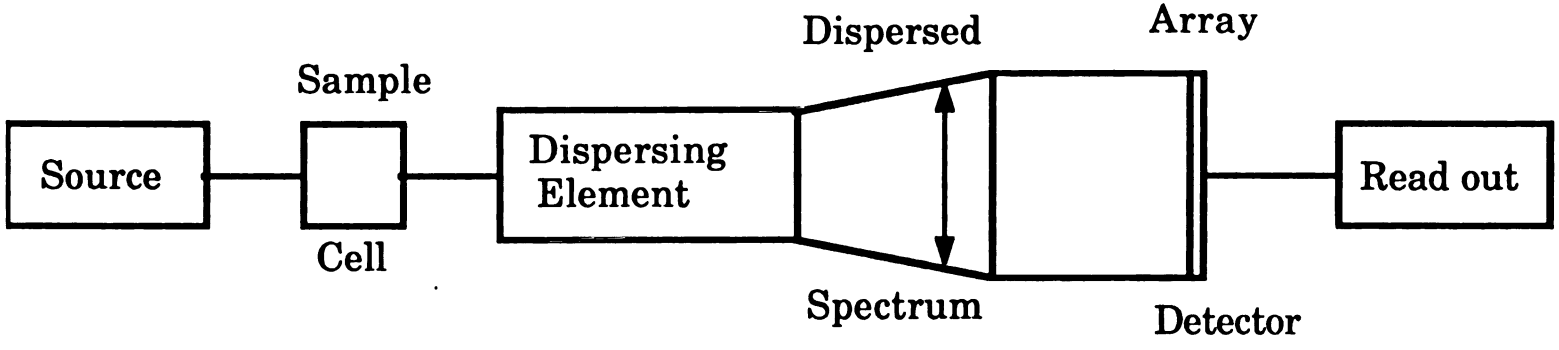

Figure 2.2 Two basic approaches to dispersin scanning spectrometers

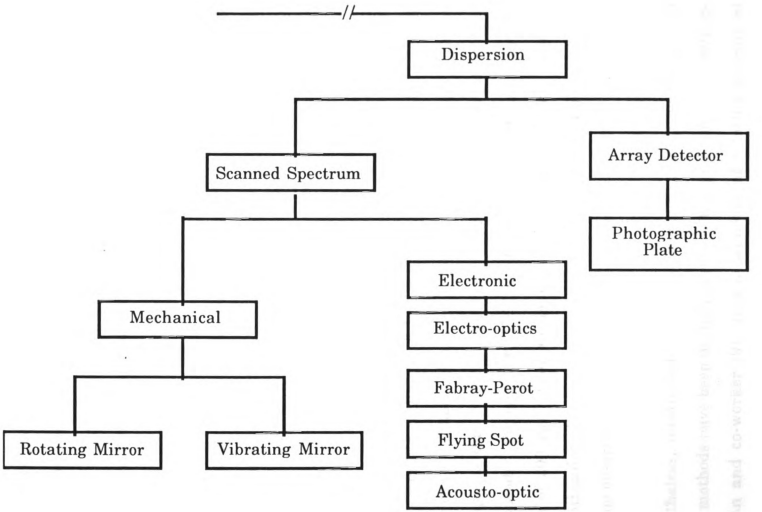

Figure 2.3 Expansion of family tree of dispersion techniques

across the exit slit and thus sweeps the frequency that reaches the detector. An advantage to this scanning technique is that M_1 is generally a rather small mirror, which permits high rotation rates. An alternate mechanical option is to move the exit slit laterally across the spectrum, as is conveniently done by placing the slit near the edge of the rapidly rotating disk. The latter technique was used by Bethke (7) in the construction of a pioneering instrument that achieved 50 microsecond scan times in the near IR with low resolution (100 cm^{-1}). Both methods, M_0 rotation and lateral slit movement, suffer from the fact that M is perfectly focussed and illumination is centered on M only at one position (usually when the beam falls on the slit jaws at normal incident).

The second method shown in Figure 2.4 is more conventional, since rotation of a littrow mirror or grating that reflects a collimated beam is the usual scanning technique in most ordinary spectrometers. The littrow mirror can be either oscillated or rotated. The disadvantage of this optical technique is that a relatively large mirror (or grating) must be moved at high speeds. Pimental et al. (8) used a polished aluminum mirror up to speeds of 200 rps. Then to improve resolution, they have substituted a conventional replica grating on glass, and routine operation at 60 rps has given no observable deformation to the grating.

Nevertheless, rotation of this large mirror is a limiting factor, and two clever methods have been devised to relieve this problem. One, developed by Terenin and co-worker (9), uses a sequence of rotating mirrors at the Littrow position so that their rotation rate are additive. More elegant is the method used by Hexter and Hand (10), in which the Littrow mirror deflects

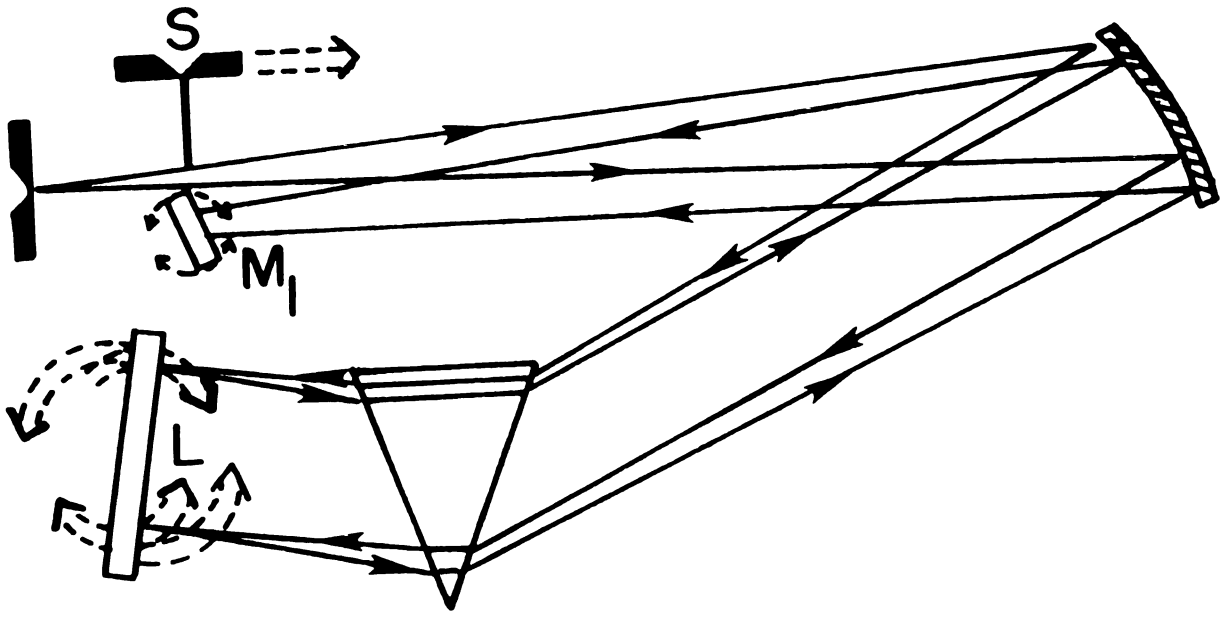

Figure 2.4 Rapid scan methods in dispersion spectrometer, S is the exit slit, M1 is the rotating or oscillating mirror, L is the rotating or oscillating littrow mirror or grating.

the collimated beam into a gallilean telescope to direct the light onto a smaller mirror which is usually driven at rates as high as 2000 rps. Not only this instrument permit 10 microsecond scan times, also a rapid repetition rate that is quite desirable for kinetic studies. There are also other spectrometer based upon one or another variant of the methods described(10-13).

The most widely used design of an RSS based on mechanically scanned monochromator incorporates a series of 24 corner mirrors mounted on a rotating drum to scan the spectrum across the exit slit (14). The wavelength scanning principle of this instrument allow the dispersing optical train to be held fixed. The spectrum is scanned by rotating the scan wheel; this sweeps the corner mirrors through the intermediate focal plane formed after the first pass through the monochromator. Each time a corner mirror sweeps through the focal surface, the spectrum is scanned once. The scan repetition rate equals the number of corner mirrors times the rotation speed of the scan wheel. Figure 2.5 shows the optical schematic of the instrument.

This method of scanning, which is applicable to both prism and grating monochromators, has some important advantages. Because the moving element is outside the dispersing train and is dynamically balanced, the optical quality of the spectrometer is not affected by the rapid scanning, and performance is limited by the signal-to-noise ratio of the detector system, as in a well designed, slow scan spectrometers. Also, the output is linear in time and wavelength, the scan time is variable up to 80% of the repetition time, the entire useful first order of a grating spectrum can be covered in

one scan, and the design inherently provides for simultaneously scanning two contiguous wavelength intervals. The device achieves high scan rates with low drum velocity, but requires exact matching of the corner mirrors for high photometric accuracy.

Another device employs a vibrating mirror to scan the spectrum (5,15). The angular velocity of the vibrating mirror is controlled by the frequency of a triangular wave which provides drive current. A beam splitter divides the energy from the exit slit into a sample and reference beam, and a logarithmic amplifier generates an output linear in absorbance. This instrument scans the region from 370 to 700 nm (or any portion thereof) with scan rate between 0.01-4000 scan/sec. The zero absorbance line is constant to within 5% T between 380 and 650 nm, and the absorbance range is 0.02-2.0 with spectral resolution of 2 nm at 1000 scan/sec. The instrument was used to study the electrochemical reduction of methyl violigen at an optically transparent electrode (16).

Electronic designed scanned spectrum methods (Electro-optic materials, Fabry-perot, etc.) have not been able to gain popularity among analytical spectroscopists and therefore they will not be discussed here. Multiplex method (FTS, HTS), even though quite popular, but it is too far afield from the main topic of this research and will not be presented here either. A brief discussion of the photographic emulsion plate as an example of an array (parallel) detector will be made in comparison to optoelectronic image devices in the next section.

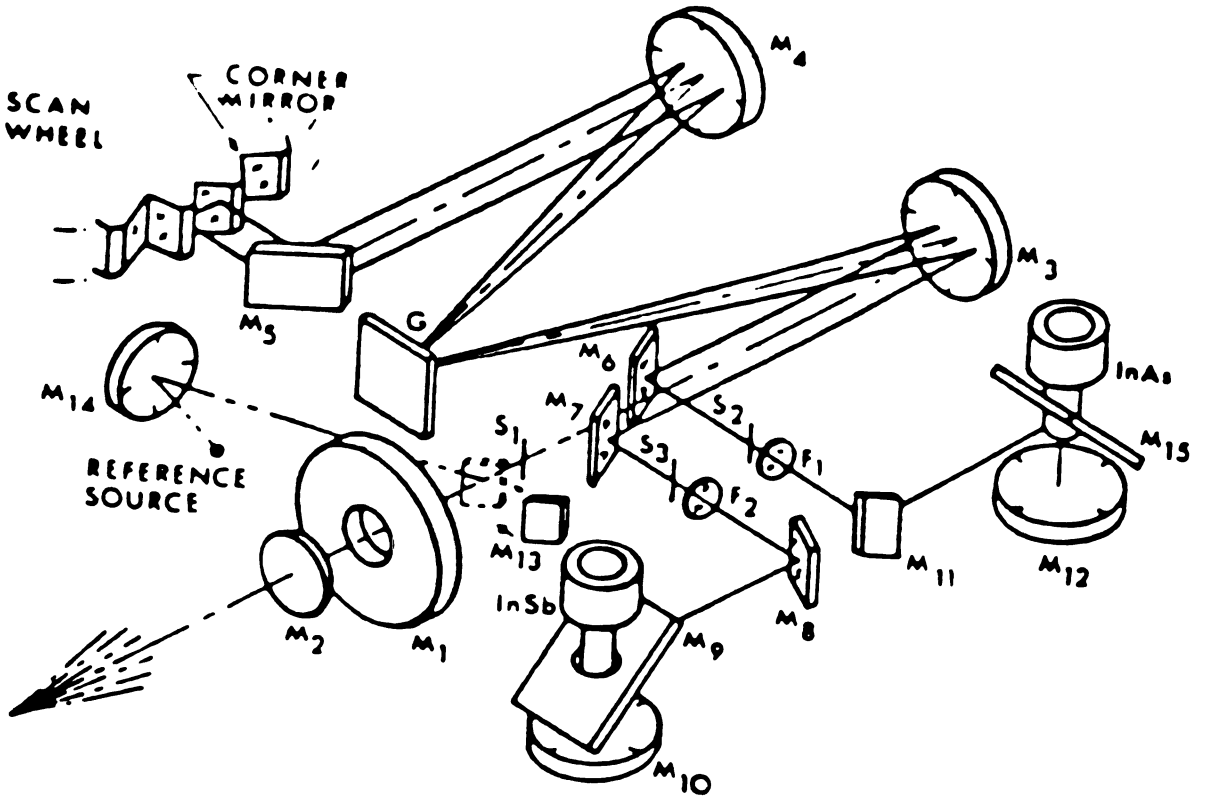

Figure 2.5 Optical schematic of the corner mirror rapid scan spectrometer.

Limitation of Conventional (Mechanical) RSS

Both of the multiplex methods and the more common spectrum scanning methods involve mechanical devices. This factor limits the fastest speed which can be obtained by use of these approaches. All spectroscopic measurements involve some trade-offs among spectral resolution, photometric accuracy, and measurement time. An ideal spectrometer would include the capability of varying each of these measurement parameters over a relatively wide range. Conventional spectrometers which feature mechanical scan mechanism have tended to emphasize spectral resolution and/or photometric accuracy at the expense of scan speed.

There are problems of inertia associated with moving parts. A common problem of conventional (mechanical) RSS techniques, specially in scanned spectrum methods, is irreproducible baselines, brought about by multiple mirror reflectance, mismatch, and differential aging.

Another problem associated with scanned spectrum RSS is that information is obtained at only one wavelength at a given time. This gives rise to longer analysis time and poorer signal-to-noise ratio. The technique also offers limitations in situations where there are shifts of wavelength or fast transient processes are studied.

It appears that the alternative to the field of rapid scanning analytical spectroscopy is high speed "parallel detection" with wide spectral coverage.

That is how the optoelectronic image devices operate and their advent has attracted the attention of many rapid scan spectroscopists. This will be discussed in the next section.

OPTOELECTRONIC IMAGE DEVICES (OIDs)

Introduction

Considering all the limitations that various conventional (mechanical) rapid scanning spectrometers have, it was concluded in the previous section that an attractive alternative approach is the simultaneous detection of multiple wavelength segments. The idea of parallel detection was realized long before the age of optoelectronic image devices was put into practice in the form of spectrographs (photographic plate detector). Actually, for a long time, the most widely used and commonly available parallel detector has been the photographic emulsion. It has a fixed and accurate geometric registration that allows for reliable wavelength calibration. Its operation is simple, its cost is affordable and its physical dimension, and therefore spectral resolution practically unlimited, depending only on the design of the spectrograph. Unfortunately, the sensitivity (quantum efficiency) of the photographic plate is poor, its transfer characteristic is non-linear, its accuracy and precision are marginal and it requires tedious and time consuming calibration procedures. Worse yet, the validity and usefulness of the spectral data gathered can be verified only after the "plate-development" process. This can result in a loss of invaluable, and at times, irreproducible experimental data.

A more recent multichannel (parallel-detection) approach is based on the use of PMTs, because of their wide acceptance as a VUV-near IR spectrometric detector. An array of PMTs is optically arranged across the focal plan of a spectrograph. Although excellent sensitivity, wide dynamic range, and rapid response are achieved, in practice this detector provides a limited number of channels aligned for a predetermined specific application (17,18). It does not provide the optimal flexibility in the interaction between the spectroscopist and his/her experiment that would be desired of a multichannel detector for general purpose and research applications.

The newest approach involves optoelectronic image devices which can provide several hundred independent optical channels in the linear mode and many thousands in a two dimensional mode, e.g., echelle spectroscopy. These detectors, when interfaced to a microcomputer (19) or a microprocessor, provide unprecedented flexibility in spectroscopic data handling, including signal processing, scan rate selection, various modes of integration, ultra-rapid data accumulation and real-time display, and elimination of undesired spectral information through software manipulation or even through "on-target" random access capability.

In the last decade, as the state-of-the-art optoelectronic image devices have adequately matured, their use as spectrometric parallel detectors has been demonstrated, and they have gradually gained acceptance among spectroscopists.

Common Characteristics of OIDs

Generally, all optoelectronic image devices (OID), including TV-type or solid state imagers, are, by their very nature, multichannel parallel photon detectors which can accurately transform optical images into their corresponding electronic images. Nevertheless, all these devices implement the three basic functions of conversion, integration and readout as elaborated in the following.

Charge Conversion

The role of a charge conversion component is to absorb photons and cause the removal of electrons from the charge storage area in proportion to the number of photons absorbed and in positions where the photons were incident (20). In other words, it converts the photon images into their electrical analogs, i.e., a pattern in electrical current or charge. The mechanism of charge conversion varies from one type of OID to another. Some operate by photoconductivity, some by photoemission, and some like silicon vidicon by discharging the stored charge on the depletion region of a reverse biased photodiode and then reading the remaining charge and so on. In a photoconductor, the electrical conductivity is approximately proportional to the irradiance to which it is subjected (21). An electric field is applied to the photoconductor for example, by applying a fixed positive potential at the transparent conducting signal plate as shown in Figure 2.6, and driving the exposed surface to near gun-cathode potential through the action of the periodically scanning electron beam. The field decays across

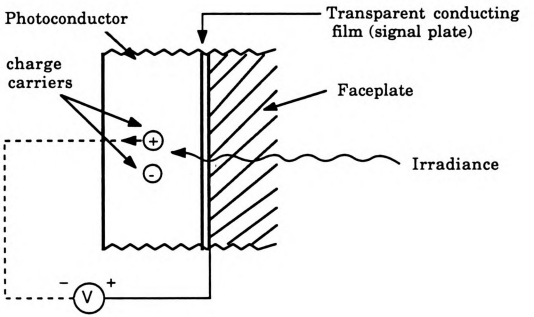

PHOTOCONDUCTIVE PHOTOCATHODE (initial electrical potential is applied to the exposed surface of the photoconductor through the action of the electron beam)

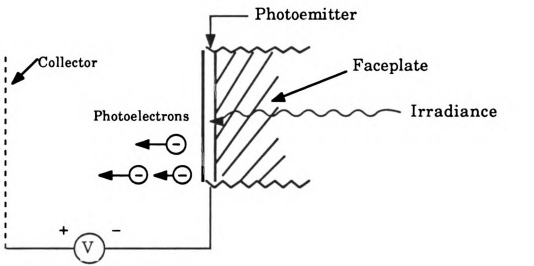

PHOTOEMISSIVE PHOTOCATHODE

Figure 2.6 Transducing charge into electrical signal

the elemental capacitance according to the resistance-capacitance time constant of that element. The resistance is controlled by the irradiance, so that during the exposure interval the electrical potential at the scanned surface of an element will be more or less positive, depending on the irradiance. In this way, a pattern in positive electrical potential is formed at the free surface that is reproduction of the optical image.

Photoemissive photocathodes are used in the image orthicon, the image isocon, the SEC CAMER, and SIT. The photoemitter is a very thin semiconductor film formed on the inside of the faceplate of the camera tube. Light incident on the photoemitter excites into the vacuum an emission of photoelectrons which is proportional to the irradiance. In more modern tubes, the photocathode is a continuous electrode which does not hold a charge image. Instead, the photoelectrons are imaged either electrostatically or electromagnetically to produce a pattern of charge on a separate storage medium.

In other kinds of OIDs such as the silicon vidicon, the charge conversion component are the depletion regions of a planar array of reversed biased silicon photodiodes which are charged up to a known voltage. When irradiated, they become discharged leaving a charge pattern corresponding to the light intensity pattern. This remaining charge pattern is eventually read out as will be discussed in this chapter.

There is apparently a fourth option for the transducer, the photovoltaic effect, the same as is used to generate power in solar cells. The photovoltaic effect is not used in camera tubes because the voltage modulation produced

across a single junction by a convenient irradiance is not sufficient for a usefully sensitive device. It is conceptually possible, however, to devise a photovoltaic pick-up tube that depends on the series of voltages developed by multiple junctions.

Integration and Storage

Again, different mechanisms for storage and integration of charge are implemented in different OIDs. Aside from different mechanisms of storage they are either integrating or non-integrating detectors. In an integrating detector, such as a vidicon, the electrical charge image developed by the charge conversion component is in general accumulated on a storage medium throughout the entire exposure time. The charge pattern is stored for subsequent read-out by the scanning electron beam. The storage medium may be the photosurface itself, for example, the photoconductor film in the vidicon, or the photoemissive mosaic in the orthicon. In a non-integrating detector such as plumbicon the signal is not integrated for the entire exposure time but rather the charge pattern present at the storage medium on the arrival time of the electron scanning beam becomes read out.

Read-out

The final product of a read-out system is a video signal. This might be done by an electron beam scanning like in TV-type OIDs, or by some electronic circuitry as in solid state OIDs. In TV-type camera tubes the stored electrical charge pattern is read out by the scanning electron beam to form

the video signal. An electron gun in conjunction with electron optics, provide a means of uniformly depositing electrons on the photoconductor or target surfaces. Electrons emerging from the gun are made to form a beam and are focused at the surface noted above. The focused electron beam follows a predetermined pattern of movement tracing out scanning lines designed to provide uniform coverage of the surface. The process is called a raster scan and might simply consist of the focused beam moving across the surface in parallel horizontal lines, beginning at the upper left corner and ending at the lower right corner as in Figure 2.8. The process is repetitive and the time it takes for the electron beam to cover the surface is called the raster period.

In normal operation, the substrate of the detector is biased positively with respect to the cathode of the electron gun. The substrate potential relative to cathode potential is called the target voltage and is typically 5-10 V. The impinging electron beam thus strikes the substrate with a maximum energy of 10 eV and removes the charge pattern from small sections of the storage area so as to be able to reconstitute the intensity and position relations of the original signal.

As mentioned already, all OIDs have the above basic three components in common, but the methods of implementation vary from one type of device to another. Historically the trend in the OID industry has been toward simplification via consolidation of these components. In some OIDs, all three components including the video amplifier itself are combined on a single monolethic silicon crystal wafer (22).

Classification of OIDs

Optoelectronic image devices can be classified into at least three rather broad categories:

I. TV-type image devices also referred to as electron beam imagers.
II. Intensified imaging devices.
III. Solid state imaging devices (SSID).

Figure 2.7 outlines the family tree of OIDs. The variety demonstrated in this outlines implies that there are important and careful decisions that have to be made by the chemist who is interested in using one of these detectors. The decisions are first of all whether the general idea of the OID is compatible to his/her problem. Secondly, which of the detectors will best fit his/her need and will be his/her optimum detector of choice. As will be seen later there is no simple answer to these kinds of questions, since the compromise and trade-offs involved in going from one device to another are quite important in some cases.

All of the varieties of image devices listed have been applied as spectroscopic detectors. Not all of them, of course, have found widespread applications. Only a few of them have gained particular attention in the field of rapid scan spectroscopy and their attractiveness and promising features are continuously growing among analytical chemists. Therefore, only those devices that have successfully been used as an RSS detector

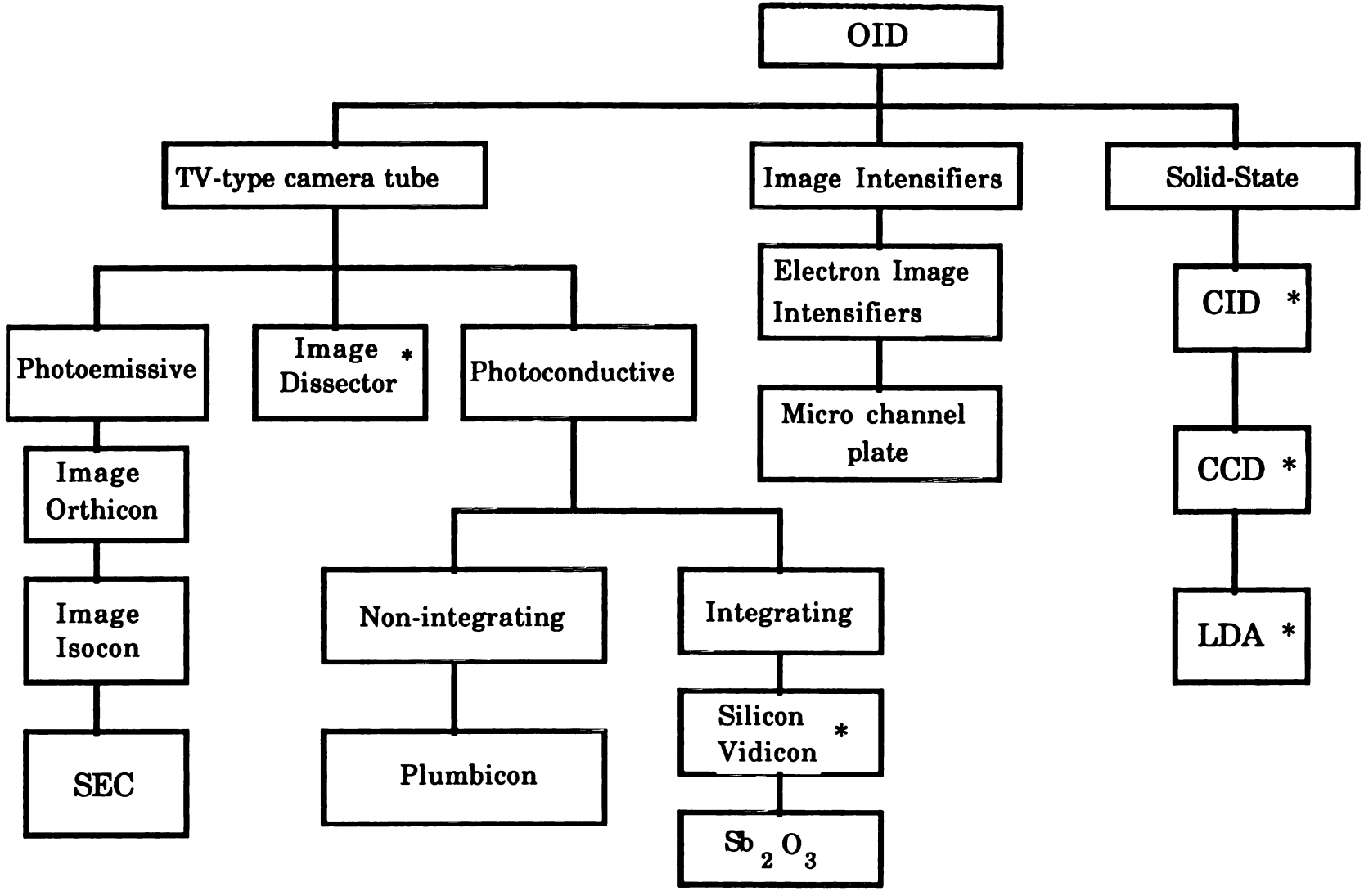

Figure 2.7 Familytree of optoelectronic image devices

(designated with an asterisk(*) in the family tree) will be discussed in a fairly detailed manner here. The reader can refer elsewhere (23-25) for brief discussions of the rest.

TV-Type Camera Tubes, Silicon Vidicon (SV) and Silicon Intensified Target Vidicon (SIT) Tubes

The term vidicon is frequently used as a generic term for photoconductive camera tubes. There are many types of vidicons in use today such as silicon vidicon, plumbicon (PbO) and Sb_2O_3 (often referred to as vidicon), which differ in the material used to form the photosensor and target, mechanism of read-out and whether they are integrating or non-integrating type. Among all the types of vidicon, the silicon vidicon has found the widest application in analytical rapid scan spectroscopy for a number of reasons which will be explored in this section.

The heart of the silicon vidicon (SV) is a single monolithic silicon crystal wafer with a microscopic array of a few million diode junctions grown on it. The p-regions of the diodes acts as charge-storage regions and the p-n junction depletion region is the light transducer. All diodes have a common cathode and their isolated anodes are selectively addressed by a scanning (readout) electron beam. Figure 2.8 and 2.9 show the vidicon tube geometry, beam scan pattern, and mechanism of signal production.

In normal operation, the diode array substrate is positively biased with respect to the electron gun cathode. The substrate potential relative to the

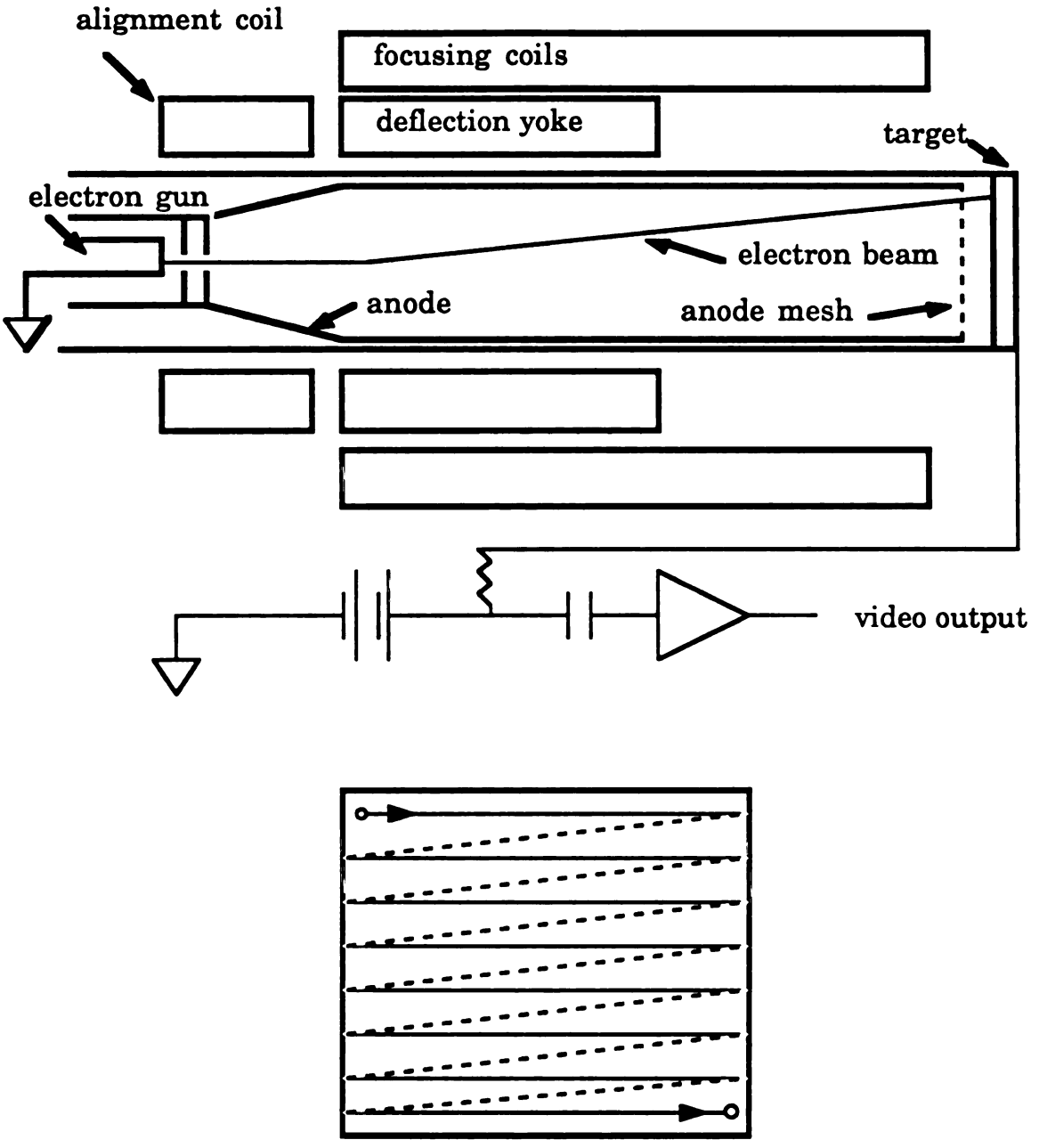

figure 2.8 vidicon tube geometry and beam scan pattern

cathode potential is referred to as the target voltage and is typically 10 V. The impinging electron beam thus strikes the mosaic and deposits electrons on both the p-type islands and the silicon dioxide film surrounding the diodes, which isolates the substrate from the beam. Since the resistivity of the silicon dioxide film is very high, the electronic charge accumulates on this surface and charges it to some voltage very close to the cathode potential, where it remains until the next readout.

The beam diameter as indicated in Figure 2.9, is generally larger than the diode spacing to eliminate any need for registration between the beam and the mosaic. The electronic charge deposited by a sufficiently intense beam will place a reverse bias of 10 V on the diode as it scans over the array. This bias will create a depletion width of approximately 5 M with a 10 ohm-cm substrate, giving a junction capacitance that result in an effective charge-storage capacitance for the target of approximately 2000 PF/cm^2. Notice that, at this bias, the silicon surface under the oxide will normally be depleted, as indicated in Figure 2.9 with very low values of diode leakage currents (less than 10^{-13}A/diode). The diodes remain in the full reverse biased condition throughout the entire frame period, if they are not illuminated.

Almost all of the incident light associated with the image is absorbed in the n-type region, each absorbed photon giving rise to one hole-electron pair. Since the absorption coefficient for UV/VIS light in silicon is very large, the majority of the photo-generated carriers will be created near the illuminated surface. This will increase the minority carrier (i.e., hole)

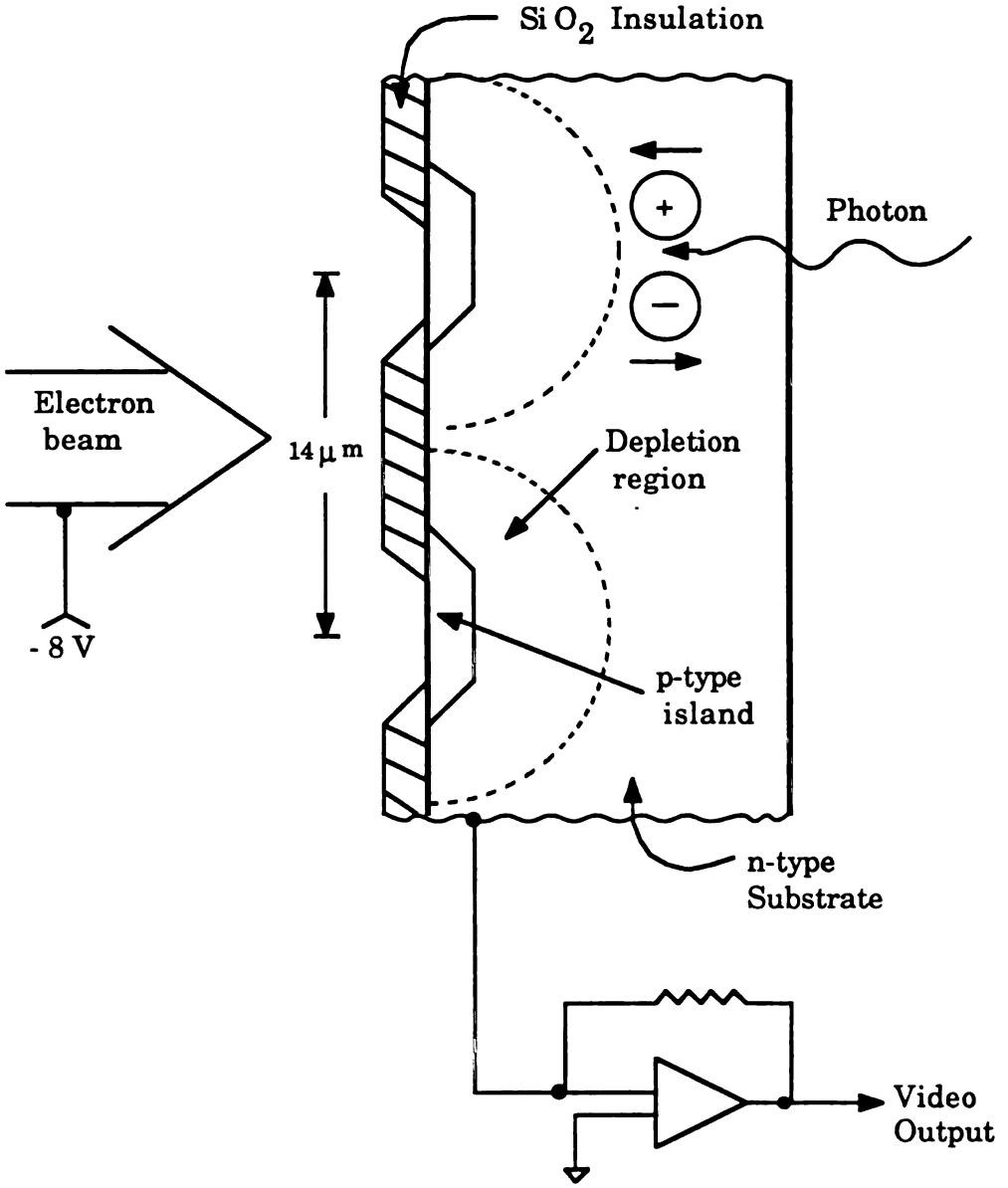

Figure 2.9 The vidicon target and signal generating mechanism

above its thermal equilibrium value and cause a net diffusion of holes towards the reverse-biased diodes. If the lifetime of the holes is sufficiently long and the illuminated surface has been treated properly to reduce recombination effects, a large fraction of the photon-generated holes will diffuse to the electric fields associated with the depletion regions of the diodes and will contribute to the junction current. The light induced junction current will continue to flow and discharge the junction capacitance throughout the frame period as long as the diodes remain in the reverse-biased condition. Thus, high light levels require high values of reverse-bias voltage or high values of junction capacitance to avoid saturation. The video output signal from each diode is created when the electron beam returns to a diode and restores the original charge by reestablishing the full value of reverse bias.

Because of the insulating properties of the depletion region, one can think of each photodiode acting as an elemental capacitor which is charged to an initial potential by the electron beam (26). In this manner each diode storage capacitor has a portion of its original charge neutralized, creating a charge pattern which is stored on the beam side of the target between successive passage of the readout beam. This charge pattern is an electronic image corresponding to the optical image focused on the transducer side of the target. The electron beam recovers this spectral information and returns the diode array to its initial condition by depositing an amount of charge equal to that discharged by the light (over the interval of time since the last scan of the beam). The elemental capacitor recharging current is capacitively coupled in the external circuit and amplified to produce a position encoded photocurrent (27). The relationship

between the observed photocurrent from any area (A) of the target and the photon flux (N) on that area over the exposure time (T_e) is given by:

$$I = QeGAT_r^{-1} \int_0^{T_e} (N)\gamma \, dt \qquad \text{amps}$$

Where

Q = quantum efficiency of the photosurface;

e = electron charge, coulombs;

G = target gain (G = 1 for SV);

A = area of target scanned as unit of information, cm^2;

N = incident photon flux, $cm^{-2}sec^{-1}$;

γ = slope of current vs. luminous flux curve (γ = 1 for SV);

T_r = readout time to scan area A, sec; and

T_e = detector exposure time between readout, sec.

With a constant photon flux over the exposure time the above equation reduces to $I = KAN (T_e/T_r)$ where K = QeG. Typical signals are on the order of a few nanoampers. As can be seen from the equation there is a linear relationship between the intensity of the incident light and the magnitude of the resulting photocurrent.

Vidicon detectors and particularly the silicon vidicon with its various image-intensified derivatives offer a number of unique advantages and, of course, some limitations as detectors for rapid scan spectroscopy. The most useful imager for UV to near-IR spectrometric application is the silicon vidicon. Their behavior and performance are better controlled (even if not

always fully understood). The ability to control the time and sequence of the beam readout (not yet taken advantage of) can provide the user with a great deal of flexibility in the operation of the device.

Silicon vidicon tubes use flat, thin-layered sensors, placed at the focal plane of a spectrograph, with an excellent geometrical registration between wavelength and position on the detector surface (spectral-to-spatial conversion). Once the detectors are calibrated, there is no need to verify this registration periodically, unless their position in relation to that of the light dispersive element has been altered. The monitored spectra can be observed in real time and any gross deviation from the expected result can be detected immediately and corrected. In this way a great deal of time can be saved and the loss of highly valuable data can often be prevented.

A large portion of the sensitivity of the device is due to combination of the advantage of a multichannel detector and integrating detector. The "integration" mode of detection is derived from their storage characteristics. Since the vidicon responds to energy (rather than power) it can be used as a very efficient storage device. The procedure by which SVs integrate is called "charge integration". This integration capability can be used to enhance weak signals by increasing the exposure time by means of blanking the electron beam an inhibiting the deflection circuit for an integer number of frames (time required to record one spectrum).

Charge integration can be utilized only until the most intense feature saturates. If integration continues after an intense region has saturated, the charge from the saturated channels will spread into adjacent channels,

in contrast to linear diode array (28). The dark current charge also increases linearly with exposure time, so that it,too places an upper limit on the integration time that can be used for signal enhancement. Cooling of the SV significantly lowers the dark current (23) and permit longer integration time.

Another attractive feature of SV is that it is a two dimensional OID with an area-array target comprising a few hundred thousands discrete photodiodes. Since these diodes can be randomly read out by the scanning beams, the detector is capable of performing some very useful spectrometric tasks:

1. 2D spectral contours, such as obtained in "total luminescence spectroscopy" (Ex. vs. Em.) (29) can be simultaneously acquired, and actually monitored in real time.

2. The electronic division of the target into a large number of individual tracks, each of which has ~500 channels, provides the means for a rather unique dual-beam and more generally poly-beam spectroscopy.

3. The adverse effect of blooming (explained later) and spectral interference, whereby spectral features masked by dominant neighboring features, can be largely reduced.

For detection of low light levels (i.e., single photoelectron), an image intensification section is added to the silicon vidicon. The resultant imager,

the silicon intensified target (SIT) vidicon has a photocathode (transducer) that converts the photon image into a corresponding photoelectron image. The generated electron image is accelerated (typically 7-9 KV) and focused onto the silicon target. Since the number of electron-hole charge pairs produced on the target is proportional to the potential of the incident electrons (approximately one charge pair per 3-6 eV) an internal gain of approximately 1500 is typically achieved, i.e., this is the number of electrons produced from each photoelectron emitted form the photocathode. With this gain, the signal is sufficiently enhanced (compared to readout noise) to allow the detection of very weak signals.

Even though SV tubes are preferred over SIT tubes for detection below 360 nm and above 850 nm and whenever cooling capability ($T<40°C$) and experimental conditions allow for long observation periods, in the case of low light level spectroscopy (such as luminescence) the SIT tube with its high in-target gain makes a superior detector.

Finally, the SV tube is a better detector than the other two: vidicon (Sb_2O_3) and plumbicon. It responds over a wide spectra range (generally 350-1000 nm, but tubes with limited response down to 200 nm are available) with high sensitivity, whereas the other two are limited to use between 400 and -600 nm. SIT has lower lag (will be explained later), lower dark current, linear response ($g = 1$), high resolution, freedom from image persistence or damage from intense sources, and linear dynamic range of at least 10^4 (30).

Two of the most serious technical problems with the vidicon are the lag and blooming characteristics. Lag is the incomplete erasure of images on the

first few readout cycles after storage. This phenomenon is caused by target capacitance and reduced beam acceptance at low discharge levels. This characteristic is more of a problem for low level signals. Blooming, or signal spreading, is caused by the lateral diffusion for charge from a region of high spectral intensity to a region of low spectral intensity. The migration of charge is caused by the potential gradient existing between the two regions and is a result of finite target conductivity. Blooming increases with increasing signal levels and causes a loss of resolution. Blooming may also prohibit the acquisition of information from a low intensity line in close proximity to a strong line.

Another undesirable feature of SV that limits its multichannel detection performance is a substantial coherent pattern noise caused mainly by diode-to-diode variations in the response and in the dark current.

The choice between operation in the single-frame and cumulative integration modes presents a dilemma. With successive readout (cumulative) at a standard TV-rate, the target reaches steady state and the output response is linear, but the SNR is substantially reduced by the introduction of amplifier noise with each readout. Alternatively, a long exposure terminated by a single readout (single frame) eliminates this effect but produces a non-linear response as a result of the incomplete readout (lag) of the only slightly discharged pixels (at region of low light exposure (31). However, ways have been proposed to remove this effect (32).

The list of photometric applications to date includes: astronomical observation (33), scanner and imaging system for earth observation (34),

flame multielemental atomic emission (35-41), and absorption (42-45), molecular absorption (46-48), molecular fluorescence (49,51), picosecond (laser) flash photolysis and molecular absorption spectroscopy (52), picosecond (laser) molecular fluorescence (53), including a single living cell fluorescence (54-55), time resolved resonance raman spectroscopy (52), HPLC detection (56-57), stopped-flow kinetic detector (58-59), electro-optical ion detectors in mass spectroscopy (60), and others.

IMAGE DISSECTOR

The image dissector is one of the oldest and simplest non-storage camera tubes. It has been used in earlier studies (61-62), and recently received some attention (63) but not comparable with either vidicon or solid state devices.

An image dissector, in reality, is nothing more than a photomultiplier with a small, electronically movable photocathode area which can therefore be operated as an all electronic low inertia microphotometer. In other words, it exactly functions as an electronically movable exit slit of the spectrometer. As Figure 2.10 shows the image dissector acts like a PMT in which a field of view is electronically scanned across a small aperture. It consists of a photocathode separated from a conventional dynode chain electron multiplier by a plate corresponding to the light image

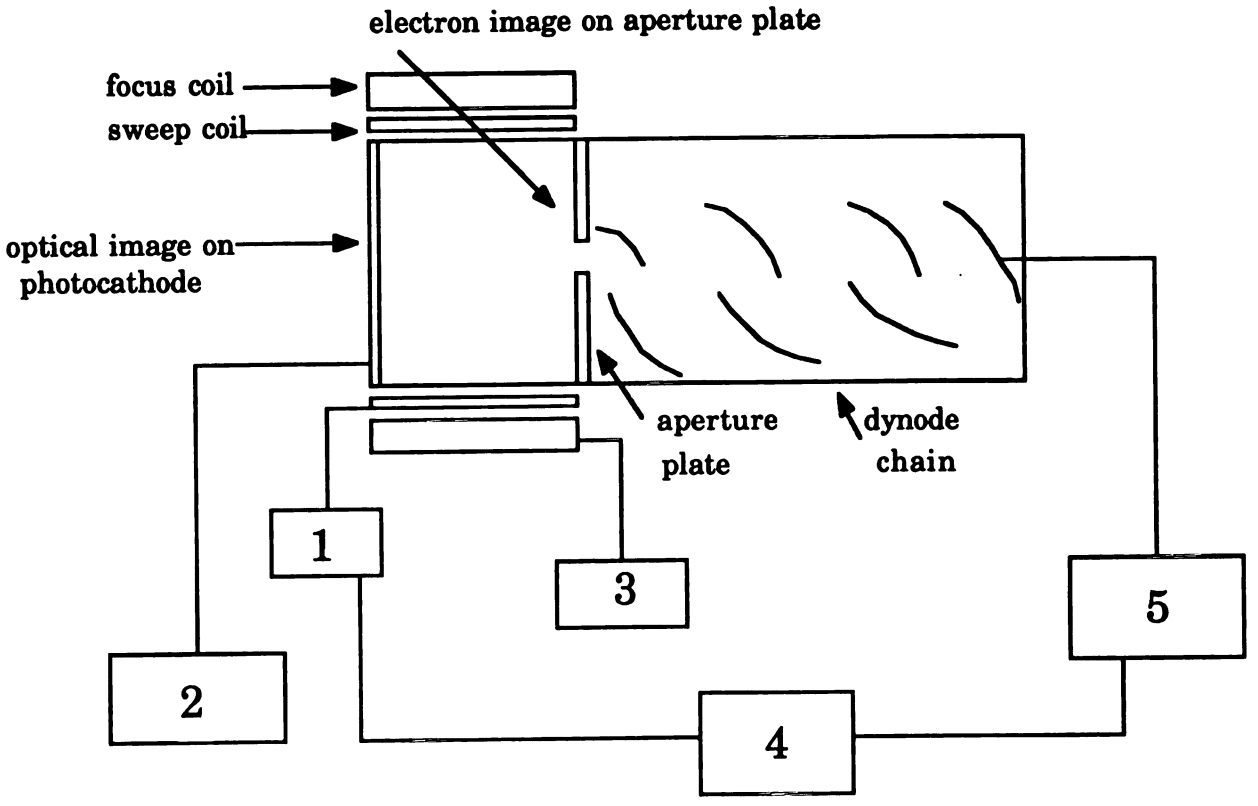

Figure 2.10 Image dissector photomultiplier. (1) Sweep coil electronics, (2) Photomultiplier power supply, (3) Focus coil electronics, (4) Display, (5) Signal amplification

incident on the photocathode. Electronic scanning is accomplished by electromagnetic sweep coils surrounding the tube, which sweep the electron image across the face of the plate. Only the portion of the electron image which pass through the hole in the aperture plate can reach the first dynode and be amplified by the dynode chain. As with other scanning systems, signal averaging techniques can profitably be employed with image dissector systems. These tubes have been employed with both one and two dimensional dispersive systems.

Danielsson and Lindblom (64-65) and Danielsson, et al. (66) have recently designed an image dissector/echelle system and have described its application to multielement analysis. This system provides wide wavelength coverage at high resolution. For example, the system covers the whole spectral range from 200-800 nm with resolution on the order of 0.001 nm.

Some of the major advantages of an image dissector are the excellent resolution, extremely high scan rates (up to 1 scan/nsec), easy random access, relatively simplified computer interfacing, large dynamic range (typically 10^5-10^6), and the virtual absence of lag and blooming effects. Unlike vidicon, the image dissector can be operated at stationary deflection, which greatly simplifies software control and permits more rapid acquisition of spectral information. Although blooming does not occur with the image dissector, an analogous phenomenon may reduce the available linear dynamic range. If bright images are incident on the photocathode when a measurement of illumination at a low level is being made, the back

scattered flux from internal tube parts may limit the available dynamic range to only 2 to 3 order of magnitude, depending on the area, brightness, and location of the disturbing flux. Another limitation of the device is that it is not an integrating sensor, such as the vidicon. This means the device can not accumulate and store information from one part of an image while another region is being integrated. Thus, if one is scanning N resolution elements in a given time, then the random component of the signal to noise ratio for each element would be degraded by a factor of N as compared to the continuous monitoring of a single resolution element for the same time period, assuming that noise is limiting.

SOLID STATE IMAGING DEVICES

Introduction

Solid state imaging devices consist of arrays of discrete photosensitive elements which are scanned by means of electronic circuits that are integrated on the same semiconductor wafer. The various solid state devices also referred to as silicon self-scanned array devices are similar in the mechanism, limitations, and capabilities of the sensing elements, but differ most significantly in the arrangement for signal amplification and scanning.

In the last decade, there has been an intense development effort in the design, manufacture, and application of solid state (SSIDs) devices. Even though the development of such devices was primarily aimed at capturing high commercial markets, spectroscopic detection technology is becoming a major beneficiary. Among various solid state devices, the photodiode array has been the most popular detector for analytical spectroscopy. The photodiode array (PDA), also referred to as linear diode array (LDA), will be discussed in detail in the next chapter. Two other solid state devices, charge coupled devices (CCD) and charge injection devices (CID) have recently received attention and seem promising for the future. They are discussed here.

CHARGE TRANSFER DEVICES (CTDS)

Charge transfer devices are solid-state integrating optoelectronic image devices constructed by employing conventional VLSI photofabrication technology. In contrast a photomultiplier tube (PMT) which produces a current proportional to the instantaneous photon flux, CTDs similar to PDAs integrate the photogenerated charge as light strikes them. The mechanism of charge collection, storage, and read out in CTDs is different from PDAs. In PDAs, the photon generated charge is collected and stored in a reverse-biased photodiode whereas in CTDs the charge collection and storage occurs in a metal-oxide-semiconductor (MOS) capacitors. The amount of photogenerated charge stored in each detector element is proportional to the number of photons that strikes that detector element.

There are two mechanism by which the accumulated signal information in CTDs can be measured (read out). These two charge sensing mechanisms are known as inter-cell and intera-cell charge transfer modes. Based on these two different charge sensing methods, two types of CTD detectors have been designed. The charge coupled device (CCD) utilizing inter-cell charge transfer mode and the charge injection device (CID) using the intera-cell charge transfer mode. An individual detector in a CTD array consists of a doped silicon region used for generation and storage of photogenerated charge. This doped silicon region is separated by an silicon oxide layer from a series of conducting electrodes used for signal information read out. A basic operation of a single CTD detector in shown in figure 2.11.

The negative voltage on the conductive electrodes with respect to the silicon creates a charge inversion region which is energetically favorable location for the mobile minority carriers (holes) to reside. An electron-hole pair is generated by the absorption of a photon of appropriate energy. The proton is promoted into the semiconductor conduction band and the hole moves toward and is stored in the inversion region. When one electrode is held at a more negative potential than the other, the positive charges (holes) will be more favorably stored under this more negative electrode.

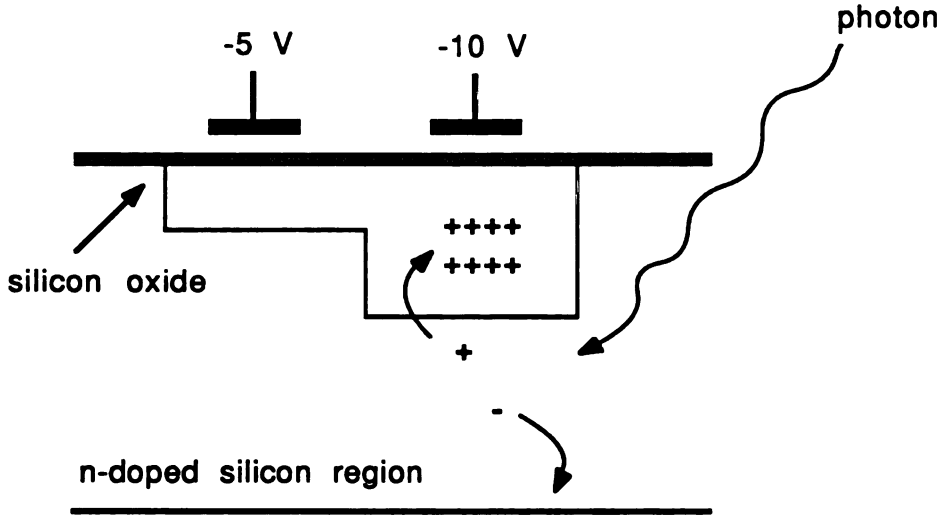

Figure 2.11 A single CTD detector element.

One can measure the amount of accumulated charge using either of the above mentioned inter-cell or intera-cell charge transfer modes. The charge measurement process consists of either shifting the charge from the detector element where it is stored to a charge sensing amplifier as in

CCDs (inter-cell charge transfer), or by the measurement of the induced voltage change which results from the movement of the charge within the detector element as in CIDs (intera-cell charge transfer).

Since their introduction in the early 1970s , there have been a great deal of research efforts aimed at exploring the capabilities of CTDs as multichannel detectors for analytical spectroscopy (70-73). These research activities have been mainly motivated by the historical desire to replace the single channel PMTs with an ideal multichannel detector (74-76). Earlier attempts at accomplishing this task were the use of television-type camera tubes such as silicon vidicons, SIT tubes, and image dissectors which were previously described. These devices possess a large number of pixels for rapid coverage of a wide wavelength range, while being compact in size. However, as previously explained, these detectors all employ an electron beam to carry the video signal information. It is absolutely necessary for this electron beam to be precisely controlled. Any uncertainties in the control of this electron beam can hamper the precise pixel selection in these devices. Moreover, silicon vidicons and SIT tubes suffer from blooming and lag problems under high light level conditions.

In an attempt to avoid these problems, solid-state multichannel image detectors were developed. The PDAs were the first solid-state multichannel detectors to be successfully used in scientific spectroscopic measurements. Throughout the late 1970's and early 1980's, PDAs have found widespread application and acceptance in the field of analytical rapid scan spectroscopy and several commercial instruments based on its technology are now available from a number of manufacturers. In many situations, however,

neither the televesion-type camera tubes nor the PDAs are capable of competitive performance with PMT in terms of sensitivity, dynamic range, and noise. This has limited the successful applications of these devices to those circumstances where the multichannel advantage outweighs the sensitivity, dynamic range, noise, and bloomig (less in PDAs) disadvantages.

Recently, the extensive research by Denton and coworkers in evaluating the spectrometric performance of CTDs has demonstrated that when compared on detector-element by detector-element basis, these devices are capable of superior sensitivity and dynamic range to that of the PMT and some of these devices can even exceed the sensitivity and dynamic range of all available detectors (77-80). A number of manufacturers are currently producing a wide range CTD devices with different electro-optical characteristics, formats, and operating requirements. Current CTD detectors can have peak quantum efficiencies over 80%, a high spectral responsivity from the soft X-Ray to the near IR regions, very low dark count rate that allow very long integration times, and read noises several orders of magnitude lower than those of commercially available photodiode arrays (81).

The detailed operation of the CCDs and CIDs along with their performance characteristics influencing analytical spectroscopy have been described by Denton and coworkers (77,79). Here, a brief description of the CCD and CID devices as well as their major advantages for and their applications in analytical spectroscopy is presented next.

Charge Injection Device (CID)

CID imaging device utilizes an x-y addressed array of charge storage capacitors which store photon generated charge in metaloxide semiconductor (MOS) inversion region. Each single detector element consists of a pair of charge storage MOS capacitors (figure 2.11) of which one is controlled by an x-row drive line, and the other by a y-column drive. The two storage MOS capacitors are formed by two conductive electrodes and an n-type silicon region separated by a silicon oxide insulating layer. A schematic representation of a typical CID detector is shown in figure 2.12.

A unique feature to note about the CID device is its random access readout capability. High speed shift registers (addressing registers) are used to randomly address any single detector element. As shown in figure 2.12, these addressing registers sequentially connect rows and columns to the output amplifier and drive signal, respectively. The photon generated charge during the integration is stored in the potential wells formed by by applying negative voltages (with respect to substrate) to both conductive electrode in each detector element (figure 2.11). One of the electrode (storage) is held at a more negative potential than the other, making the storage of photogenerated charge more favorable under this electrode. This energetically more favorable charge storage location is indicated by the depth of a potential well under the more negative electrode.

As was pointed out earlier, the accumulated charge in the CID device is measured using the intera-cell charge transfer mode. This involves

shifting the charge from under the more negative storage electrode to the other less negative (sensing) electrode and measuring the potential change induced on the sensing electrode. The induced potential change is dV = dQ/C, where C is the capacitance of the MOS sensing capacitor and dQ is the quantity of charge transferred. A differential charge sensing scheme is employed where two charge sampling, one before and one after the charge transfer, is performed. The difference in charge (dQ) between the two sampling is proportional to the amount of photogenerated charge. In practice, one can accomplish this process by first driving the voltage of storage electrode from its integrating negative potential to positive causing the collapse of the inversion region under this electrode and; thus, transfering the charge to the only remaining potential well under the sensing electrode. Next, the voltage of the sensing electrode is driven positive which results in the collapse of inversion region under both electrodes and the injection of charge from the entire detector element into the substrate.

The charge readout sequence in the CID device can be completed in one of two ways (79). In one way known as the nondestructive readout (NDRO); after the second voltage measurement on the sensing electrode is made, the charge is shifted back under the storage electrode (original position) by re-establishing the potential well under this electrode. This returns the detector element to its condition prior to charge measurement nondestructively, i.e., without any change in neither the amount nor the location of the photogenerated charge information. The second option is that upon completion of the differential voltage measurement, the potential well under the sensing electrode is made to collapse. This is known as

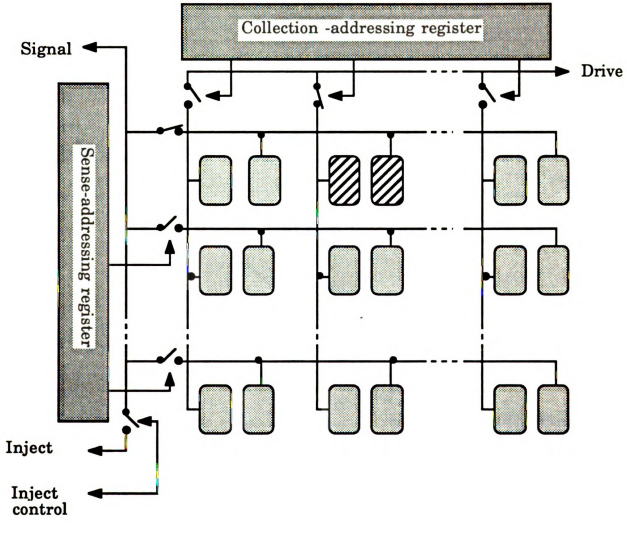

Figure 2.12 A hypothetical CID device

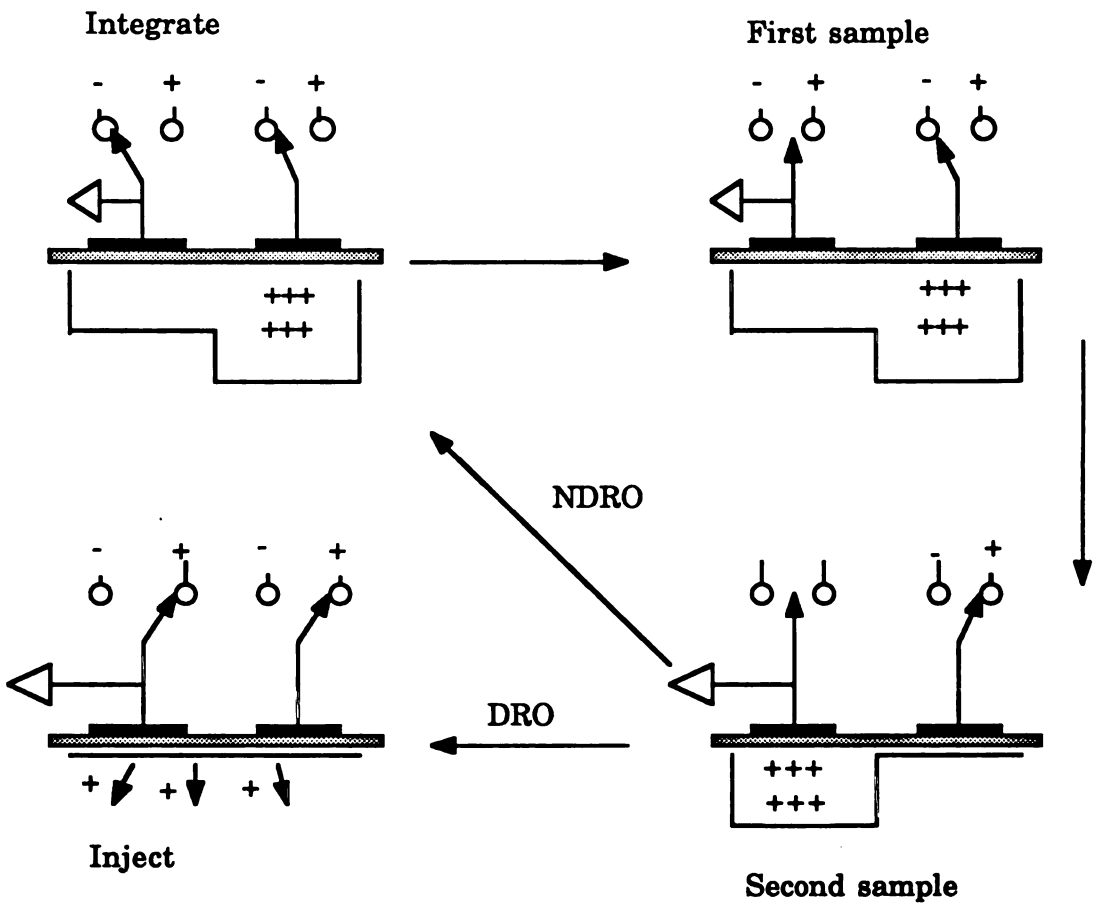

Figure 2.13 The destructive and nondestructive readout scheme in the CID

destructive readout (DRO), since it causes electron-hole recombination and destructive elimination of charge from the detector element. These two readout methods are shown schematically in figure 2.13.

The CID device has several unique features which makes it very useful as a spectroscopic detector. First, it can be operated with random access readout instead of sequentially scanning through the whole array as is the case in other solid-state devices. This allows for faster readout speed for rapid analysis. Second, it is very resistant to cross talk (blooming) between detector elements except under extremely intense illumination conditions where the charge migration across the substrate junction may not occur at sufficient rate. Third, the read noise in the CID device can be significantly reduced through the use of NDRO readout. Besides photon counting PMT detectors which essentially have no noise associated with their readout system, almost all other spectroscopic detectors including solid-state devices have some read noise introduced by the detector and its associated readout electronics. The read noise in solid-state imaging devices varies from more than 1200 electrons for PDAs to less than 5 electrons for some CCDs (77). The S/N ratio of a photon flux measurement can be increased by averaging a number of NDROs with the CID. Contrary to typical signal averaging which is subject to various photon noises, NDRO averaging in the CID is free from photon noise and only subject to the read noise. Therefore, if the read noise is random, the NDRO averaging can result in a factor of 10 reduction in the effective read noise (81).

Now, that many of the earlier problems with the CID devices such as low response in the UV region and the absorption of light below 350 nm by their

glass windows have been removed (72), and in light of some important new developments discussed above, the CID technology appear to be ready and well suited to many interesting spectroscopic applications. A recent application of a two dimensional CID to multielement ICP emission spectroscopy (82) is a very good example. In this regard, the CID device offers several important advantages. These include full utilization of the enormous information available in the emission signal, random access readout and random access integration through NDRO which leads to a very wide dynamic range as well as clean background correction and dynamic optimization of the experiment (78).

Charge Coupled Device (CCD)

Like most imaging devices, charged coupled devices (CCD) were not first intended for use in spectroscopy but rather for a wide variety of military, industrial and consumer imaging applications. Presently, however, a variety of CCD detectors optimized for scientific imaging applications are available from many manufacturers.

Similar to the CID, the structure of CCD also consists of a series of MOS capacitors for storage of photogenerated charge packets (figure 2.11). The two detectors do, however, differ in a number of ways. First, CCDs are usually manufactured with p-type materials (as opposed to n-type in CIDs), so that electrons are stored in the potential wells. Second, the structure of CCDs does not allow for random access readout and the entire array must be read before the next exposure. Third and the most important difference

between the two detector is in the way which the charge packets are read out. As mentioned before, CCDs employ inter-cell charge transfer mode for charge information readout. Analogous to the CIDs, a number of independent conductive electrodes are used in each detector element to effect the charge transfer. The number of electrodes used may range from one to four giving rise to uniphase to four phase CCD device (83), respectively. By changing the voltages of these conductive electrodes in a controlled way, the charge from one detector element is sequentially shifted to the next (analogous to an analog shift register) and on to a single on chip charge detector diode and voltage sensing amplifier located at the edge of one or two dimensional arrays of detector elements.

A schematic diagram of a typical two dimensional CCD is shown in figure 2.14. Columns are clocked in parallel causing the charge in an entire array to be shifted, one row at a time, toward a serial shift register where it is serially moved to a single low capacitance output node for readout. The migration of charge from one column to another is prevented by means of fixed potential barriers between them. The sequential shifting of charge from each detector element to a single low capacitance output node allows for higher S/N ratio to be achieved in the CCD output compared to the CID and the PDA which employ mutiplexed architecture. The capacitance at the input of an off-chip amplifier in the CID, for example, is relatively higher than that of the CCD and; thus, the voltage change induced on this capacitance ($dV = dQ/C$) for a given quantity of charge is lower in the CID device. In fact, the dominant noise source in the CID is directly proportional to the capacitance at the input node of this off-chip amplifier.

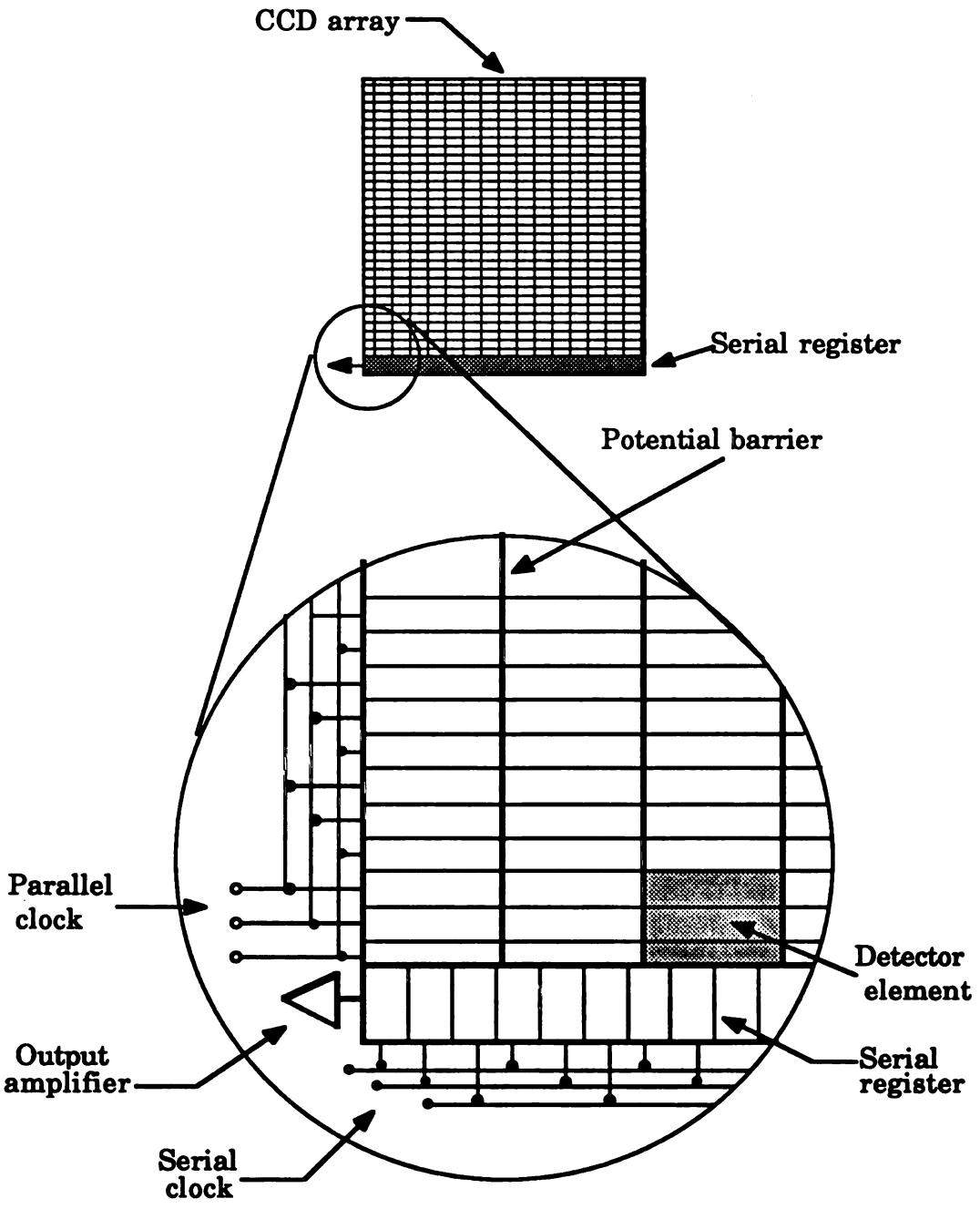

Figure 2.14 Diagram of a hypothetical three-phase CCD

The elimination of the multiplexed circuitry and its replacement with a single low capacitance readout node provides for an ultra low read noise observed in the CCD device. However, before the charge from a given detector element reaches the output node, it undergoes numerous transfers from detector element to detector element, as well as from the parallel register into the serial register, and finally from the serial register into the output node. This demands for an extremely efficient charge transfer process where after several thousand transfers, the amount of charge in each packet stays substantially the same with minimal signal degradation. Charge transfer efficiencies on the order of 0.99999 is required for this purpose (79) and fortunately CCD devices charge transfer efficiencies on the order of 0.999995 are available.

A very important characteristic of the CCD which makes it unique among all other imaging devices is its ability to utilize a special charge readout mechanism called binning (84). Binning is a process where the photogenerated charge packets from more than one detector elements is physically combined into one single charge packet (bin) and is subsequently transferred to the output node for readout. With the CCD device, it is possible to perform serial, parallel, as well as two dimensional binning of any number of consecutively arranged detector elements.

The summing of the photogenerated charge packets from multiple detector elements has a direct effect on the S/N ratio and the dynamic range of spectral intensity measurements. The on-chip analog summation (binning) is definitely advantageous over digital summation in a computer memory. This is because the binned charge packet (charge from a group of

detector elements) is subject to only one read noise, whereas digital summation adds the read noises from every detector elements in the group. Under detector read noise limited situations (very low-light-level), the noise in a digitally summed signal is greater by a factor equal to the square root of the number of summed detector elements. Moreover, the number of analog to digital conversion required to process a group of charge packets is reduced by binning which, in turn, reduces the total detector noise and increases the readout speed. It is also important to point out that the sacrifice in resolution accompanied with the gain in sensitivity brought about by binning may not be that significant due to the original large number of resolution elements in the CCD arrays.

As evident from the above discussion, there are several unique characteristics of the CCD device that encourages its application in analytical spectroscopy. First, it is the most sensitive multichannel detector for low-light-level scientific applications. The high sensitivity of the CCD device is due to its high quantum efficiency, ability to integrate charge for a long time, negligible dark current, and most importantly, its ultra-low detector read noise. Second, all elements integrate over precisely the same time frame before the signals of all elements are simultaneously moved into the analog shift register and serially clocked into the output node. One disadvantage with regard to spectroscopic applications may be the spatial format of two dimensional CCDs where the height to width aspect ratio of a single detector element does not match that of a typical slit image found in spectroscopy. However, the added flexibility provided by binning in the CCD can easily overcome this spacial format disadvantage. Appropriate number of detector elements may be binned to exactly match

any desired slit image. In fact, if so desired the entire two dimensional CCD can be binned into a single channel detector with a large active area, or into a linear array detector with a high aspect ratio or, with appropriate optics, into two stacked linear array for truly multichannel dual-beam operation(84).

The high sensitivity obtainable with the CCD device, makes it a particularly suitable detector for low-light-level spectroscopic applications such as luminescence and raman spectroscopy. Recently, very promising results have been obtained with the application of the CCD device to chemiluminescence (85) and molecular fluorescence (86). In both cases, significant improvements in sensitivity and dynamic range have been realized through the use of CCD array detector. The case of molecular fluorescence is particularly interesting in that despite the use of a mercury pen lamp as excitation source that is modest in both cost and photon flux, a wide dynamic range (over 6 orders of magnitude) as well as very low detection limit of 1 fmol has been obtained (86). Based on this kind of performance, the authors conclude that these type of CCD based luminescence detection systems can be well suited for use in conjunction with FIA and HPLC analysis.

Device Comparison

Comparison among various SSIDs and their advantages and limitations as rapid scan multichannel spectroscopic detectors appear in previous sections of this work. By now the reader must be very well aware of the fact

that it a difficult , if not impossible, task to single out one particular detector as the best detector for all RSS applications. All of them involve some trade-offs among resolution, photometric accuracy, and measurement time. Other areas which also merit significant attention in selecting an appropriate multichannel detector for a given situation are sensitivity, dynamic range, spectral response, and addressing schemes. In fact, the desire for improvement in these areas has been the motivation behind analytical spectroscopists to keep on searching for new devices and technological advancements in other areas and exploit them for spectroscopic application. Actually, that is how the imaging devices came to be used in analytical spectroscopy.

However, it is obvious at this point that the optoelectronic image devices are superior detector over conventional mechanical systems at least for analytical rapid scan spectroscopy in the UV/VIS regions. Their applications have already broadened the field and will continue to do so.

Within the OIDs, solid state devices have recieved greater attention in recent years and have become well accepted among analytical spectroscopists. This is due to the fact that these devices offer long life, small size, low power consumption, ease of cooling, simplified circuitry and thereby ease of interfacing to the computer.

Among solid state devices, the photodiode array (PDA) has been the most popular multichannel detector for many years. This has been in part due to the develpment of PDAs specifically for spectroscopic application. Additionally, the spectroscopic performance of the PDAs have been well

studied and the device has been successfully applied to many areas such as atomic and molecular spectroscopy, stopped-flow kinetics, and HPLC detection. These factors as well as commercial availibility of PDA-based spectrometers in recent years have contributed ti its popularity. In fact, many spectroscopists had predicted that PDAs would eventually become the detector of choice.

Recent developments in charge transfer devices (CTDs), however, have begun to change the equation. Notice, that PDAs do still suffer from several drawbacks including fixed sequence of scanning, one dimensional format, higher read noise (due to multiplexed readout scheme), and finally, lag and blooming. Moreover, the PDA's sensitivity and dynamic range does not still quite match those offered by the PMT, particularly in low-light-level situations. Even the use of intensified PDAs does not totally eliminate the problem, since the dark current noise associated with the photocathode materials used in the intensification stage will still place a limit on the S/N ratio that can be achieved.

CTDs, on the other hand, provide a number of unique advantages compared to the PDAs. These include higher density of detector elements, ultra-low read noise (particularly in CCDs), and random access capibility. Their sensitivity and dynamic range have been shown to even exceed those of the PMT when compared on detector element- by-detector element basis. The imaginative readout schemes offered by the CTDs along with their very low read noise allows these devices to acheive high S/N ratio measurements specially at low-light-level.

The author believes that once a few remaining obstacles for the CTDs are resolved in the future, they will most likely dominate the field of rapid scan spectroscopy. One problem is their high cost which is not still affordable by many potential users. Secondly, the small size of the CTD detector elements does not match those of the slit-like images encountered in most spectrometers. Therefore, specific spectrometers need to be designed to match the CTD detector elements physical geometry. Third, and most importantly, intellegent software needs to be developed for control of the device and efficient processing of the enormous amount of information that is generated. When these issues are properly addressed and the demand for their applications increases, the presently high cost of the CTDs will perhaps become more affordable.

CHAPTER 3

DESCRIPTION OF A RAPID SCANNING LINEAR DIODE ARRAY SPECTROPHOTOMETER FOR STOPPED-FLOW KINETICS

Introduction

The purpose of this chapter is to provide a complete presentation of the instrument developed throughout this research. This is done by first giving a brief historical review of linear diode array applications in rapid scan spectroscopy in conjunction with stopped flow and then presenting an overview of the basic parts of the instrument; the function of each part of the instrument is described. Advantages and disadvantages of the LDA versus other optoelectronic image devices described in the previous chapter are discussed wherever necessary so that, this chapter is complementary to the previous one.

History of the LDA as an RSS Stopped-flow Detector

Only a few of the great many techniques that have been developed for rapid scanning spectroscopy have been applied to stopped-flow kinetics. Both of the two general techniques of RSS, i.e., conventional mechanical and optoelectronic image devices (OID) have been used in conjunction with stopped-flow and they have been reviewed by E. M. Carlson (87).

Until recently the application of the linear diode array to rapid scanning spectroscopy, especially stopped-flow kinetics, has been somewhat limited. This has been due to the low manufacture yield which limited the commercial availability and also the number of sensor element per array. Now that they have become commercially available with a large number of elements at a relative low price, these compact integrated circuits are beginning a new trend. Most experts predict that the self scanned solid state imagers, especially the LDA will eventually become the OID of choice.

However, the only report of a rapid scanning stopped-flow spectrophotometer which utilizes a linear diode array as a detector is that of Dessey (88). No data have appeared on the characterization or application of this system.

Functional Description of the Instrument

In traditional stopped-flow spectrophotometers, the reaction under study is monitored by recording the absorbance change with time of either a product, a reactant, or in some cases, an intermediate in the reaction. Because these measurements are done at a single wavelength, they require a repetitive process of performing the experiment for each wavelength at which the reaction is to be studied.

The rapid scan diode array stopped-flow spectrophotometer discussed here with its multiwavelength capability enables one to monitor the light intensities over a large spectral region simultaneously in a time comparable to that which a traditional spectrophotometer takes for a single

wavelength experiment. This multiwavelength capability provides the user with the choice of observing any abrupt change of formation of intermediate species at any wavelength during the course of the reactions. This kind of information is very helpful for a variety of theoretical studies such as determining the mechanism of a chemical reaction, rate constant, or rate expression. The system very quickly provides the analytical chemist with information over a large spectral region, which allows him/her to look at all spectral features in a given region and immediately locate the optimum wavelength desired for the analysis.

Figure 3.1 shows the block diagram of the instrument. The upper half of the figure shows the stopped-flow mixing system which is used as a solution handling system. The sample and reagents are rapidly mixed and brought into the observation cell. To monitor the subsequent reactions that take place in the observation cell, a beam of light focused by a double convex lens is passed through the cell and then into a polychromator module. Since it is very important for the linear diode array to have a focused spectrum across its flat surface, the polychromator module employs a holographic grating. The holographic grating design technology has made possible the production of flat field spectrographic, concave, abbertion-corrected gratings which by themselves produce a flat field image across the photosensitive elements of the detector with a minimum of stray light. The polychromator module which contains the holographic grating, linear diode array and other required optics all in one package has been designed by P. J. Aiello and is explained in detail elsewhere (89); so, it will not be further discussed here.

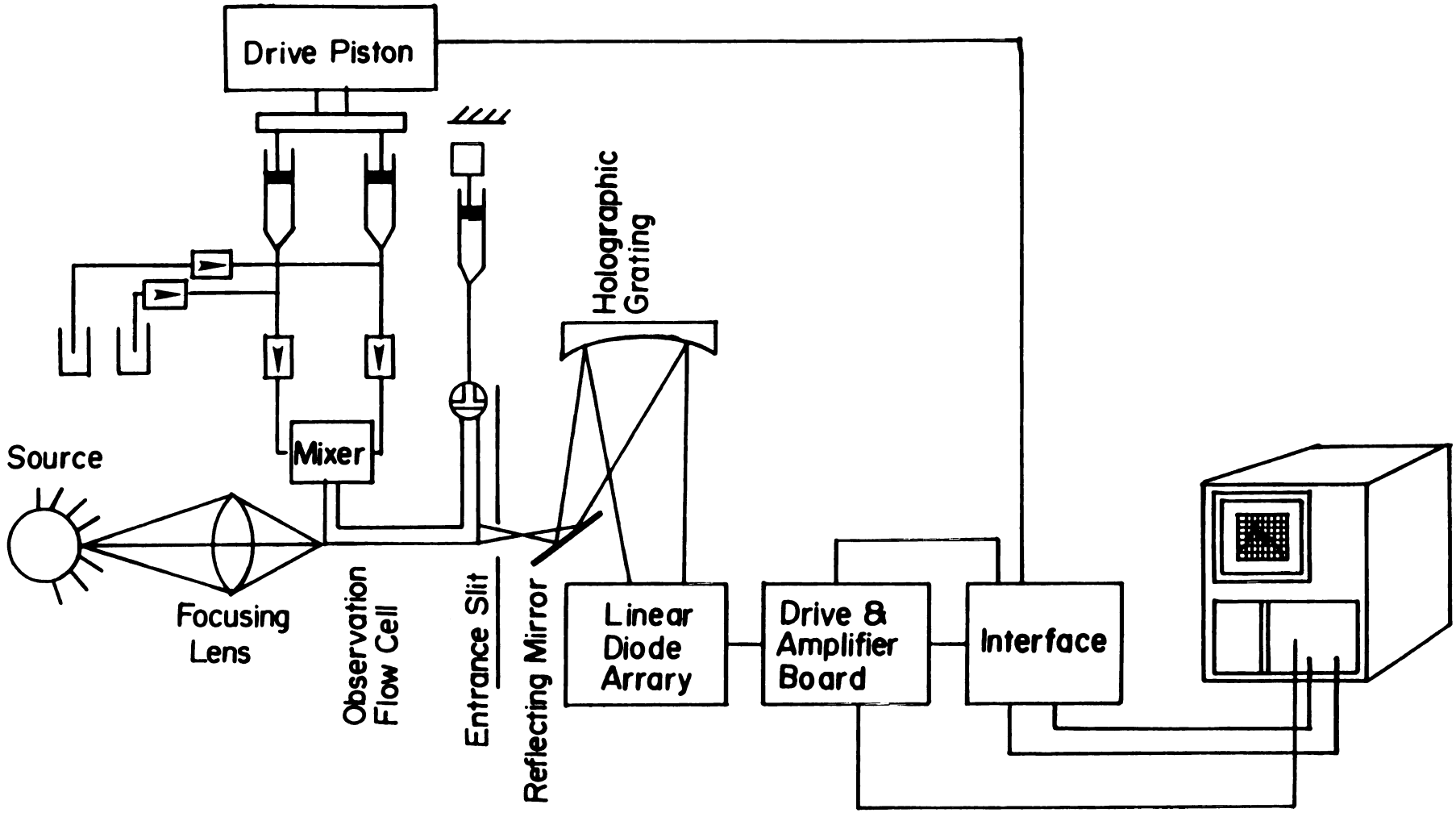

Figure 3.1 Block diagram of the rapid scanning photodiode array stopped-flow spectrometer.

The light dispersed by the polychromator eventually hits the rapid scan linear diode array, the output of which is recorded by a Tektronix storage scope. Other important parts of the instrument include: the linear diode array, the stopped-flow mixing systems and the control interface. The discussion of each follows.

Linear Diode Array

The linear diode array (LDA) used in this research was purchased from Reticon Corp. (90). This is a Reticon "S" series Type Rl-512S which has 512 sensor elements and is the first solid state image sensor designed specifically for spectroscopy applications.

The Reticon "S" series is a family of monolithic self scanning linear photodiode arrays. The devices in this series consist of a row of silicon photodiodes, each with an associated storage capacitor on which to integrate photocurrent and a multiplex switch for periodic readout via an integrated shift register scanning circuit. The device is packaged in a 22 lead dual-line integrated circuit package with choice of a ground and polished quartz window or a fiber optic faceplate. The pin configuration of the 512 element array used here is shown in Figure 3.2.

The Reticon S-series self scanning photodiode arrays here consists of 512 sensor elements (silicon diode). The overall length of the array chip is 12.8 mm, and the sensors are on 25 micrometer centers which corresponds to a density of 40 diodes/mm. Each sensor has a height of 2.5 mm providing a

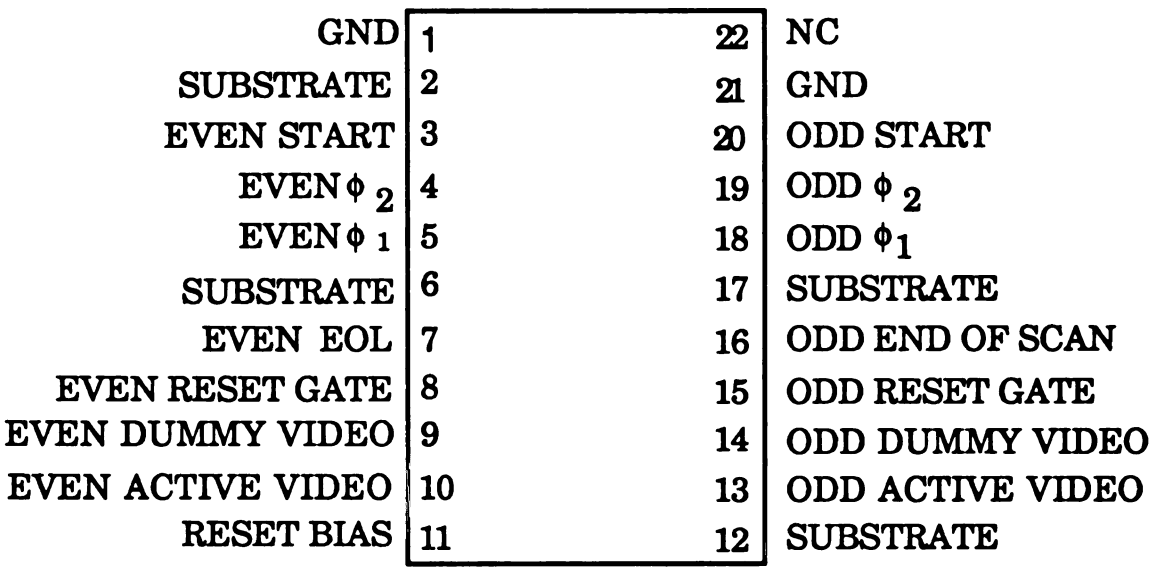

Figure 3.2 Pin configuration of the photodiode array integrated circuit

slit like geometry to each element with an aspect ratio of 100:1. This feature makes the array suitable for use in conjunction with monochromators or spectrographs. Figure 3.3 shows the sensor geometry and aperture response function. Each diode consists of an island of p-type bars diffused in an n-type substrate. Upon irradiating the sensing area, a charge proportional to the amount of light is generated. The generated charge is collected and stored on the p-type islands during the integration time. The stored charges are then transferred to the video line readout. Both the p-type and n-type silicon substrates are photosensitive. The charge generated on the p-type region is stored on the corresponding diode, and the charge created on the n-type substrate between two p-type regions will divide between the neighboring diodes to yield the response function shown in Figure 3.3.

Figure 3.4 shows the simplified equivalent circuit of an RL512S linear diode array. As can be seen each element contains one photodiode and one dummy diode, with each having its corresponding storage capacitance. The diodes are connected to dummy and video recharge lines through multiplex switches. All the odd sensor elements are connected to one pair of recharge lines and all the even sensor elements are connected to another pair. The shift register scanning circuit sequentially turns the multiplex switches on and off and thereby periodically recharges each element to 5 volts. As a result, a charge of Q_{satn} is deposited on its capacitance. A two-phase clock drives the shift registers. The clock also produces a periodic start pulse for initiation of each scan. The clock frequency determines the element-to-element sampling rate. The interval between start pulses is the

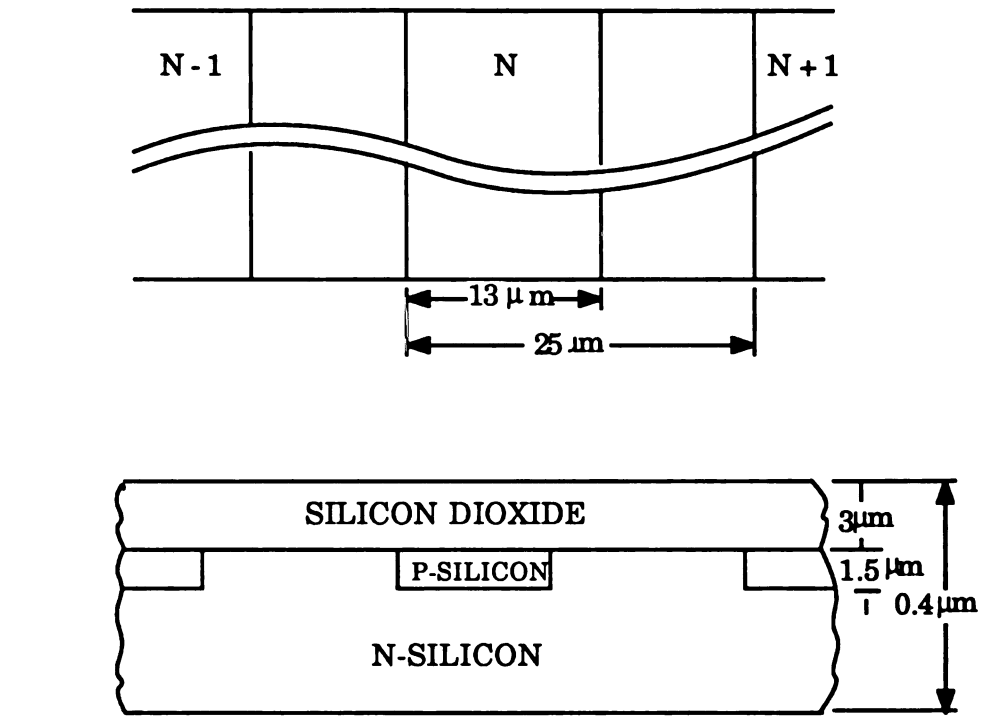

Figure 3.3 Sensor geometry and the response function of the aperture

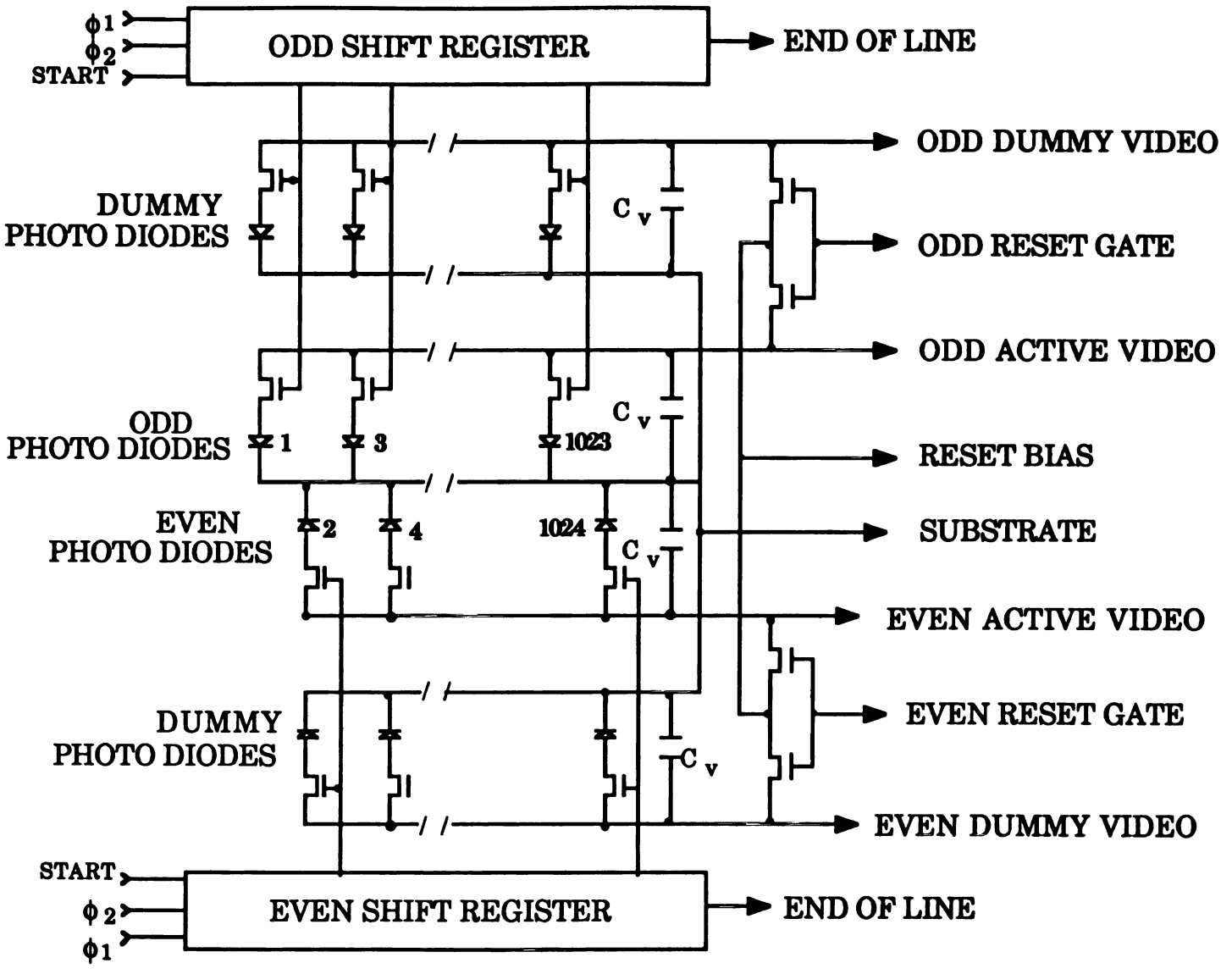

Figure 3.4 LDA ELECTRICAL EQUIVALENT CIRCUIT

integration time. During the integration time the reverse current flowing in each photodiode gradually discharges the charge on its associated capacitor. This reverse current consists of two components: the photocurrent i_p and the dark current i_d which is often negligible.

The photocurrent is the product of the responsivity of diode and the intensity of light. In a given line scan time the amount of charge which is discharged from each element is the product of the photocurrent and the line time. The video line must replace this charge when it samples each element once each scan. Therefore, each scan from a given N-element array produces an output signal which is a train of N charge pulses each being proportional to the light intensity on the corresponding photodiode. All of the diodes can be sampled in proper sequence by correctly phasing the two shift registers to the clock drives. Then by simple connection of the two video lines together a continuous train of output charge pulses will be produced. Switching transients are also capacitively coupled into the video lines by the multiplex switches. The transient are fed into the dummy lines, so that, they can be eliminated and a clean signal extracted by reading out the dummy and video lines differentially. Some of the key features of the LDA employed in this research are in summary:

1) Simultaneous integration of 512 photodiode sensor elements with 25 micrometer center-to-center spacing.

2) Integration time as short as 0.5 ms (according to the Reticon data sheet) or as long as 0.3 s are possible at room

temperature. however, in our experience the detector did not work properly with integration times of less than 4 ms.

3) Clock controlled sequential readout at arbitrary rates up to 2 MHz and simple square wave clock.
4) Differential output to cancel clock switching transients and fixed patterns.
5) Low output capacitance (2 pF) for low noise.
6) High saturation signal charge (14 C) for wide dynamic range.
7) Wide spectral response (200-1000 nm).
8) Quartz window for UV application.

Stopped-Flow Mixing System

The stopped-flow mixing system described here is a solution handling system whose purpose is to mix two solution rapidly together and deliver them to an observation cell where the reaction can be monitored by the diode array spectrophotometer. A complete schematic diagram of the stopped-flow mixing system is shown in Figure 3.5. As can be seen in this figure, it consists of two delivery syringes, a pneumatic drive piston, four pneumatically driven check valves, mixing chamber, observation cell, 3-way pneumatically driven slider valve and a stopping syringe assembly.

Two pairs of check valves works in opposition to one another so that the syringes are either connected to the reagent or to the observation cell depending on the direction of pressure. In a normal stopped-flow run (or

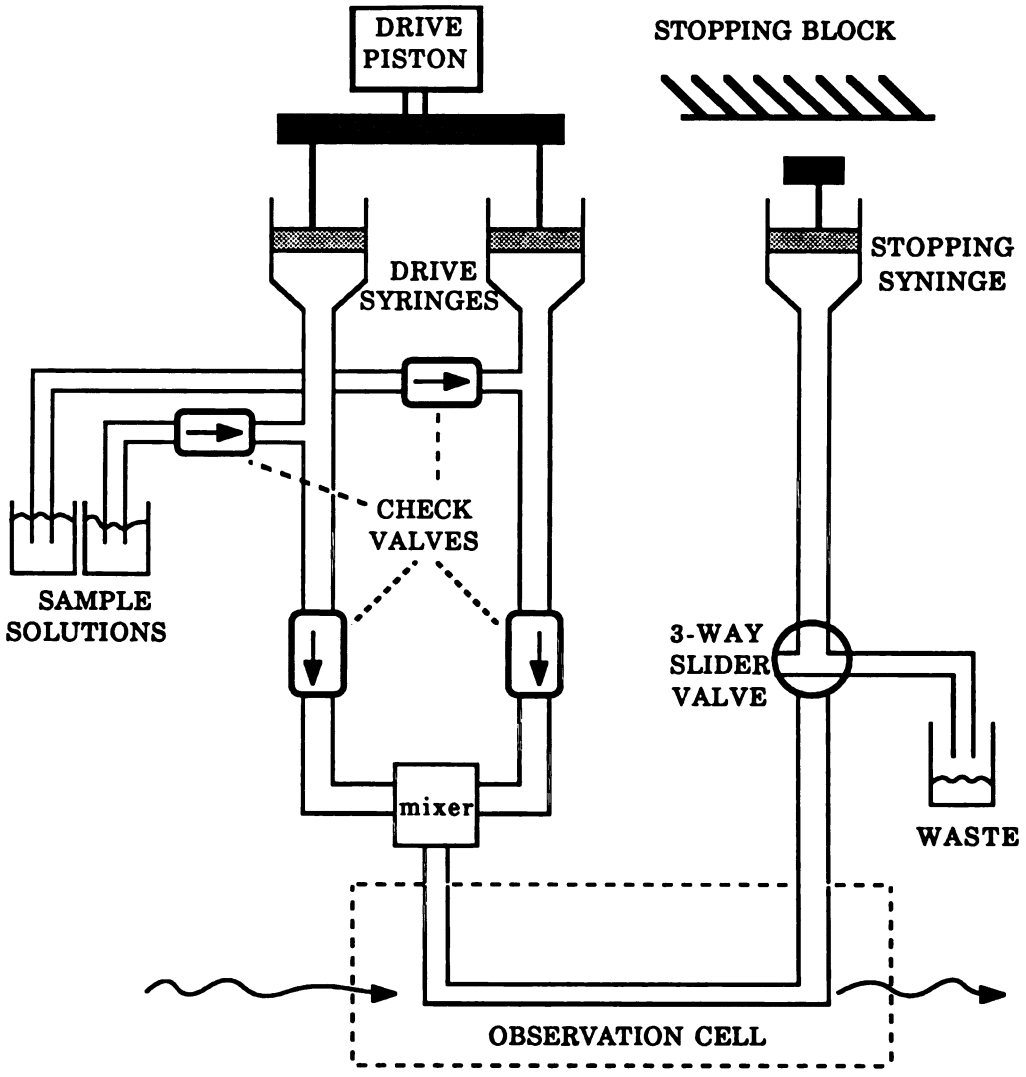

Figure 3.5 Block diagram of the stopped-flow mixing system (87)

push), the first operation is the filling of the drive syringes with the solutions. The pneumatically driven piston shown at the top performs this operation. The drive syringe piston moves upward, drawing reagent and sample solutions into the syringes. During this time the check valves insure that the syringes are filled with the sample solutions only. Then, the direction of air pressure is switched and with the 3-way slider valve in closed position, no solution flows at this time. The drive syringes become energized, and the check valves prevent the solution from returning to the sample reservoirs. The solution starts to flow when the position of the 3-way slider valve is switched to connect the flow system to the stopping syringe, and the syringe drive piston rapidly strokes forward, forcing the solution through the mixing chamber. The flow is automatically stopped when the springloaded stopping syringe comes to rest against a mechanical stopping block. The reaction occurring in the observation cell is then monitored. Upon completion of the reaction the 3-way slider valve is switched, connecting the spring loaded stopping syringe to the waste and forcing old solution in the stop syringe out the waste port.

The connection of various parts of the system are accomplished by 1/8 inch Teflon tubing (1.5 mm I.D.) with Altex chemically inert tubing end fittings (Altex Scientific Inc., part No. 200-15). The exact dimension and part numbers of both drive syringes and the stopping syringe (constructed by the Michigan State University glass shop) or the drive, air valves and check valves (purchased from outside) are given in the Ph.D. thesis of R. M. Carlson (87). The same author also explains the stopping syringe velocity/position transducer (originally designed by F. J. Holler (91)

mounted on the stop syringe; this device enables the user to determine the position of the stopping syringe plunger at any time during the stopped-flow push.

Figure 3.6 shows a cross-cut view of the stopped-flow mixer and observation cell. The whole cell assembly, except for the Teflon adaptor, is made of a block of stainless steel and was made by the chemistry department machine shop of Michigan State University. Same Altex end fitting is used here for connection. Quartz rods (2 mm) with ground and polished ends (Wilmad Glass co., Inc.) are sealed to the ends of the observation cell and are kept tight by the compression of Teflon washers, rubber o-ring and aluminum compression fitting. These quartz rods also play a role as light pipe and have a tremendous effect on light throughput. The mixer used here is a Notz-type Kel F mixer (92), which is sealed to the observation cell by compression from Teflon mixer adaptor.

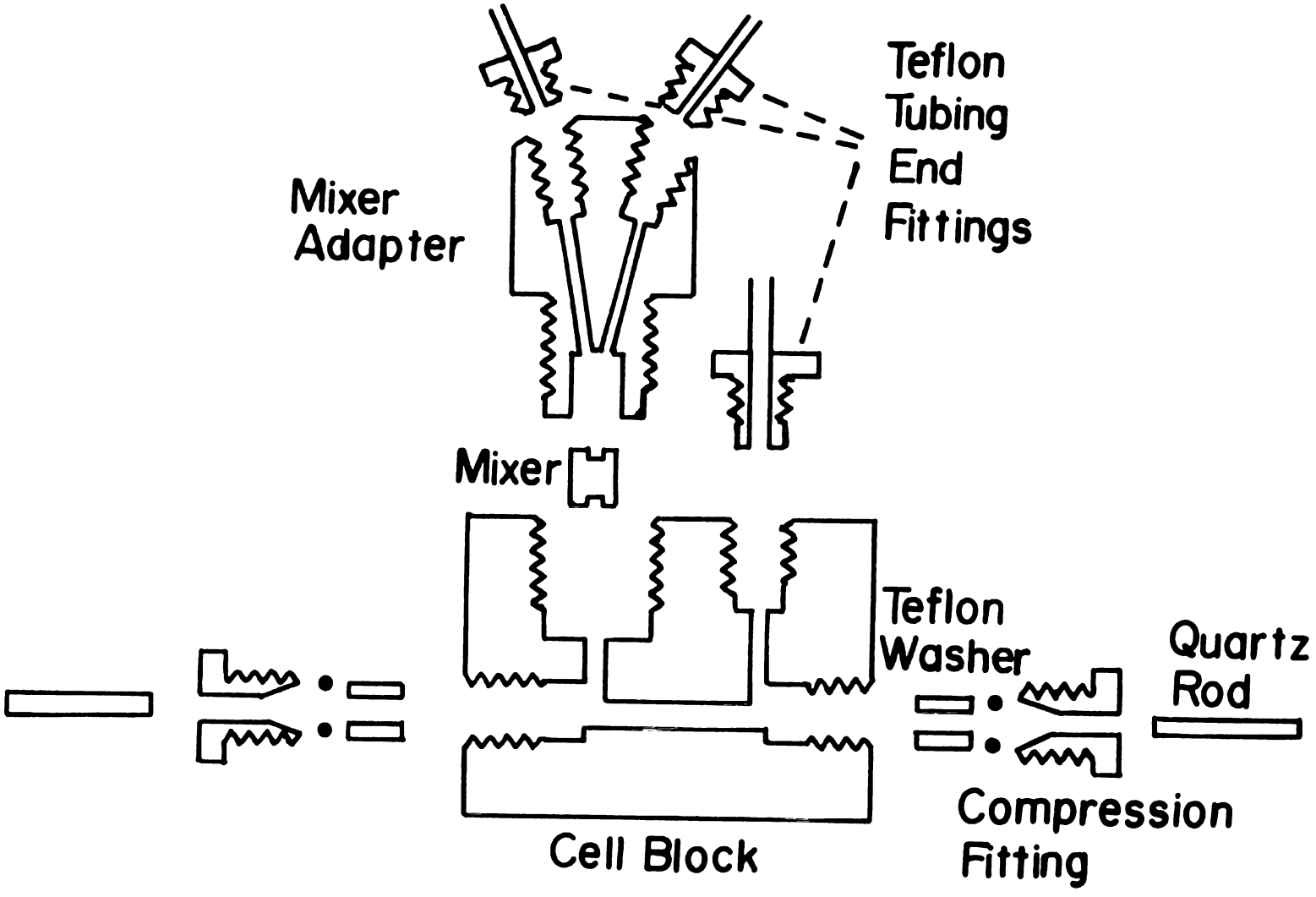

Figure 3.6 Stopped-flow mixer and observation cell (87).

Control Interface

In order to control the overall operation of the rapid scanning stopped-flow diode array spectrometer a digital interface has been built. The circuit block diagram of the interface is shown in Figure 3.7. The digital interface has been designed to provide the following functions:

1. provide a variable integration time for the LDA.
2. provide a variable delay time to allow the user to obtain a spectrum at different times during the reaction.
3. provide proper signals to run the stopped-flow.
4. provide a triggering signal for the storage scope.

The integration part of the interface consists of four presettable 4-bit synchronous binary counters which are cascaded to one another to form a 16-bit integration counter; this can be expanded to any number of bits if desired. The integration time is set by a 16-bit dip switch; once an optimum integration time is set for a specific experiment it need not be changed. The input to the integration counters is a 16 micro second clock pulse from the Reticon board, and the output from integration counters is the START pulse. The start pulse is an input to the Reticon and continuously scan the diode array with a preset integration time. The range of integration times available is from 4 ms up to about 1 min.

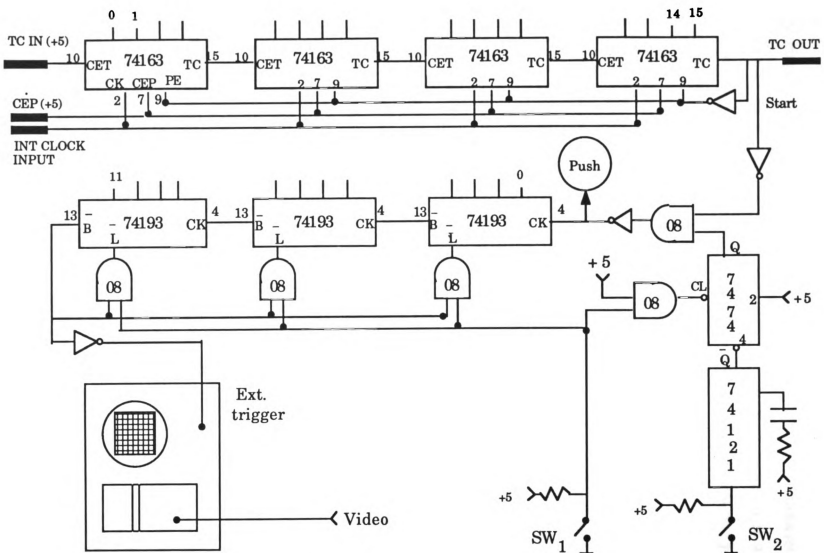

Figure 3.7 Control interface

Another set of three presettable 4-bit down counters are cascaded together to form a 12-bit presettable delay counter. The delay time is actually a multiple of the integration time or, in other words, it is the integration time multiplied by the preset number on the delay counter. Therefore, the delay counter simply counts the preset number of start pulses and then triggers the storage scope to record a spectrum. The operation of the delay counter is controlled by two manual switches. Switch 1 loads the preset delay time from the dip switches into the delay counters, and clears the stopped-flow push flip flop. Now as soon as the push button switch 2 is pushed, it triggers the monostable (MS) which produces a low signal of a few microsecond duration to the preset input of the stopped-flow push F/F. Once the push F/F is set, it enables the delay counters, which after counting the preset number of start pulses, trigger the scope and a spectrum is acquired. In this way one spectrum per push can be obtained and the process must be repeated for multiple spectra. In order to synchronize the time that the scope is triggered and the time that the flow stops for a precise determination of the time, a counter-time-frequency (CTF) card is used as a period meter to measure the time between the push and stop

Determination of the System Dead Time

One of the single most important characteristics of a stopped-flow mixing system is its dead time. The stopped-flow dead time can be defined as the time between the theoretical start of the reaction and the time at which the reaction can be monitored, or it could practically be defined as the time for the solution to flow from the mixer to a point halfway through the

observation cell. The procedure employed here to determine the dead time is known as the extrapolation technique (93). The technique is based on a determination of the amount of the reaction occurring before the first observation is made. To carry out the experiment a 5×10^{-4} M solution of Fe(III) in 0.05 M H_2SO_4 and a 0.02 M solution of KSCN in 0.05 M H_2SO_4 were mixed by the stopped-flow. The spectrum at different times during the reaction was obtained by the diode array spectrophotometer at 8 ms integration time and the course of the reaction was followed at 450 nm. Then the dead time was determined by extrapolating the slope of the absorbance vs time plot back to the initial absorbance of the reaction mixture. The dead time is the time between the intersection of the extrapolated curve with the initial absorbance line and the time of the first observation of the reaction curve. The dead time of the system was determined to be 7.9 + 1 ms.

Determination of Mixing Time

The mixing time of the stopped-flow system was determined by mixing 0.01 M NaOH with 0.01 M p-nitrophenol solution. The spectrum of this very rapid reaction was monitored at different integration times with the diode array spectrophotometer. The oscilloscope was triggered as the plunger of the stopping syringe came to rest against the stopping block. It was observed that the minimum integration time of 2.048 ms a constant spectrum was obtained each time, so it can be stated with certainty that mixing time was complete in less than 2.048 ms.

CHAPTER 4

APPLICATION OF THE DIODE-ARRAY STOPPED FLOW SYSTEM TO THE KINETIC ANALYSES OF BOTH SINGLE AND MULTICOMPONENT SAMPLES

Introduction

There are a number of significant advantages associated with the diode-array spectrometer for qualitative and quantitative analyses of both single and multicomponent samples. Ordinarily, due to its relatively low information content, UV-VIS spectra are rarely used for qualitative analyses. However, the spectral reproducibility advantage of the diode-array permits the identification of for example two compounds with very similar spectra. This is very difficult to achieve with conventional scanning spectrometers. With conventional systems, one can never be sure whether the small differences in the spectra are real differences or only due to the instrument reproducibility errors. Therefore, the confidence on spectral reproducibility offered by the diode-array can certainly extend the application of UV-VIS spectroscopy to qualitative analyses.

The advantages of the diode-array are even more pronounced when applied to quantitative analyses of either single or multicomponent systems. In this regard, one of the major drawbacks of conventional scanning spectrometers is the wavelength resettability and drift problems which affects the precision of measurements. These problems become

continuously more serious as the mechanical linkages wear. This forces the analyst to perform all of his/her analyses at the wavelength of maximum absorption where the wavelength resettability error is at its minimum. This is despite the fact that the wavelength of maximum absorption may not be the optimum wavelength for reason of for instance selectivity. Since there are no moving parts involved in scanning a spectrum with a diode-array, the above problems are not present in such systems. The availability of the entire spectrum, virtually free of wavelength resettability errors, allows the analyst to choose the optimum wavelength for improved sensitivity, selectivity and dynamic range. Measurements at any wavelength, peak maxima or on the side of the absorption band, can be made with essentially the same accuracy and precision.

The combination of simultaneous multiwavelength detection and the wavelength resettability advantage offers a number of other benefits to the analyst for the improvement of sensitivity and dynamic range. For instance, one can compensate for source fluctuations by performing simultaneous measurements at the analytical wavelength and a second wavelength in close proximity of the analytical wavelength where there is no absorption. This is very important for situations where measurements are made at low absorption. Notice that this is, in essence, a pseudo dual-beam operation without the complexity associated with such an optical design. Conventional scanning systems does not allow for such operations, since different wavelengths are measured at different times.

Another important benefit comes from the fact that stray light is less of a practical problem with diode-array instruments which leads to an extension of dynamic range. An extension of the dynamic range at the upper concentration range may be achieved by measuring strongly absorbing samples at the side of an absorption band, where absorbance is lower compared to the band maximum. At low absorption end, the dynamic range can be stretched further with the diode-array due to higher light throughput (fewer optical surfaces than conventional instruments), and lower noise level.

Moreover, a diode-array equipped with a computer and appropriate software is capable of reducing the noise even further through the use of two noise reduction techniques known as time and wavelength averaging. For example, if one desires to obtain a full spectrum over the range of 200 to 1000 nm at 2 nm intervals, one has to make 401 measurements. Assuming each data point takes one second, a conventional scanning system will require 401 seconds to collect the full spectrum. The diode-array instrument on the other hand, measures all data points simultaneously and, therefore, can generate the full spectrum in one second. In fact, the diode-array can collect and average several spectra in one second (time averaging). This will reduce the noise level by a factor of the square-root of the number of spectra averaged together. Consequently, improved signal-to-noise and hence sensitivity is achieved.

The second noise reduction technique (wavelength averaging) stems from the multiwavelength measurement capability of the diode-array. Instead of quantitative measurements at only one wavelength (e.g., wavelength of

maximum absorption), one can measure several data points on either side of the maximum in the same time and average them together. This will again result in improved signal-to-noise and in turn sensitivity. However, for a given absorption bandwidth, there will be a limit as to how many data points can be averaged to give an optimum signal-to-noise. As more data points are included, the average absorbance is reduced which has a negative effect on the signal.

It should be pointed out that it is possible to do both time and wavelength averaging with a conventional scanning spectrophotometer. However, the required time is considerably longer which makes it more susceptible to drift errors. One may also perform wavelength averaging by widening the slit-width in a conventional system, but then the linearity is seriously affected.

It can be concluded from the above discussion that the diode-array spectrophotometer is clearly superior to conventional systems in all applications where speed and full spectrum acquisition is of major concern. Undoubtedly, the speed of diode-array data acquisition makes it a clear choice both for kinetic analyses and for fundamental kinetic studies. The diode-array spectrometer in combination with the stopped-flow, as a rapid mixing technique, can further expand the horizon of the instrument to the study of those reactions which occurs in a very short time scale.

This chapter describes the application of the developed system to the kinetic analyses of some clinically significant species. In fact, many clinically important processes, in addition to being in a complex media, also occur at

a moderately fast rate. Therefore, the diode-array stopped-flow spectrometer appears to be well suited for the analysis of such samples. The kinetic determination of total serum protein is studied as an example of single component sample followed by the simultaneous kinetic analysis of glucose and alcohol in blood serum as a representative case of multicomponent system.

DETERMINATION OF TOTAL SERUM PROTEIN BY BIURET METHOD

Background

One of the most significant clinical test often performed in any clinical laboratory is the determination of total blood serum protein. The evaluation of the result of the test is normally used to decide whether further analysis of subfractions of protein is necessary. Among many methods available for determination of blood serum protein, the biuret method is one of the most widely used procedure. This is because the method has been shown (94) to be least affected by variation in protein composition. The sensitivity of the method , although not as good as some other ones, but has been evaluated (94) as sensitive enough.

The principle of the biuret method is based on the fact that all protein contain a large number of peptide bonds. When a solution of protein is treated with cupric (Cu^{+2}) ions in a moderately alkaline medium, a colored chelate complex of unknown composition is formed. The reaction takes place between the carbonyl (- C = O) and imine (= N - H) groups of the peptide bonds of the protein and cupric ions. It turns out, that the organic compound biuret (H_2N - CO - NH - CO - NH_2) also undergoes similar type of process with cupric ions and, therefore, the reaction is referred to as biuret reaction (Figure 4.1).

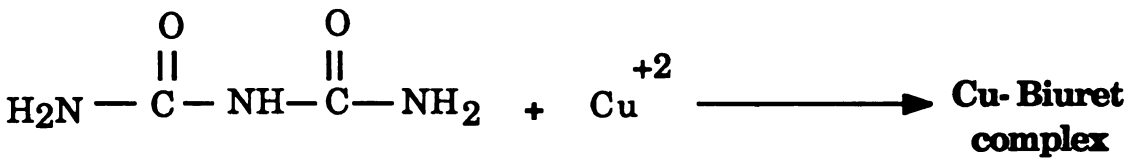

Buiret **(Blue)**

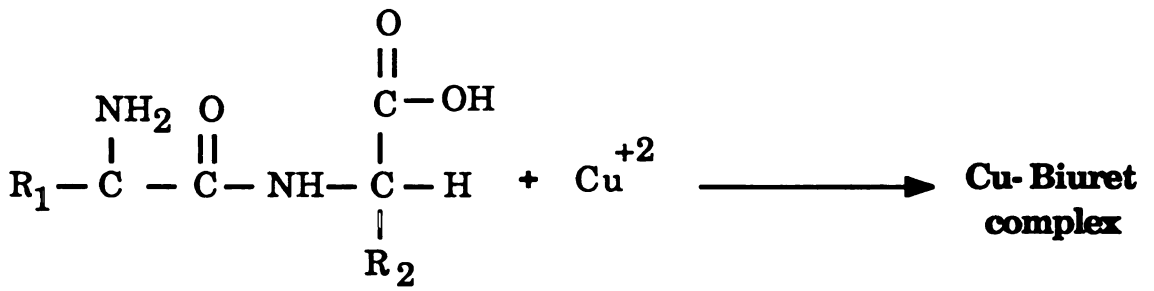

Protein **(Blue)**

Figure 4.1 The buiret reaction

The reaction appears to take place between the cupric (Cu^{+2}) ions and any compound containing at least two H_2N - CO - , H_2N - NH_2 - , H_2N - CS - , and similar groups directly joined together or through a carbon or nitrogen atom. However, aminoacids and dipeptides do not undergo this reaction, but tri- and polypeptides and proteins react to produce a pink to reddish violet color product.

The biuret method was first introduced by Kingsley (95) in 1939. Since then, there have been many modifications to the method (94,96). In a typical procedure the blood serum or solution of standard protein are mixed with biuret reagent and the absorbance is measured after 30 minutes waiting period for the equilibrium to be established. Certainly, this rather long waiting period (30 min.) is the main disadvantage of the equilibrium methods. In an effort to shorten the analysis time , many investigators have been working toward the applicability of various reaction-rate methods to the determination of total serum protein by biuret method (94,96).

Hatcher and Anderson (97) were the first to describe the determination of serum total protein with the fast analyzer. However, according to Koch and coworkers (94) , " they did not study many samples from patients nor did they discuss the characteristics and requirements of the kinetic approach". Koch, Johnson, and Chilcote (94) employed a fixed time kinetic approach using the "Centrifichem" centrifugal analyzer. Although fixed time kinetic analysis is limited to those substances undergoing a first order (or pseudo-first order) reactions (98-99), they did not find biuret reaction to follow a simple first order kinetics. Nevertheless, they found it suitable for fixed

time kinetic analysis and described their method as being rapid, accurate, and reasonably precise. But, Savory and coworkers (96) suggested that the method was found to be relatively imprecise in their hand and subject to errors in analyses of sera from patients with dysproteinemias.

In an attempt to develop a more precise and rapid rate method, Wai-Tak-Law and Crouch (100) examined the biuret method using stopped-flow mixing system. In agreement with previous investigators, they also found that the biuret reaction did not follow a first order or pseudo-first order kinetics. They, nevertheless, pointed out that the reaction is still suitable for the two point fixed time reaction rate approach. They, in fact, indicated that one is able to obtain an analytical curve long before the reaction is over. They performed experiments both with 0.1 second and 10 seconds time interval and because of the rapidity of biuret reaction, found that the 10 seconds time interval gave more precise results with standard deviation of 1.4 %.

As a test of our system's performance, we decided to carry out the analysis of serum total protein by biuret method using the linear diode-array stopped-flow spectrometer.

Kinetic Determination of Total Protein in Blood Serum by Linear Diode-Array Stopped-Flow System

As pointed out in the previous section, this experiment was chosen to demonstrate the ease and flexibility with which single component analysis can be accomplished with the diode-array stopped-flow instrument. There are several major advantages which becomes immediately apparent to the analyst as the system is applied to situations such as the one studied here. The stopped-flow mixing system facilitates the achievements of an extremely short analysis time. It also demands a very small sample volume. The rapid acquisition of the entire spectrum with the diode-array, not only satisfies the requirement of the stopped-flow, but also displays the spectrum instantly for the analyst 's visual inspection. An appropriate optimum wavelength for the analysis may be selected at a glance. This relieves the analyst from having to have preknowledge of the analysis wavelength. Multiple spectra can be acquired by multiple push of the stopped flow system.

Based on Wai-Tak-Law and Crouch observations, it was decided that two point fixed time reaction rate method be employed and the Δt of 8 seconds was chosen as a good compromise between precision and analysis time. It should be pointed out, that since the system can acquire data almost instantaneously after mixing, it could provide for more exact definition of blank and, therefore, improvement in precision over other rate methods using two point fixed time approach.

The reagents and solutions used for the experiment were as follows:

Biuret reagent: This reagent contains cupric sulfate (2.4 g L^{-1}) , sodium potassium tartarate (8 g L^{-1}) , sodium hydroxide (48 g L^{-1}) , and potassium iodide (1.0 g L^{-1}).

Standards: The human serum protein standards (Dade Division, American Hospital Supply Corp., Miami, FL 33152 ; Cat. No. B5158) were diluted to proper concentrations in saline solution (NaCl, 9 g L^{-1}).

Quality Control Sera: Lyophilized control serum samples (Moni-trol I, Cat. No. B5103 ; Moni-trol II, Cat. No. B5113 ; Patho-trol, Cat. No. B5110 ; Dade Division, American Hospital Supply Corp., Miami, FL 33152) were reconstituted according to manufacturer's instructions and diluted to proper concentrations.

All protein solutions were prepared fresh from vacuum sealed prepackaged bottles which were stored at 2 - 8 ^{o} C. The biuret reagent was kept in dark place in plastic bottles.

Figure 4.2 shows the calibration curve for serum protein standards using the two point fixed time (Δt = 8 s) reaction rate analysis. The 0% T was recorded with the light source blocked. A spectrum was then recorded (first push) with the diode array integration time set at 8 ms and was treated as a blank avoiding the need for running a separate blank. The integration time was then changed to 8 seconds and a second spectrum was recorded (second push) . The difference in absorbance (ΔA) was used in

the standard curve. The standards concentration range along with the statistics of the standard curve is shown in table 4.1.

The statistical calculations were based on the assumption that measurement precision is determined by the standard deviation(σ_T) in the measurement of Transmittance (T) which is constant and independent of the magnitude of Transmittance. This is due to the fact that a fixed stopped flow cell was used for all measurements which leads to a negligible contribution of random error due to cell positioning. Also, the photon detector shot noise is negligible compared to the somewhat limited resolution of the readout system (oscilloscope). Under these conditions (%T noise-limited), the following equation was used (101) for error calculations.

$$\frac{\sigma c}{C} = \frac{0.434}{\log T} \times \frac{\sigma T}{T}$$

Three replicate measurements of each standard solution were overlaid and the thickness of the scope trace were used as a measure of precision. A

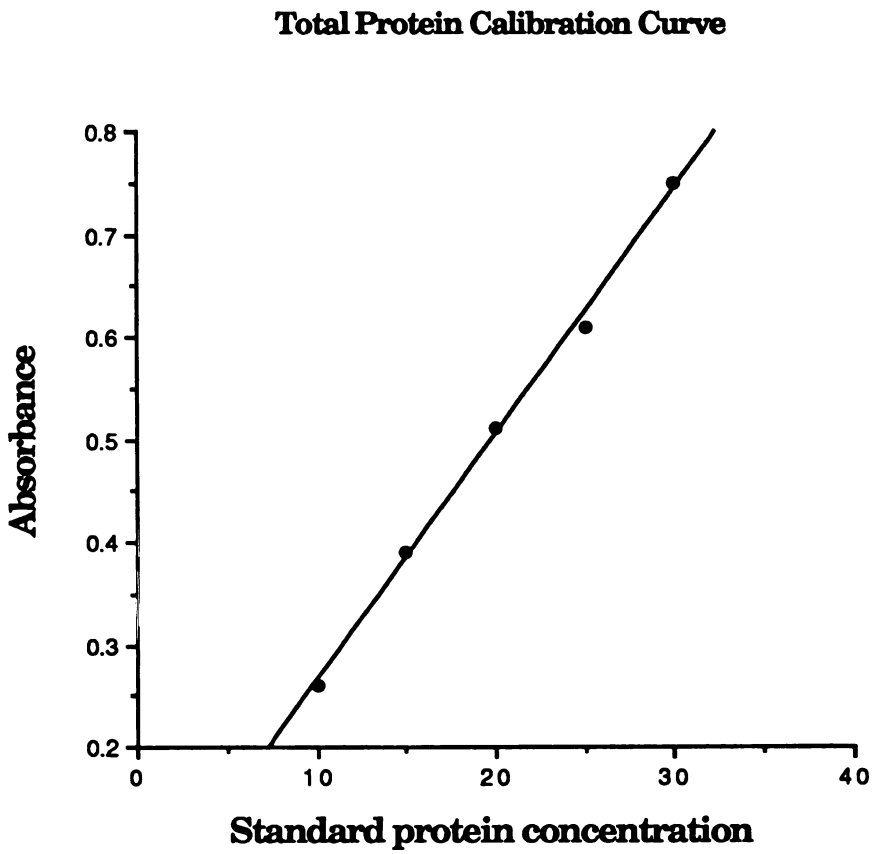

Figure 4.2 Calibration curve for total serum protein

Table 4.1 Results for standard solutions of serum protein (Δt = 8 s)

Protein concentration (g/L)	Absorbance (A average)	RSD (%)
10	0.26	1.5
15	0.39	1.4
20	0.51	1.4
25	0.61	1.5
30	0.75	1.6
Slope	= 2.40×10^{-2}	A g^{-1} L
Intercept	= 2.40×10^{-2}	A
Correlation coefficient	=0.998	

typical standard deviation of $\pm$ 0.005 T was found in the measurement of %T which turns the above equation into:

$$\frac{\sigma c}{C} = \frac{0.434}{\log T} \times \frac{0.005}{T}$$

which was used for the calculation of relative standard deviations.

The standard curve is linear over the range of standards concentration with the correlation coefficient of 0.998. The maximum relative standard deviation obtained was 1.6 %, which is slightly greater than that obtained by Wai-Tak-Law and Crouch (100).

To experiment with real serum sample, three lyophilized sera (Moni-trol I, Moni-trol II, and Patho-trol) were analyzed as controls. Assigned values of total protein for these sera based on the analyses with well-established methods are given by the manufacturer.

The results obtained for these sera with diode array stopped-flow system utilizing fixed-time rate method is presented in table 4.2. The results reported by three other methods namely improved biuret (equilibrium method), centrifichem (rate method), and the PMT-based stopped-flow (fixed-time rate method) of Crouch et.al. are also listed for comparison.

Table 4.2 Results of determination of Total protein in real human serum

	Reported values		Measured values
	Mean (g/dL)	Range	(Δt = 8 s)
Moni-trol I			
method 1	7.0 ± 0.06	6.7 - 7.2	
method 2	6.5 ± 0.35	5.8 - 7.2	7.0 ± 0.09
method 3	6.79 ± 0.01		
Moni-trol II			
method 1	5.3 ± 0.07	5.0 - 5.6	
method 2	4.5 ± 0.05	4.2 - 4.8	4.5 ± 0.07
method 3	5.14 ± 0.04		
Patho-trol			
method 1	5.3 ± 0.12	5.0 - 5.6	
method 3	5.85 ± 0.08		5.31 ± 0.08

Method 1 : Improved biuret (equilibrium method)
Method 2 : Centrifichem (rate method)
Method 3 : PMT-based stopped flow (fixed-time rate method)

The data in table 4.2 shows that the results obtained for the analysis of Moni-trol I and Patho-trol are in good agreement with those of both the improved biuret and the PMT-based stopped-flow methods, while the results for Moni-trol II is more closer to that reported by centrifichem method. Nevertheless, the results for all three samples are well within the acceptable range given by the manufacturer.

Based on the overall results of the experiment, it can be concluded that not only it is possible to carry out single component reaction rate analysis with the LDA-stopped flow system, but one can perform such analyses with far greater speed, flexibility, and convenience compared to instruments with single channel detection. However, the real power of the LDA-stopped flow spectrometer can be realized when applied to multicomponent systems. This is demonstrated in the next section.

SIMULTANEOUS KINETIC DETERMINATION OF GLUCOSE AND ETHANOL IN BLOOD SERUM

Introduction

Optical spectroscopy in the UV-VIS region accounts for a large portion of all analyses performed in a modern clinical laboratory. However, most spectrophotometers used in clinical laboratories are based on a design concept in which a single resolution element is isolated by a filter or some type of a dispersion optics and slit combination, and its intensity is subsequently monitored by a photoelectric detector. With such instruments, time consuming separation is usually required before the measurement step to separate the analyte from other species that absorb in the analytical bandpass. Because most biological samples are complex matrices, it would be advantageous in many situations to determine multiple components without a complete separation step. This, in principle, requires the ability to monitor multiple wavelengths simultaneously. The use of conventional rapid scanning instruments that require several minutes for the acquisition of each complete spectrum, can only offer a slight advantage over todays fast separation techniques.

Optoelectronic image devices such as diode array, on the other hand, are capable of collecting the entire spectrum in millisecond time scale and with repetition rates approaching 1000 spectra per second. This kind of speed is, by no means, matched by any of the existing separation technologies. The

extremely short time required for a complete scan with the diode array, is well below the time scale for most clinically important reactions to reach equilibrium. This makes the diode array spectrometer well suited for multicomponent kinetic analyses in a clinical laboratories. A brief history of the application of kinetic methods in clinical chemistry may be appropriate at this point.

Clinical chemists have long been interested in kinetic methods of analysis. The main reason for the popularity of kinetic methods among clinical chemists is the extensive application of enzymes in the diagnosis of diseases. In fact, enzyme activity determinations constitutes a major workload of a typical clinical laboratory. The main advantage of enzymes as analytical reagents is their specificity in catalyzing many complex chemical reactions ocurring in biological media. Since enzymes affects the kinetics of reactions, reaction rate methods have been used for a long time for the determination of substrates, activators, inhibitors, and also of enzyme themselves.

However, prior to 1960's the use of enzymes for analytical purposes has been rather limited. This has been mainly due to some disadvantages attributed to the use of enzymes such as unavailability, instability, poor precision, considerable time and labor required for the analyses. While these objections were quite valid earlier, numerous enzymes are now available in purified form, with high specific activity, at reasonable prices. With recognition of the enzyme instability and adoption of appropriate precautions, this potential problem can be minimized. The burden of using large amounts of expensive enzymes for routine analytical purposes has

also been somewhat alleviated by the development of immobolized enzyme techniques which allows continuous use of the enzyme for a relatively long period of time.

The question of poor precision, time and labor demand that have in the past made enzymatic kinetic methods of analysis undesirable, have been more a consequence of the experimental techniques and instrumentation than the inherent fault of enzymes or kinetic approach. Techniques and instrumentation originally developed for equilibrium methods were being used for kinetic analysis. Kinetic methods are inherently time dependent and highly sensitive to experimental variables. Equilibrium based instruments are not essentially equipped with means of accurate time measurements, temperature control, or adequate detector sensitivity or stability for monitoring small signal changes in kinetic analysis.

During the 1960's, several investigators (102-104) began to address the issue of designing appropriate instrumentation explicitly for kinetic methods. As pointed out by H. L. Pardue (105) : "the turning point for kinetic approach as a viable tool for high quality, fast, routine analyses occurred during the 1960's when a few workers focused a concentrated effort on the development of instrumentation and techniques designed explicitly for kinetic applications". During this same period and throughout 1970's, many other developments such as rapid mixing techniques, temperature control reaction cells, various analytical kinetic methodologies, and finally automation of most stages of measurement process such as sample introduction, data acquisition and processing has contributed tremendously to the maturity and acceptance of kinetic methods of

analysis. It was clearly demonstrated during this period that rate methods of analysis could be performed with speed, reliability and simplicity compared to that of most common equilibrium methods. These developments have been the subject of several texts (106-107) and reviews (108-112).

Until recently, however, the most frequent application of rate methods of analysis in clinical laboratories has been through the utilization of catalyzed reactions for the determination of single species using photometers or spectrophotometers with single channel detection. The introduction of multichannel spectrometers and their applications to a few clinical problems (113-115) in the mid to late 1970's, provided a whole new opportunities to the modern clinical chemist. When applied to clinical chemistry an array detector capable of monitoring hundreds of resolution elements simultaneously can offer several significant advantages. In addition to handling single channel equilibrium and kinetic measurements often performed with conventional systems, these instruments can also provide fast repetitive scans of optical spectra, with little or no extra effort on the part of the operator. these instruments allows for rapid and simple means of equilibrium and kinetic multicomponent analysis of complex biological samples as well as fundamental kinetic studies of clinically significant reactions. A properly designed multichannel spectrometer for clinical applications can, in effect, replace an otherwise several other instruments and, therefore, bring about a tremendous saving in the cost of equipment and personnel training.

Despite the obvious benefits of these devices, however, clinical chemists have been very slow in taking full advantage of these new developments and the application of array detectors for multicomponent clinical analysis have been quite limited. In the next section, the application of the diode array stopped-flow system to simultaneous analysis of glucose and ethanol in blood serum using enzyme catalyzed reactions is described.

Simultaneous Kinetic determinations of Glucose and Ethanol in Blood Serum

The primary objective in this work was to demonstrate the capabilities of the diode array stopped-flow system for multicomponent analysis using enzyme-catalyzed reaction rate method. Therefore, the determination of glucose and ethyl alcohol in blood serum was undertaken because established reaction rate procedures are available for each species. Some modifications to these procedures were necessary to allow for simultaneous determination of both glucose and alcohol in a blood serum sample.

The determination of both glucose and ethanol in blood serum are procedures most frequently performed in hospital chemistry laboratories. The glucose determination is often done as an aid in the diagnosis and treatment of diabetes. Early detection of diabetes allows for delay or minimization of the complications of the disease. The blood glucose level can fall below normal as a result of either overproduction or excess administration of insulin. In sever cases, the resulting extreme hypoglycemia causes muscular spasm and loss of consciousness known as

insulin shock. Therefore, it is important for a clinical laboratory to use methods which can furnish the results of glucose analysis rapidly and with high degree of reliability.

Enzymatic methods have been used very frequently for the specific determination of glucose in biological samples. One of the common procedure involves the oxidation of glucose with glucose oxidase, forming hydrogen peroxide, which in turn oxidizes a chromogenic oxygen acceptor such as o-dianisidine in presence of horse raddish peroxidase to form a colored product proportional to the glucose concentration (116-118). The measurement of absorbance is made after a long time waiting period required for the reaction to reach equilibrium.

Based upon the above enzymatic reaction, Malmstadt and Hicks (119) described a rate method which gives quantitative data within the first few minutes of the reaction by an automated spectrophotometeric system. This method avoids the waiting period for the establishment of equilibrium and greatly reduces the total analysis time. A potentiometric kinetic method for the analysis of aqueous glucose samples in which the hydrogen peroxide formed in the oxidation of glucose reacts with excess iodide, in the presence of molybdate catalyst, to form an equivalent amount of iodine has also been described by Malmstadt and Pardue (120). This method is rapid, precise, sensitive, and has the advantage of substituting molybdate catalyst in place of the expensive peroxidase enzyme. The above same chemical system has been employed by Malmstadt and Hadjiioannou (121) except that the rate of iodine formation been monitored by an automatic spectrophotometric system measuring the time required for a fixed absorbance change. They

obtained within 2 % precision for measurements on samples containing 0.08 mL of serum, plasma, or blood.

Most of the interest in the determination of ethanol in blood arises from the fact that it is the most frequent toxic substance encountered in medico-legal cases. Not only it is lethal by itself, but it is most often a significant contributor to accidents of all types. Every time that a patient is brought to a hospital in coma, a differential diagnosis of the cause of coma is performed in which the effect of alcohol must be first ruled out. This, of course, demands for a rapid and precise method of alcohol determination in biological fluids. As a result, more analytical methods have been developed for the determination of alcohol than for any other toxic substances.

Many of the chemical methods are based on the measurement of the oxidant required for the stoichiometric oxidation of ethanol. The most commonly used oxidant is dichromate in sufuric acid (122), but permanganate, vanadium pentoxide, and osmic acid have also been used (123). The major problem of the oxidation methods is their lack of specificity and, therefore, the necessity to eliminate materials such as acids, bases, aldehydes, ketones and alcohols prior to oxidation using various time consuming separation techniques (124).

Enzymatic methods (125-126), on the other hand, allows for high specificity without separation. The usual enzymatic methods are based on the use of the enzyme alcohol dehydrogenase (ADH) to catalyze the reaction between ethanol and diphosphopyridine nucleotide (DPN). A typical 60 - 90 minutes waiting period is required before the absorbance of DPNH (reduced form of

DPN) in measured at the wavelength of 340 nm. In an attempt to develop a faster method, Malmstadt and Hadjiioannou (127) applied the rapid spectrophotometric reaction rate method previously developed for the determination of glucose (128) to the determination of ethanol in blood. They measured the time required for the fixed absorbance change and were able to determine blood alcohol concentrations in the range of 0.015 to o.3 with relative errors of about 2 to 3 %.

To demonstrate the capability of the diode array- stopped flow system for multicomponent kinetic analyses, the simultaneous determination of glucose and ethanol in blood serum using enzyme catalyzed reactions was carried out. The reaction chosen for glucose involves the oxidation of glucose by glucose oxidase to form hydrogen peroxide. The hydrogen peroxide then reacts with o-dianisidine in presence of peroxidase to produce the oxidized form of o-dianisidine which absorbs at 540 nm. The procedure for ethanol was essentially based on the method used by Malmstadt and Hadjiioannou (127) which involves the use of enzyme alcohol dehydrogenase. As part of this reaction, DPN+ is converted to DPNH which absorbs light at 350 nm. These two reactions are shown in figure 4.2.

GLUCOSE

$$\text{Glucose} + O_2 + H_2O \xrightarrow{\text{Glucose oxidase}} \text{Gluconic acid} + H_2O_2$$

$$\text{o-dianisidine} + H_2O_2 \xrightarrow{\text{peroxidase}} \underset{\text{o-dianisidine}}{\text{Oxidized}} + H_2O$$

(color)

$\lambda_{max} = 540$ nm

ETHANOL

$$CH_3CH_2OH + DPN^+ \xrightarrow{\text{ADH}} CH_3CHO + DPNH + H^+$$

(color)

$\lambda_{max} = 350$ nm

Figure 4.3 Enzymatic reactions of glucose and ethanol

The reagents used are as follows:

1. Deproteinization reagents

a) Barium hydroxide ($Ba(OH)_2 . 8 H_2O$), 1.8 % solution in water. This solution was let stand for two days, then decanted and stored in a bottle.

b) Zinc sulfate ($ZnSO_4 . 7H_2O$), 2 % solution in water. This solution was balanced against barium hydroxide so that 5.00 mL of barium hydroxide is equivalent to 5.00 mL of zinc sulfate solution.

2. Buffer solution, pH 6.8

The KH_2PO_4/K_2HPO_4 conjugate pair was used to which 4.0 g of semicarbazide hydrochloride was added and the P^H was adjusted to 6.8 using a pH-meter. This solution is stable indefinitely.

3. Glucose oxidase

The enzyme packaged mixture (Worthington Biochemical Corp., Freehold, N.J. 07728) was used. A small package contains 10 mg of o-dianisidine and a larger package contains about 125 mg of glucose oxidase and 5 mg of peroxidase. The soluble o-dianisidine was completely dissolved in 1.0 mL of distilled water and drained into an amber bottle. The glucose oxidase and peroxidase mixture was dissolved in, and diluted to 100 mL with the buffer solution. This solution was added to the amber bottle and stored in the refrigerator. The solution is stable for about a month.

4. Alcohol dehydrogenase (ADH

Yeast ADH (from Worthington Biochemical Corp) was dissolved in the buffer solution, just before use and kept in ice bath during use.

5. Coenzyme DPN (diphosphopyridine nucleotide)

This solution was prepared just before use by dissolving 0.33 mg of DPN from Sigma Chemical Co. per one mL of the buffer solution and kept refrigerated when not in use.

6. Glucose standards

Stock standard glucose solution of 1.0 g/100 mL was made by dissolving 1.000 of dry reagent grade glucose in benzoic acid (2 g/L) and diluting to 100 mL with benzoic acid. This solution is stable indefinitely if kept refrigerated when not in use. Working standards were made from this solution with proper dilutions.

7. Ethanol standards

A 300 ppm stock ethanol solution was made from anhydrous ethanol. Working standards were prepared from this solution with proper dilutions.

Using the photodiode array stopped-flow system, two separate calibration curves were initially established for glucose and ethanol employing the fixed-time (Δt = 8 s) reaction rate approach similar to that explained in the analysis of total protein. This was done by preparing a composite solution composed of both enzymes (glucose oxidase and ADH), coenzyme DPN in

the buffer solution. Prior to the analysis, all solutions were kept separate because the composite solution of ADH and DPN is unstable at room temperature. The ADH was kept in an ice bath during use. The buffer solution was placed in a 37 °C water bath and the other solutions were separately added and allowed to warm up for a few minutes just before the analysis. The composite solution was adjusted to contain 1.25 mg/mL glucose oxidase and 1.5 mg/mL ADH. These values are reported as appropriate values (127-128) to provide satisfactory enzyme activity for the range of concentrations used for the standard solutions in this experiment.

The second solution consisted of either glucose or ethanol standards in buffer solution for preparation of their respective calibration curve. This solution was also allowed to warm up in the 37 oC water bath prior to the analysis. Under the above selected conditions (substrate and enzyme concentrations), both reactions follow first order kinetics and the absorbance change (ΔA) measured near the start of the reactions is proportional to initial concentration of the substrates. Also, the materials present in glucose oxidase, ADH and DPN which may absorb light at analyses wavelengths do not pose a serious problem since absolute absorbances are not measured. The possibility of side reactions is also very remote as the measurements are completed during the early part of the reactions.

However, in addition to enzymes and substrates concentrations the measured absorbance change is also affected by experimental variables such as pH and temperature. As was described earlier, every efforts were made to minimize the effect of temperature variations, but some degree of

temperature fluctuation will still be present since the system was not thermostated. The question of pH is a more difficult one since the procedure used for glucose is normally carried out at neutral to slightly acidic pH (~6.8 - 7.0), while that of ethanol is usually done at moderately alkaline pH (~8.7). This is because the second step in the glucose procedure (involving peroxidaes) is less specific and at pH values above neutral, various substances such as uric acid, ascorbic acid, and bilirubin compete with o-dianisidine for hydrogen peroxide (129). In the case of ethanol, a very small fraction of alcohol (1-10%) is consumed (127) during the measurement period and buffering at high pH values can drive the reaction more to the right.

The buffer solution used in this experiment (pH = 6.8) was in fact optimized for glucose, while the addition of semicarbazide hydrochloride to the buffer solution was intended to drive the ethanol reaction to the right by reacting with aldehyde as it is formed. Figure 4.2 and 4.3 show the calibration curves for glucose and ethanol respectively, and table 4.2 and 4.3 list their corresponding standards concentration range and statistics.

As can be seen, both calibration curves which are obtained by plotting ΔA against the standards concentrations are quite linear. Neither of which, however pass through zero because of the certain amount of glucose or alcohol which is consumed before the measurements are completed.

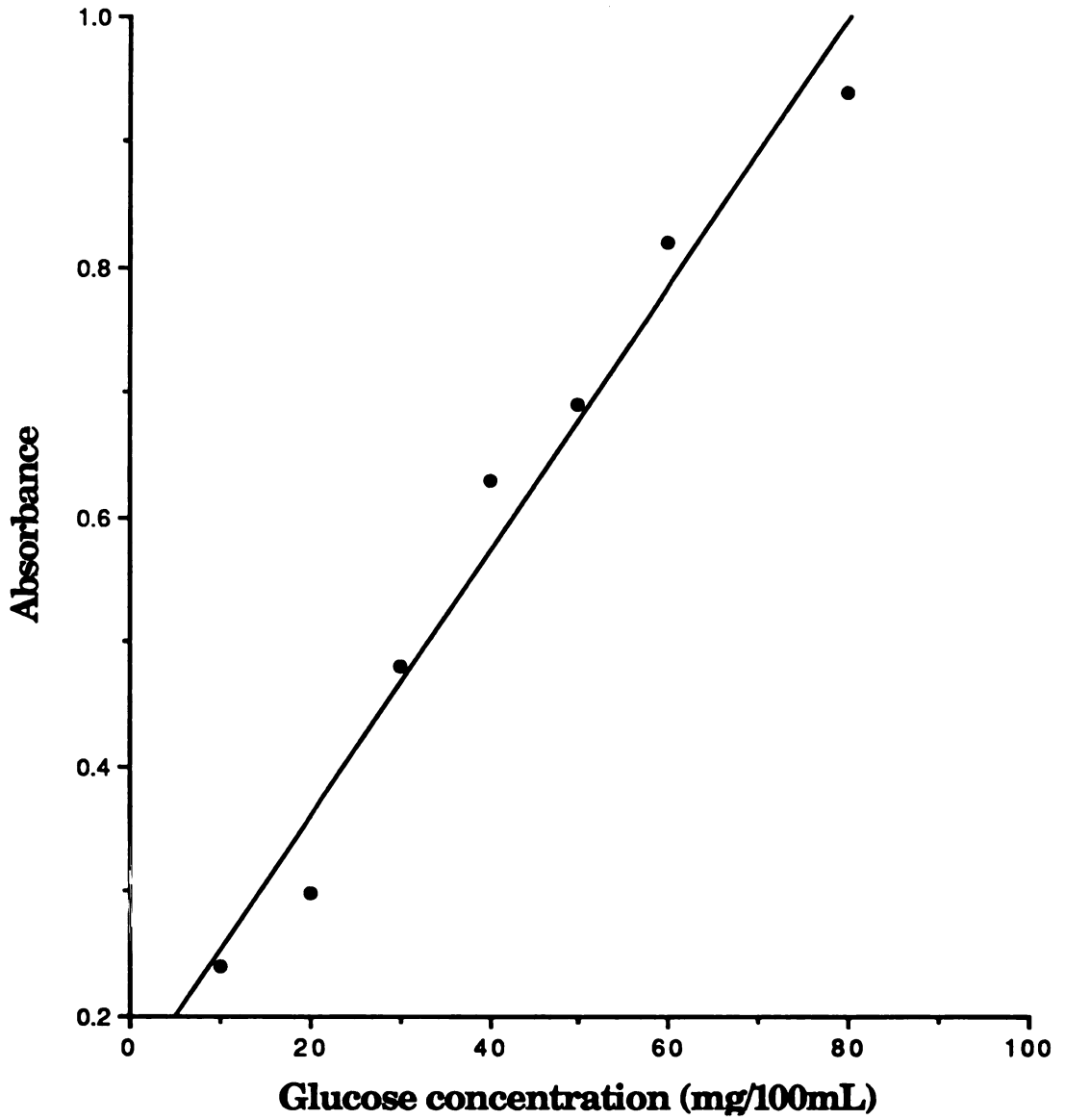

Figure 4.4 Calibration curve for glucose

Table 4.3 Results for standard solutions of glucose ($\Delta t = 8$ s)

Glucose concentration (mg/100 mL)	Absorbance (ΔA, average)	RSD (%)
10	0.24	1.5
20	0.30	1.5
30	0.48	1.4
40	0.63	1.5
50	0.69	1.6
60	0.82	1.6
80	0.94	1.7

Slope = 1.06 x 10-2 $A\,g^{-1}\,L$

Intercept = 0.145 A

Correlation Coeff. = 0.971

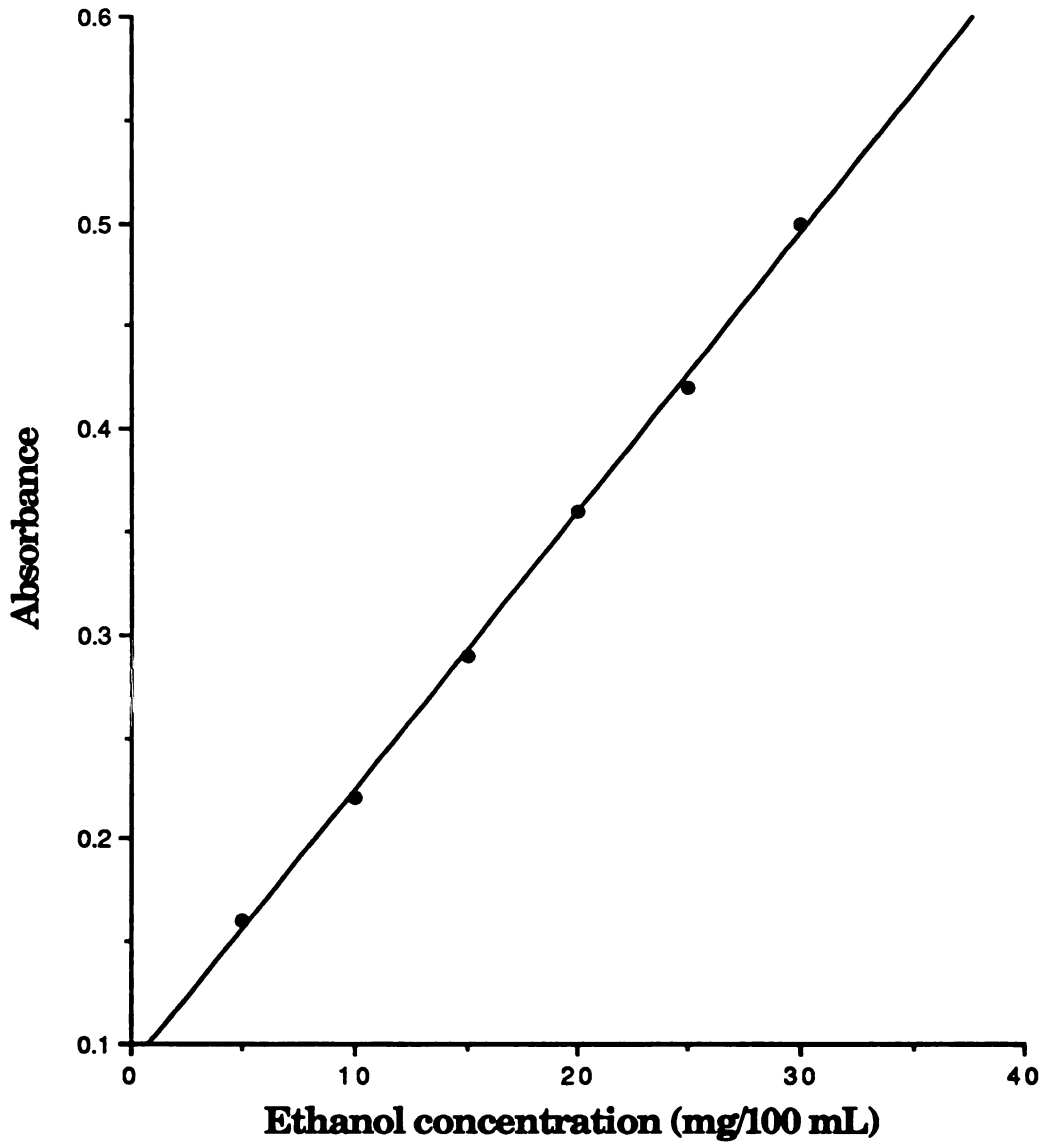

Figure 4.5 Calibration curve for ethanol

Table 4.4 Results for standard solutions of ethanol ($\Delta t = 8$ s)

Ethanol concentration (mg/100 mL)	Absorbance (ΔA, average)	RSD (%)
5	0.16	1.6
10	0.22	1.6
15	0.29	1.5
20	0.36	1.4
25	0.42	1.4
30	0.50	1.4

Slope = 1.35×10^{-2} A g^{-1} L

Intercept = 8.80×10^{-2} A

Correlation coeff. = 0.999

To carry out the simultaneous determination of both glucose and ethanol in real blood serum, a sample of human blood serum was acquired from Sparrow Hospital in Lansing, Michigan. The sample was a pooled blood serum over a large human population. .Therefore, its glucose content was expected to be in the average of the normal range. As for ethanol, normal blood serums are free from alcohol and a known amount of ethanol had to be added to the serum. Thus, after deproteinization of the blood serum sample with barium hydroxide and zinc sulfate solutions, it was diluted with ethanol solution to contain 60 mg of ethanol per 100 mL of blood serum.

Three replicate measurements ($\Delta t = 8$ s) of the blood serum sample were made (by a procedure similar to those of the standards) and the concentrations of glucose and ethanol were determined from the calibration curves. The average values determined for the concentrations of glucose and ethanol were 91 mg/100 mL and 51 mg/100 mL of blood serum, respectively. The relative standard deviations of the measurements were on the order of 6.8%. The normal value for glucose concentration in blood serum is in the range of 70 - 105 mg/100 mL (129) and, as expected, the value determined for glucose is well within this range.

However, the results of ethanol analysis is more than 15% at error. This may be explained by considering several experimental factors which were not favorable for ethanol determination. One factor which was previously mentioned is that of low pH (6.8) which can further reduce an already small fraction of ethanol which reacts during the measurement time. Secondly, the light source which was used (quartz halogen) has a very low photon flux at wavelengths below 400 nm. Both of these factors can lead to low S/N

ratio for ethanol. Small amount of ethanol could have also been lost by evaporation during the measurement period, particularly during the warm up period at 37 ° C. All of these factors could have contributed to the low value obtained for ethanol.

Also note that the measurement precision (RSD of 6.8%) for simultaneous determination of glucose and ethanol is only fair. Obviously, it is possible to improve the measurement precision by conducting a more vigorous and careful studies for optimization of the experimental variables such as pH , temperature, enzymes and coenzyme concentrations. However, since the primary objective of this work was to demonstrate the potential utility of the proposed system to multicomponent kinetic analyses, such extensive optimization studies were not carried out.

The overall results in this chapter indicate that the photodiode array stopped-flow spectrometer is certainly a powerful technique for clinical applications. The system allows for both single and multicomponent analyses to be performed with great ease, flexibility, and convenience using either equilibrium or kinetic methods. In most applications, the system provides for an essentially overdetermined analyses and, therefore, offers a greater degree of flexibility and freedom to the clinical chemist for utilizing the information of his/her interest. Undoubtedly, for modern clinical laboratories involved in many complex chemical analyses, a photodiode array stopped-flow spectrometer is clearly a viable choice.

REFERENCES

1. Mars, J.M., paper NO. 48, Pittsburgh Conference on Analytical Chemistry and Applied Spectroscopy, Cleveland, Ohio, **1972**.

2. Nunn, W.G.; Dessay, R.E. Multichannel Imaging Detectors, ACS Symposium Series.

3. Massey, V.; and Gibson, G.H., Fed. proc., **1964**, 23, 18.

4. Carr, J.D.; Libby, R.A.; and Margeram, D.W. Inorg. Chem., **1967**, 6, 1083.

5. Strojek, J.W.; Gruver, G.A.; and Kuwana, T. Anal. Chem., **1969**, 41, 481.

6. Patterson, J.I.H.; Perone, S.P. Anal. Chem., **1972**, 44, 1978.

7. Bethke, G.W. J. Opt. Soc. Amer. **1960**, 50, 1054.

8. Terenin, A.; Dimitrievsky; and Shakhverdou, P. "Spectroscopy of Short Lived Molecular Ions of Organic Compounds," Eighth European Congress On Molecular Spectroscopy, Copenhagen, August 1965.

9. Hexter, R.M.; Hand, C.W. Appl. Opt. **1968**, 7, 2161.

10. Brabov, H.J.; and Tourin, R.H. Appl. Opt. **1968**, 7, 2171.

11. Buchhave, P.; and Church, C.H. Appl. Opt. **1966**, 7, 2200.

12. Hill, R.A. Appl. Opt. **1968**, 7, 2184.

13. Greig, J.R.; and Cooper, J. Appl. Opt. **1968**, 7, 2166.

14. Denton, M.S.; Deangelis, T.P.; Yacynych, A.M.; Heineman, R.; and Gilbert, T.W. Anal. Chem. **1976**, 48, 20.

15. Dolin, S. A.; Kruegle, H. A.; and Penzias, G. J, Appl. Optics, **1967**, 6, 267.

16. Washwell, E.R.; and Cuff, E.R. Anal. Chem., **1970**, 9, 1911.

17. Geig, J.R.; and Cooper, J. Anal. Chem. **1968**, 7, 2166.

18. Koszewski, J.; Jansy, J.; and Brabowski, J.R. Anal. Chem. **1968**, 2178.

19. Harris, S.E.; and Wallace, R.W. J. Opt. Soc. Amer., **1969**, 59, 744.

20. Harris, S.E.; Nieh, S.T.K.; and Windslow, D.K. Appl. Phys. Lett. **1969**, 15, 325.

21. Biberman, L.M.; Nudelman, S., Eds. Photoelectronic Imaging Devices, **1971**, Vol. 2, Plenum Press, New York, pp. 253-57.

22. Horlic, G.; Codding E. G., Anal. Chem., **1973**, 45, 1491.

23. Talmi, Y. Anal. Chem. **1975**, 47, 658A.

24. Talmi, Y. Anal. Chem. **1975**, 47, 699.

25. Nieman, T.A., Ph.D. Thesis, Michigan State University, Chemistry Department, **1975**.

26. Biberman, L.M.; Nudelman, S., Eds., Photoelectronic Imaging Devices, **1972**, Vol. 2, pp. 253-57, Plenum Press, New York.

27. Biberman, L.M.; Nudelman, S., Eds., Photoelectronic Imaging Devices, **1972**, Vol. 2, pp. 303-6, Plenum Press, New York.

28. Horlick, G. Appl. Spectra **1976**, 30, 113.

29. Johnson, D.W.; Callis, J.B.; Christian, G.D. Anal. Chem. 49, 747.

30. Cooney,R. P.; Vo-Dinh, T.; Winefordner, J. D., Anal. Chem. Acta., **1977**, 89, 9.

31. Nieman, T.A. and Enke, C.G., Anal. Chem., **1976**, 48, 619.

32. Hornshuh, Ph.D. thesis, Michigan State University, **1978**.

33. Westphall, J.A. "Advanced Electro-optical Imaging Techniques," NASA Report SP-338, p. 93.

34. "Advanced Scanner and Imaging Systems For Earth Observations," NASA, SP-335 Report, **1972**.

35. Busch, K.W.; Howell, N.G.; Morrison, G.H. Anal. Chem. **1974**, 46, 575.

36. Busch, K.W.; Howell, N.G.; Morrison, G.H. Anal. Chem. **1974**, 46, 1231.

37. Malino, M.J.; Pardue, H.L.; Cook, T.E.; Santini, R.E.; Margerum, D.W.; Raycheba, J.M.T. Anal. Chem. **1974**, 46, 374.

38. Felkel, H. L.; Pardue, H. L., Anal. Chem., **1978**, 50, 602.

39. Howell, G.; Ganjei, J. D.; Morrison, G. H., Anal. Chem., **1976**, 48, 319.

40. Furuta, N.; McLeod, C. W.; Haraguchi, H.; Fuwa, K., Appl. Spectrosc., **1980**, 34, 211.

41. Grabau, F.; Talmi, Y., Multchannel Image Detectors, Talmi , Ed., Vol. 236, ACS symposium series, **1982**, p. 75.

42. Felkel, H. L.; Pardue, H. L., Anal. Chem., **1977**, 49, 1112.

43. Felkel, H. L.; Pardue, H. L., in Multichannel Image detectors, Talmi, Ed., Vol. 102, ch. 3, ACS symposium series, **1978**.

44. Busch, K. W.; Malloy, B., ibid, ch. 2.

45. Ganjei, J. D.; Howell, N. G.; Roth, J. R.; Morrison, G. H., Anal. Chem., 1976, 48, 505.

46. Olesik, J. W.; Walters, J. P., in Multichannel Image Detectors, Talmi, Ed., Vol. 236, ACS symposium series, **1982**.

47. Milano, M. J.; Pardue, H. L., Anal. Chem., **1975**, 47, 25.

48. Hoffman, R. M.; Pardue, H. L., Anal. Chem., **1979**, 51, 1267.

49. Talmi, Y.; Baker, D. C.; Jadamec, J. R.; Saner, W. A., Anal. Chem., **1978**, 50, 936A.

50. Johnson, D. W.; Callis, J. B.; Christian, G. D., Anal. Chem. **1977**, 149, 747A.

51. Cooney, R. P.; Vo-Dinh, T.; Winefordner, J. D., Anal. Chem., **1977**, 49, 939.

52. El-sayed, M. A., in Multichannel Image Detectors, Talmi, Ed., Vol. 102,ch. 10, **1979**.

53. Weisman, R. B.; Greene, B. I., ibid, ch. 11.

54. Kohen, E.; Kohen, C.; Thorell, B.; Salmon, J. M., Rev. Sci. Instrum., **1973**, 44, 1784.

55. Hirschberg, J. G.; Wouters, A. W.; Kohen, E.; Kohen C.; Thorell, B.; Eisenberg, B.; Salmon, J. M.; and Ploem, J. S., in Multichannel Image Detectots, Talmi, Ed., Vol. 102, Acs symposium series, ch. 13, **1979**.

56. Jadamec, J. R.; Saner, W. A.; Sager, R. W., ibid, ch. 6.

57. Jadamec, J. R.; Saner, W. A.; Talmi, Y., Anal. Chem., **1977**, 49, 1316.

58. Carlson, E. M.; Enke, C. G., in Multichannel Image Detectors, Talmi, Y., Ed., Vol. 102, Acs symposium series, ch. 7, **1979**.

59. Nieman, T.A., Holler, F.J., and Enke, C.G., Anal. Chem., **1976**, 48, 899.

60. Boettger, H. G.; Giffin, C. E.; and Norris, D. D., in Multichannel Image Detectors, Talmi, Y., Ed., Vol 102, Acs symposium series, ch. 14, **1979**.

61. Harber, R. A.; Sonnek, G. E., Appl. Opt., **1966**, 5, 1039.

62. Eberhardt, E. H.; Hertel, R. J., Appl. Opt., **1971**, 10, 1972.

63. Flekel Jr, H. L.; Pardue, H. L., Anal. Chem., **1978**, 50, 602.

64. Danielsson, A.; Lindblom, P., Appl. Spectrosc., **1976**, 30, 151.

65. Danielsson, A.; Lindblom, P., Physica. Scripta.,**1972**, 5, 227.

66. Danielsson, A.; Lindblom, P.; and Soderman, E., Chemica Scripta, , **1974**, 6, 6.

70. Ratzlaff, K.L.; Paul, S.L. Appl. Spectrosc. **1979**, 33, 240.

71. Ratzlaff, K.L. Anal. Chem. **1980**, 52, 916.

72. Denton, M.B.; Lewis, H.A.; and Sims, G.R. in Multichannel Detectors, Y. Talmi, Ed. ACS Symposium Series No. 236, Vol. 2, Chap. 6.

73. Lewis, H.A.; Denton, M.B. J. Auto. Chem. **1981**, 3, 9.

74. Talmi, Y. "Multichannel Image Detectors" ACS Symposium Series, Vol. 102, **1979**.

75. Talmi, Y. "Multichannel Image Detectors" ACS Symposium Series, Vol. 236, **1981**.

76. Nieman, T.A.; Enke, C.G. Anal. Chem. **1976**, 48, 619.

77. Sweedler, J.V.; Bilhorn, R.B.; Epperson, P.M.; Sims, G.R.; and Denton, M.B. Anal. Chem. **1988**, 60, 282A.

78. Epperson, P.M.; Sweedler, J.V.; Bilhorn, R.B.; Sims, G.R.; and Denton, M.B. anal. Chem. **1988**, 60, 327A.

79. Bilhorn, R.B.; Sweedler, J.V.; Epperson, P.M.; and Denton, M.B. Appl. Spectrosc. **1987**, 41, 1114.

80. Bilhorn, R.B.; Epperson, P.M.; Sweedler, J.V.; and Denton, M.B. Appl. Spectopsc. **1987**, 41, 1125.

81. Sims, G.R.; and Denton, M.B. J. Opt. Eng. **1987**, 26, 1008.

82. Sims, G.R.; Denton, M.B. in "Multichannel Image Detectors," Y. Talmi, Ed., ACS Symposium Series, Vol. 2, Chap. 5.

83. Dereniak, E.L.; Crowe, D.G. Optical Radiation Detectors, John Wiley, New York, 1984.

84. Epperson, P.M.; Denton, M.B. Anal. Chem. **1989**, 61, 1513.

85. Jalkian, R.D.; Denton, M.B. Appl. Spectrosc. **1988**, 142, 1194.

86. Epperson, P.M.; Jalkian, R.D.; Denton, M.B. Anal. Chem. **1989**, 61, 282.

87. Carlson, E.M., Ph.D. Thesis, Michigan State University, Chemistry Department, 1978.

88. Dessey, R.E. Anal. Chem. **1977**, 49, 1100A.

89. Aiello, P.J., Master's Thesis, Michgian State University, Chemistry Department.

90. Reticon "S" Series Solid State Line Scanners, Reticon Corp. 910 Benicia Ave., Sunnyvale, California 94086.

91. Holler, F.J., Ph.D. Thesis, Michigan State University, Chemistry Department.

92. Notz, P.K., Ph.D. Thesis, Michigan State University, Chemistry Department.

93. Stewart, J.E. Dionex, Applications Note No. 4.

94. Koch, R.; Johnson, G.F.; and Chilocote, M.E. Clin. Chemistry **1974**, 20, 392.

95. Kingsley, G.R. J. BIol. Chem. **1939**, 131, 197.

96. Savory, J.; Heintges, M.G.; Sonowave, M.; and Cross, R.E., Clin. Chem. **1976**, 22, 1102.

97. Hatcher, D.W.; and Anderson, N.G. Amer. J. Clin. Pathol. **1969**, 52, 645.

98. Ingle, Jr., J.D.; and Crouch, S.R. Anal. Chem. **1971**, 43, 697.

99. Pardue, H.L. Advan. Anal. Chem. Instrum. **1969**, 7, 141.

100. Wi-Tak-Law, Ph.D. Thesis, Michigan State University, Chemistry Department, **1978**.

101. Rothman, L. D.; Crouch, S.R.; Ingle Jr., J. D., Anal. Chem. **1975**, 47, 1226.

102. Malmstadt, H.V.; Enke, C.G. "Digital Electronics for Scientists" W.A. Benjamin Menlo Park, California, **1969**.

103. Javier, A.C.; Crouch, S.R.; Malmstadt, H.V. Anal. Chem., **1966** ,41, 239.

104. Pardue, H.L.; Frigns, C.S.; Delaney, C.J. Anal. Chem. **1965**, 37, 1426.

105. Pardue, H.L. Clin. Chem. **1977**, 23, 2189.

106. Mark Jr., H. B.; Rechnitz, G. A., Kinetic in analyticalchemistry, Wiley-Interscience, New York, **1968**.

107. Yatsimerskii, K. B., Pergamon, Oxford, **1966**.

108. Greinke, R. A.; Mark Jr., H. B., Anal. Chem., **1974**, 46, 413R.

109. Greinke, R. A.; Mark Jr., H. B., Anal. Chem., **1976**, 48, 87R.

110. Malmstadt, H.V.; Delaney, C.J.; and Cordos, E.A. Anal. Chem. **1972**, 44, 79.

111. Crouch, S.R.; Holler, F.J.; Notz, P.K.; and Beckwith, P.M. Appl. Spect. Rev. **1977**, 13, 165.

112. Mark, H.B., Jr. Talanta Rev. **1972**, 19, 717.

113. Pardue, H.L.; McDowell, A.E.; Fast, D.M.; and Milano, M.J. Clin. Chem. **1975**, 21, 1192.

114. Milano, M.J.; Pardue, H.L. Clin. Chem. **1975**, 21, 211.

115. Milano, M.J.; Kim, Kwang-Yil Anal. Chem. **1977**, 49, 555.

116. Hugget, A. St. G.; Nixon, D.A. Biochem. J. **1957**, 66, 129.

117. Keilin, D.; Hartree, E.F. Biochem. J. **1948**, 42, 221.

118. Kingsley, G.R.; Getchell, G. Clin. Chem. **1960**, 6, 466.

119. Malmstadt, H.V.; Hicks, G.P. Anal. Chem. **1960**, 32, 394.

120. Malmstadt, H.V.; Pardue, H.L. Anal. Chem. **1961**, 33, 1040.

121. Malmstadt, H.V.; Hadjiioannou, S.I. Anal. Chem. **1962**, 34, 452.

122. Widmark, E.M.P. Biochem. Z. **1922**, 131, 473.

123. Lundquist, F. "Methods of Biochemical Analysis", **1959**, Vol. 7, P. 247, Interscience, New York.

124. Friedemann, T.E. J. Biol. Chem. **1938**, 123, 161.

125. Brink, N.G.; Bonnichsen, R.K.; Theorell, H. Acta. Pharmacol. Toxicol. **1954**, 10, 233.

126. Kirk, P.L.; Giber, A.; Parker, K.P. Anal. Chem. **1958**, 30, 1418.

127. Malmstadt, H.V.; Hadjiioannou, S.I. Anal. Chem. **1962**, 34, 455.

128. Malmstadt, H.V.; Hadjiioannou, S.I. Anal. Chem. **1962**, 34, 452.

129. Fundamentals of Clinical Chemistry, Tietz, N. W., Ed., Saundres, 2nd. Ed., **1978**.

PART II

THE DEVELOPMENT OF A NEW CHEMOMETRIC APPROACH FOR COMPUTERIZED COMPOUND IDENTIFICATION USING IR SPECTRAL DATA

INTRODUCTION

Computer compound identification was one of the first data handling applications to appear after the computers were interfaced to spectroscopic instruments. Ever since, the bond established between analytical chemistry and computers has become continuously stronger. In recent years, the integration of computers with just about all modern spectroscopic instruments, has created a new enthusiasm for research activities in the field of automated compound identification. Beyond the significant effect of these efforts on the work of experts, it has made an impact of far greater dimension on the way that chemical analysis is performed by users who are not specialists.

Clearly, chemistry continues to play an increasingly important role in today's modern life. For members of every society , almost all aspects of life such as health, food, environment, consumer products, etc. are more and more influenced by chemistry or, as perceived by the general public by "chemicals". This influence is not limited to the material aspects of life, but also effects the formulation of much legislation and many public policies which govern the society. In many situations, accurate identification and thereby undrestanding the nature and properties of these "chemicals" is of key importance. This is a complicated problem when considering the fact that the vast majority of users of such "chemicals" at best possess minimal knowledge about their characteristics and behavior. This, of course, creats a large demand for qualified personnel which is

near impossible to achieve considering the extent and the magnitude of the issue.

A better understanding of the technical problem involved is achieved by drawing an analogy with that of a chemical equation which is too far from equilibrium. One side of the equation consist of a small chemical society (expert domain) with a great deal of knowledge about these so called "chemicals", and the other side includes a large body of various users with little or no knowledge (user or public domain). To bring a sensible equilibrium in this equation, there is a definite need for transfer of knowledge and expertise from the former domain to the latter. Although this interdomain information transfer appears to be a thermodynamically favorable process (large information gap) , until recently it has been kinetically very unfavorable. This is due to the the fact that positioning a qualified human expert at every conceivable user interface becomes rapidly prohibitive both from resources (including human experts) and economical perspectives. The only logical alternative appears to be the utilization of some kind of a "magic catalyst" which can facilitate the transfer of knowledge with high speed, accuracy and efficiency. In reality, the goal is not to transfer the kowledge in advance and make experts of the public as a whole,but rather one only need to facilitate access to information that is accurate and relevant. Computers has truly played an indispensable role as such a magic catalyst through various scientific databases and expert systems.

It should be noted that the scope of the above rather abstract discussion is not limited to chemistry only and is certainly applicable to any user/expert

domain interaction within any scientific discipline. Analytical chemists, however, have long been concerned with the characterization and identification of various compounds. In this process, they rely on a vast body of chemical knowledge and expertise in interpreting a great variety of characteristic spectroscopic information about numerous compounds. Certainly, these kinds of human experts do not, by any means, come easy or free of cost. High levels of training along with many years of experience are in fact invested into the production of these qualified individuals. It is within this context that many efforts have been focused at reducing the demands for human experts by their possible replacement with computerized expert systems. Specifically, the field of automated compound identification, perhaps more than any other area, has employed this role of computers as interdomain information mediators. Today, with the high-throughput computerized instrumentation and the scarcity of human experts, the development of sophisticated procedures for computerized processing of spectroscopic information must and has become a high priority.

One should be cautioned, however, that to this date automated compound identification systems are still far from being perfect and the computers have not, quite yet, turned into a spectroscopist in a box. They have at best become a valuable tool for the experienced chemist and a marginally useful tool in the hands of inexperienced users. There are still many problems with spectroscopy itself as well as instrumentation, operators and sampling errors. Great deal of work needs to be done toward standardization of sampling and spectral data acquisition parameters, software utilities and computers and networking protocols. Nevertheless,

we are not far from the time when a universal automated system across all spectroscopic disciplines will become a reality. This will not only free the experts from performing many routine and repetitive tasks but, when combined with today's communication technology, will greatly enhance collaboration among world experts to investigate issues of global dimension such as health and environmental matters. The network approach will not, of course, help a user with one or two instruments which have dedicated data systems. Therefore, localized automated systems with a greater degree of intelligence in performance than those currently available still need to be developed.

It is hoped that the brief discussion above can serve to generate some excitement on the part of the reader in regard to the area of automated compound identification. It also will hopefully make him/her appreciate the impact of the research activities in the field which may be of far greater dimension than the mere curiosity of individual researchers. This chapter begins with a a brief conceptual overview of automated compound identification pertinent mostly to IR spectroscopy. Subsequently, a new chemometric approach for qualitative and quantitative infrared spectroscopic analysis developed in this research is described. Finally, the application of the method to the analysis of pure samples and mixtures and to the resolution of unseparated chromatographic peaks is demonstrated.

AUTOMATED SPECTRAL PROCESSING
A CONCEPTUAL OVREVIEW

While chemists study the characteristics, properties and structure of compounds based on first principles as well as various spectroscopic probes which may directly or indirectly reveal exploratory information, these compounds find numerous applications in the hands of users who are not expert chemists. Therefore, the development of automated compound identification systems intended for users who are not expert spectroscopists has become increasingly important.

The determination of the structure and identity of organic compounds is typically done by spectroscopic methods such as infrared spectroscopy (IR) , mass spectrometry (MS) , nuclear magnetic resonance (N.M.R) and ultraviolet-visible (UV-VIS) spectroscopy. Among these, mass spectrometry and infrared spectroscopy occupy the first and second place respectively, in terms of automated tools already developed for their spectral processing. Although there exists a variety of computerized spectral processing systems, these may all be broadly classified into two major categories. Those based on spectral matching (library search) and those relying on artificial intelligent programs (interpretive methods) often referred to as "expert" or "knowledge based" systems. Regardless of the approach used, the goal is to ultimately determine the identity of an unknown compound based on various spectroscopic information.

In order to develop an appreciation of the basic mechanism operating in automated spectral processing, a brief discussion of an abstract mathematical model proposed by J. T. Clerc (1,2) is presented at this point. The reader may refer to the original references for a more detailed treatment. The Clerc's model also serves to make a clear distinction between the two categories of automated spectral processing mentioned above.

The underlying assumption of all approaches to spectra interpretation is the fact that the spectrum of a compound is a function of its structure. This functional relationship may be depicted in the following form:

$$\text{Spectrum} = \mathbf{F}\,(\text{Structure}) \qquad (1)$$

To obtain an unknown structure, one only needs to invert the function **F** and apply it to the spectrum:

$$\text{Structure} = \mathbf{F}^{-1}\,(\text{Spectrum}) \qquad (2)$$

At the first glance, the operations suggested by equations (1) and (2) may appear to be very simple. However, the theoretical evaluation of the function **F** , i.e, the exact calculation of, for example, all IR frequencies absorbed by a given molecule from basic principles, is not possible except for very small or highly symmetrical molecules. The majority of compounds are structurally too complex to be treated theoretically which leaves the empirical data treatment as the only practical choice. This empirical treatment of spectral data is, in fact, a task performed everyday by

practicing spectroscopists which may very well provide an insight for approaching the problem of spectra interpretation. The way that a spectroscopist performs structure elucidation by spectral interpretation is by breaking the total function **F** into a set of smaller and simpler functions G_i relating subspectra to substructures. The criteria for selection of G_i functions is that they must be relatively simple and invertible:

$$\text{Subspectrum}_i = G_i\,(\text{Substructure}) \qquad (3)$$

and,

$$\text{Substructure} = G_i^{-1}\,(\text{Subspectrum}) \qquad (4)$$

The total structure may then be recovered by combining various substructures:

$$\text{Total Structure} = \sum_i (\text{substructures})_i \qquad (5)$$

The utilization of the scheme suggested by equations (3), (4), and (5) does not, however, lead to a unique total structure. This stems from the fact that the simplification offered by considering only partial G_i functions instead of the total **F** function comes at the expense of losing context information. The influence of structural surrounding (neighboring groups) on a given substructure are no longer considered which can result in G_i^{-1} functions being fuzzy. Consequently several substructures are often found to be compatible with a given subspectrum or vice versa.

The trend in alleviating this problem has been through the simultaneous application of various sets of G_i^{-1} functions obtained with the orchestrated

use of several spectroscopic techniques (3,4). This strategy is well founded when one considers a spectrum of a compound as the projection of the compound from structure space into spectrum space. Since some loss of information is accompanied with any projection, ambiguous results can be obtained when the reverse projection is performed. Just as the shape of an object can be better deduced by combining different projections, the structure of a molecule can also be determined with greater certainty when spectral information from different spectroscopic techniques (i.e. different projections) exhibiting different potentialities and limitations are combined.

Thus, the combined use of, for example, IR and MS spectral data for a given compound is far more powerful than the single use of an extremely precise and highly resolved spectrum of either. Additionally, other parameters such as source of the sample and its physical properties may also be incorporated into such schemes as constraints to further focus the flow of information toward a more strictly defined possible structures, i.e., achieving selectivity enhancement among an otherwise informationally homolog candidates.

The main steps for a general algorithm for spectra interpretation proposed by Clerc is listed in table 5.1. These five steps are followed in almost all automated spectra interpretation systems (4-9) differing mainly in the emphasis placed on each step and the degree of sophistication used for their implementation.

TABLE 5.1 : General algorithm for spectra interpretation

---

1. partial structures

Apply the G_i^{-1} functions to compile a list ofstructures possibly present in the compound at hand.

2. consistent sets

From the list compiled in step 1 select all sets of structural elements possibly present simultaneously in the compound at hand which are self-consistent and not at variance with nonspectroscopic evidence.

3. Structure assembly

From all the sets generated in step 2 generate all possible full structures that are in accordance with the rules of chemistry and not at variance with nonspectroscopic evidence.

4. Spectra prediction

Predict the spectral data for the next tentative structure from the list of step 3 , using either of the F function or approximate G functions, taking into account the structural context.

5. Spectra comparison.

Compare the predicted spectrum with the experimental spectrum. If the two spectra are closely similar, keep the tentative structure as a possible solution. Then repeat step 4 and 5 until the list from step 3 is exhausted. Then stop. The list generated in step 5 now contains all possible solutions to the problem.

From reference (1).

The major consideration in step 1 is the selection of a complete set of G_i^{-1} functions with an appropriate degree of fuzziness. Different complications may arise if the range is made either too narrow or too wide. With a narrow range, one can miss a substructural element in a complex environment; and with a wide range, one may end up with too many solutions which can drive the processes in step 2 and step 3 out of hand. Steps 2 and 3 are not basically chemical problems, although they demand a very involved and certainly nontrivial programing effort. Step 4 is essentially an information recovery step. This means that the context information lost in step 1 by considering isolated substructures is to be recovered for the prediction of total spectra. In order for this step to be useful and lead to a reduction of the list in step 3, the G_i functions used here must be far more precise than the G_i^{-1} functions used in inference step. It is possible to achieve better precision by implementing more sophisticated rules in this step than the inference rules used in the first step. The accuracy of step 4 is also very important. Erroneous prediction here can cause the acceptable solution to be missed in the last step. Finally, the last step consists of a similarity check. All the instrumental parameters (reproducibility, spectrum registration, etc.) as well as the accuracy and precision used in step 4 must be taken into account for an accurate definition of similarity.

As mentioned previously, the general algorithm outlined in the above five steps closely resembles the approach followed by human spectroscopists. With a finite level of training and experience, the human analyst makes many logical decisions on an everyday basis and also learns from his/her

experiences. For this fundamental reason, the interpretive methods based on rule programing and full utilization of the above general algorithm have received a great deal of attention in recent years. To this end, one of the most notable example of interpretive software for use with infrared spectra is the "Program for Analysis of Infrared Spectra" (PAIRS) developed by Woodruff and Smith in 1980 (9-13) .

This program originally designed for liquid phase spectra, has been later modified to also accommodate vapor phase spectra (14) . The software consists of two Fortran programs, a rule compiler, an interpreter, and a set of interpretation rules written in an English-like language called CONCISE. These concise rules are converted into integer strings by the rule compiler and stored for later use by the system for interpretation of the unknown spectra. An important feature of the PAIRS program which is responsible for much of its success is that the rules and the interpreter are kept separate as opposed to being integrated in one program. This enables the user to change rules or teach PAIRS new rules without being an expert computer programmer. One version of PAIRS is available to run on IBM systems, and a most up-to-date version exists for DEC VAX systems. Some version of PAIRS also exist on Nicolet (10,15) and Digilab (16) and IBM (17) FT-IR instruments.

Since the interpretive methods are not the focus of this research, they will not be further discussed here. However, the reader may refer to several recent reviews on the general subject (18) and as applied to infrared (19) and mass spectrometry (20) .

Although research in the development of various interpretive algorithms in recent years has led to many useful concepts for spectral interpretation with computers, they have not yet found widespread application in the chemical laboratory. The library search, on the other hand, has become a mature technique and is routinely used for compound identification and structure elucidation.

In library search systems, the spectra are not interpreted at all; and therefore, no interpretation rules are used in the process. Theses systems, as the name suggests, rely on a large library of reference spectra of known compounds. The unknown spectrum is then compared to all library members and a list of best hits from those references exhibiting closely similar spectra to that of the unknown is presented to the user. Whether any of the compounds in the hit list are exactly identical or only bear some structural similarity to the unknown is something that must be entirely determined by the user.

Although a variety of matrices are used for spectral matching, the mechanism operative in a library search can also be understood in terms of the five steps outlined in Clerc's general algorithm. Since library search systems make no attempt at interpreting the unknown spectrum, step 1 (partial structure) is skipped entirely. Consequently, the selection of consistent sets of partial structures (step 2) is no longer applicable. It should be emphasized, however, that these two steps which essentially utilizes spectroscopically relevant information are perhaps the most important steps in interpretive methods and are responsible for making them distinctly different from search systems. In step 3 (structure

assembly) all of the library members are considered as possible structures; and since the library contains the real spectra of all references, Step 4 (spectrum prediction) becomes a straightforward retrieval operation.

The only major step left in the library search is that of spectra comparison (step 5). Since all library entries are compared to the unknown spectrum, the accuracy of the search results is critically dependent upon the quality of similarity measure employed. In this step, a bad performance by the similarity filter will produce a hit list dominated by noise structures with no relation to the unknown. For successful results, the library search also relies on high quality reeference spectra, uncontaminated samples, and the presence of unknown in the data base.

For interpretive methods, this final step is generally much less critical. With a fairly rational structure generation step, a rather limited number of tentative structures with reasonable similarity to that of the unknown is obtained. This makes step 5 not to be a very involved operation for these systems.

In summary, it may be concluded from the above discussion that, while from two distinctly different perspectives, both interpretive and library search systems share the same ultimate goal of structure elucidation of unknown compounds. This goal of structure elucidation is very explicit in an interpretive system as opposed to implicit in library search. Note that the cornerstone assumption of all library search systems is that if two compounds have similar spectra, then they must have similar structure. In fact as the search routine compares spectra, the user compares

structures and the success of the search system may be evaluated by how closely these two processes match.

The most striking difference between the two systems is perhaps on the degree of intervention by the human expert. This human intervention varies from zero to a minimal level in search routines compared to an extensively involved level in interpretive systems. The integrated use of both matching and interpretive algorithms may be more fruitful in aiding the human interpreter than either alone. Since matching system require the least human intervention, they may be utilized first. If a plausible match is not found in the library, an interpretive algorithm can be subsequently used to provide structural information. This information can then be utilized as feedback to the matching routine in order to insert compounds of appropriate structures into the library. McLafferty and Stauffer (21) have, in fact, used the combination of PBM (Probability Based Matching) matching routine (22,23) and STIRS (Self Training Interpretive and Retrieval System) interpretive algorithm (24) with mass spectral data.

As the interpretive systems find their history in the earlier work in matching routine, the future development in both fields can also be very much linked. Most likely, attempts at developing a hybrid between the two types of algorithms tailored to a specific application domains will be the trend of the future.

The remainder of this chapter describes the theory and applications of a new method developed in this research for computerized infrared analysis of organic compounds. The advantages of the new method are evaluated for

the analyses of both pure samples and mixtures using a small reference library. The performance of the method is then compared to other conventional search routines such as absolute differences and dot product matrices. Finally, the application of the proposed method as a curve resolution technique is described. Before all this, a brief history of automated compound identification with infrared spectroscopy is presented.

LIBRARY SEARCH BY INFRARED SECTROSCOPY
A BRIEF HISTORY

Infrared spectroscopy is one of the oldest and well established techniques for the identification of organic compounds. The identification ability of IR stems from the fact that the peaks in the spectrum generally correspond to two types of vibrational modes, those that are characteristic of complete molecular structure and those that are directly associated with specific functional groups. This combination of the fingerprint region (1400 - 400 cm^{-1}) and the functional group frequencies makes the IR spectrum one of the most structurally sensitive types of information that can be obtained. Therefore, strong evidence for the identity of an unknown is provided by the exhibition of a close match between a peak-to-peak comparison of the unknown spectrum with those of references. This is, of course, the foundation of library search systems.

In early days, compound identification was done by manual comparison of an unknown spectrum with those of reference compounds stored in reference books. The advantages of this approach are twofold. First, the reference spectra are in their original analog forms; thus, no loss of information through digitization has occurred. Second, the human brain is used as a pattern analyzer for similarity matching which is essentially unsurpassed by any computer. However, the great deal of time and effort that must be invested in manual searching of a large library of reference compounds makes the appeal of this approach quickly disappear.

Researcher then began to look into a more efficient way of matching unknown spectra with a digitized library of reference spectra via the use of computers. The earliest attempt which made use of punch cards for representation of digitized spectra, was reported by Kuentzel (25) in 1951 and later by Baker and coworkers (26) in 1953. A mechanical card sorter was used to search for the cards with similar patterns. This system was subsequently made to operate with an automatic card sorter and eventually turned into a computer readable format known as the ASTM (American Society for Testing and Materials) database. The ASTM database basically consisted of binary representation of spectra along with some limited structural information. Though the information in this database was limited, it did certainly serve as a good beginning for automated library search routines.

With the advances in computer technology and the introduction of magnetic tapes and disks with greater storage and faster retrieval times, some workers began utilizing them for faster search times based on ASTM system (27-29). Various techniques such as spectral compression (29-31) , hash coding (32) and file inversion (33) have been used to further decrease the search time and storage requirements. It should be pointed out ,however, that the decrease in search time and storage requirements which is frequently achieved by the use of spectral compression comes at the cost of a reduction in the information content of the spectra in the library. The condensation of the spectra is typically done by deresolving both the intensity and resolution producing thereby library spectra that are usually inadequate for visual inspection One solution to this problem reported by Lowry and coworkers (34) utilizes low resolution spectra for search

purposes while storing higher resolution spectra on a hard disk for visual display and inspection. To this end, a very interesting paper by Divis and White (35) describes an IR spectrum compression technique based on deconvoluted band representation which can reduce the storage space for 4 cm^{-1} resolution by 95% with minimal loss of spectral information content. However, because of the requirement of spectra reconstruction, the search time is longer in a deconvoluted band compressed library compared to a digitized reference library.

The main disadvantage of the ASTM system mentioned earlier is in the way that the spectral information is represented (binary format) . In this system, the spectrum is partitioned into a series of equally spaced intervals; and the presence or absence of a peak in a given interval is indicated by setting a corresponding bit to one or zero, respectively. Aside from the problems associated with peaks on the interval borders, the system essentially does not utilizes the intensity and peak-shape information contained in an infrared spectrum.

A major step forward in IR library searching was the development of the EPA vapor phase library by Azaraga (36). This was the first large library which utilized true digital IR spectra acquired with an FT-IR spectrometer. The low noise level and the wavelength accuracy offered by the FT-IR instrument has provided the basis for many full spectral search methods in use today (37-45). A detailed review of various methods for computer retrieval of spectral data by Hippe and Hippe (46) and a through evaluation of various aspects of library search techniques by Zupan (47) are available in the literature.

However, the automated IR spectral analysis has been, for a long time, suffering from the lack of a large, high quality and easily accessible database. In this regard, it has certainly lagged behind other techniques such as, for example, mass spectrometry. This is in part due to the fact that the IR absorption band consists of both peak shape and frequency information as opposed to a series of mass/intensity pairs found in mass spectrometry. Therefore, automated IR spectroscoy requires the use of fully digitized spectra which has only recently become available on a routine basis.with the introduction of FT-IR instruments. The after-the -fact digitization of existing large IR databases is neither cost effective nor free of error. Therefore, work must be done toward the creation of a large and high quality FT-IR based database.

Moreover, in terms of the quality of IR spectra, the lack of a standard method for spectral quality assessment such as the one developed for mass spectrometry (48) poses a serious problem. Although the design and implementation of a quality index is more difficult for IR than MS, it is nevertheless of extreme importance and a prerequisite for the development of high quality IR library. Fortunately, the Coblentz society (49) has recently begun work at addressing both the issue of IR spectral quality and the coordination of efforts toward the creation of high quality database. When these issues are properly resolved in the near future, it will definitely generate a new wave of enthusiasm and activity in the area of computerized Infrared spectral analysis.

At present, there are several computerized IR databases in existence. These include a rather large database (ASTM) gathered on grating and prism instruments along with various smaller FT-IR based systems. The ASTM database contains over 100,000 spectra in binary format compiled during 1950-1974. Although this library is no longer updated, it is still available on magnetic tape and distributed by Sadtler Research Laboratories (50). A collection of 94,000 spectra originally obtained on grating instruments has also been digitized by Sadtler; in addition a smaller vapor phase FT-IR database containing about 8600 spectra has been produced. However, these are only available as parts of instrument data systems which incorporates the database. Due to the advantages of FT-IR mentioned before, all other existing databases are essentially FT-IR based systems. Most of these systems are relatively small in size with differing and undefined spectral quality. Some of the most popular ones are mentioned here.

A condensed phase FT-IR database containing about 11,000 spectra is available in book form (51), floppy disk for searching (52) or on nine track magnetic tapes for use with any instrument or computer system available. This database has been created collaboratively by Nicolet Instruments and Aldrich Chemical Company using only Aldrich chemicals. Another FT-IR database available in a computer readable format is that of the Georgia State Crime Laboratory (49) which contains 1422 solid phase spectra of various drugs. In 1979, Satdler Laboratories under the direction of Leo Azarraga, created a library of some 3300 vapor phase FT-IR spectra. The public domain availability of this database has greatly facilitated the development and testing of search algorithms. This library is being

continuously updated and current version containing about 10,000 spectra is commercially available from Sadtler Laboratories.

THE DEVELOPMENT OF A CHEMOMETRIC APPROACH FOR COMPUTERIZED IR ANALYSIS OF PURE AND MIXTURE SAMPLES

Introduction

It was pointed out in the previous section that the research activities in computer-based spectral identification of organic compounds has been continuously increasing in recent years. This recent momentum in the field can be attributed to the introduction of inexpensive microcomputers with high speeds and large storage capabilities as well as the availability of a large number of digitized reference spectra. This has, in turn, resulted in the development of a wide range of library search algorithms and spectral interpretation systems. Today, the number of routine qualitative analyses performed by computerized spectral matching far exceeds those of any other method.

The problem is, however, that while one rarely deals with pure samples in real life situations, almost all spectral matching algorithms are designed to handle pure compounds. This certainly poses a serious limitation to the use of these systems in real life applications. As it will become more evident later, to be able to achieve automated mixture analysis one has to inevitably utilize more involved mathematics than the typical matching factors employed in most ordinary library search routines.

One attempt at handling mixtures has been through the concept of reverse searching. In reverse searching, the reference is compared to the unknown. The question is how many features of the reference spectrum exists in that of the unknown. A mixture will obviously contain some features from all the pure components found in it. When these features are combined, it will not probably match any member of a library containing only pure spectra. The best matches will, at best, be the spectra of the mixture. More likely however, they may just be spectra that contain various combinations of the functional groups from the pure components of the mixture.

Another major approach for direct spectroscopic analysis of mixtures is that of curve fitting. A common assumption among all these techniques is that there is a linear relationship between concentration and absorbance (Beer's law is obeyed), whereby each component in the mixture acts essentially as an independent absorber. Therefore, the mixture spectrum must be a linear combinations of component spectra.

Within the framework of curve fitting, there exist two basic approaches for solving the problem of the identification of unknown mixtures. One approach is to perform a single fit of all reference spectra to the unknown, i.e., to determine the linear combination which provides the best approximation of the mixture spectrum. Each reference spectrum should contribute in proportion to the concentrations of the corresponding compounds in the mixture. Compounds not present in the mixture should yield coefficients approaching zero. Therefore, any compound producing a coefficient above a certain threshold value would, in principle, be present in

the unknown. However, the number of floating point operations required to carry out such an analysis is extremely large precluding the use of this approach in conjunction with a large library. If one assumes that the unknowns are only binary mixtures, one can achieve a significant reduction on the number of required math operations. Nevertheless, for a library containing N compounds, there would still be N(N-1)/2 combinations to be tested making the approach time-prohibitive for a large database.

The second approach is to perform the inverse of the above process, i.e., to fit the spectra of each library member by linear combinations of the spectra of a series of mixtures. In this approach, one always needs to compute only N fits regardless of the number of pure component in the mixture. If the mixture is composed of n components, for example, the n compounds in the mixture can be identified from the n best fits. The algorithm for such analysis can be easily drived within the framework of factor analysis as demonstrated by Gillette and Koenig (52-53) . A dramatic reduction on the number of floating operations (~ N(NPTS) n^2) is generally achieved with the use of this approach because the number of components in a typical mixture is often much smaller than the number of reference compounds in the library. The successful application of this approach, however, depends upon the availability of a series of mixtures containing independent concentrations of the same compounds which may not always be obtainable.

The method described in this research will also attempt to fit the unknown spectrum (pure or mixture) to linear combinations of library specrta. The unique feature of the method is that all library spectra are

orthonormalized. This results in a computationally more efficient analysis (to be discussed later). In fact, the use of a orthonormalized library combines the best features of both previously mentioned approaches in that it is computationally efficient and it can be done with a single sample of the mixture. Next, the necessary mathematical background for undrestanding the proposed method is presented.

MATHEMATICAL BACKGROUND

An Algebraic and Geometrical Description of the Gram-Schmidt Orthonormalization process

The Gram-Schmidt orthonormalization process is a method employed by mathematicians for the generation of coordinate systems in multidimensional space. First, to develop an appreciation as to how an orthonormalized vector space may be constructed, a number of vector algebra definitions pertinent to the process are briefly presented. A reader familiar with these definitions may skip this part. An analytical as well as a geometrical step by step description of the Gram-Schmidt process followed by the application of the method to IR spectroscopy and the generation of an orthonormalized library of IR spectra is discussed.

Let's begin by considering a given vector space. A vector space V may be defined as any set of arbitrary objects on which two basic operations of

a. Addition, and
b. Multiplication by scalars (real numbers)

are defined. By addition, it is meant that for each pair of objects $\mathbf{x}$ and $\mathbf{y}$ in V one can associate an element $\mathbf{x} + \mathbf{y}$ called the sum of $\mathbf{x}$ and $\mathbf{y}$; and scalar multiplication is a rule of associating an element $k\mathbf{x}$ called the scalar multiple of $\mathbf{x}$ by k for each $\mathbf{x}$ in V and each scalar k. Each element in this set is then called a vector.

A very useful vector operation is that of linear combination. If a given vector $\mathbf{y}$ can be expressed as the sum of scalar multiples of a set of other vectors like $S = (\mathbf{x}_1, \mathbf{x}_2, ..., \mathbf{x}_n)$ such as:

$$\mathbf{y} = k_1 \mathbf{x}_1 + k_2 \mathbf{x}_2 + ... + k_n \mathbf{x}_n$$

where $k_1, k_2, ..., k_n$ are scalars, then vector $\mathbf{y}$ is called a linear combination of vectors $\mathbf{x}_1, \mathbf{x}_2, ..., \mathbf{x}_n$. The set of vectors $S = (\mathbf{x}_1, \mathbf{x}_2, ..., \mathbf{x}_n)$ is said to span a vector space V if they are in V and every vector in V is expressible as a linear combination of $(\mathbf{x}_1 + ... + \mathbf{x}_n)$. In general, a set of vectors S may or may not span the vector space V. If they span the space, then every vector in V can be expressed as a linear combination of $(\mathbf{x}_1, \mathbf{x}_2, ..., \mathbf{x}_n)$ and if they do not, then some vectors are so expressible while others are not. If all the vectors in V that are expressible as linear combinations of S are grouped together, a subspace is obtained which is referred to as the **space spanned by S.** These spanning sets S are very useful in many situations, for it is often possible to study a vector space V by first studying the vectors in the spanning set S, and then extending the results to the rest of V. It is therefore, desirable to keep the spanning set S as small as possible. The question of finding this smallest spanning set for vector space V depends on

the notion of linear independence. For instance, if for the spanning set S, the following vector equation,

$$k_1 \mathbf{x}_1 + k_2 \mathbf{x}_2 + \ldots\ldots + k_n \mathbf{x}_n = 0$$

has only one solution, namely

$$k_1 = 0 \, , k_2 = 0 \, , k_n = 0$$

then S is called a linear independent set. The set of S will be linearly dependent if there are other solutions. An important conclusion which may be drawn from the concept of linear independency is that a linear independent set for an n-dimensional space (R^n) can contain at most n vectors. This simply means that a set in R^2 with more than two vectors or a set in R^3 with more than three vectors are linearly dependent.

Utilizing the ideas of linear independency and a spanning set, one can arrive at a precise definition for the **basis** and **dimension** of a vector space. We normally think of a line as being one dimensional, a plane as two dimensional, and space around us as three dimensional. This intuitive notion of dimension may be made more precise in the following general way. A set of vectors S is called a basis for a given vector space V if

a. S is linearly independent
b. S spans V

When a vector space V contains a finite set of vectors $S = (\mathbf{x}_1, \mathbf{x}_2, ..., \mathbf{x}_n)$ which forms a basis, then V is called finite dimensional. Also it is a known property of vector spaces that if S is a basis for vector space V , then every set with more than n vectors (elements) is linearly dependent.

These properties of vector spaces allow the interpretation of the idea of dimension. The dimension of a finite dimensional vector space V is defined to be the number of vectors in a basis for V. Since as mentioned previously, a basis for a vector space is some linearly independent set of vectors that span the vector space, it follows that the dimension of a vector space is the minimum number of vectors required to span the vector space. As an example, consider the vectors (1, 0, 0) , (0, 1, 0)., and (0, 0, 1) in R^3 (3-D space). These are just unit vectors in R^3 and any vector in R^3 may be expressed as a linear combination of these three unit vectors. Notice, that no two vectors are sufficient to span R^3, but four vectors, say, (1, 0, 0) , (0, 1, 0) , (0, 0, 1.) , and (1, 1,.1) contains redundancy. Any one of them could be omitted and the remaining three would span R^3. Of course, not all sets of three vectors span R^3. The vectors (1, 0, 0) , (0, 1, 0) , and (1, 1, 0) although three (the dimension) in number, do not span 3-D space. These vectors are linearly dependent and so one is redundant. The concept of linear independence is, therefore, the key in consideration of the dimension of vector spaces.

To be able to fully apply vector ideas to Euclidean geometry, one must have a means of introducing concepts such as length, angle and perpendicularity. These concepts can be defined by introducing a kind of multiplication of

vectors called **dot product** or **inner product** . The dot product of two vectors $\mathbf{x} = (x_1, x_2, \ldots, x_n)$ and $\mathbf{y} = (y_1, y_2, \ldots, y_n)$ is defined to be a number

$$\mathbf{x} \cdot \mathbf{y} = x_1y_1 + x_2y_2 + \ldots + x_ny_n \ .$$

The length (norm) of a vector can then be easily expressed in terms of the dot product. For instance, one can think of the length of $\mathbf{x} = (x_1, x_2, x_3)$ in R3 as the distance from the origin to the point with coordinates (x_1, x_2, x_3) . It can be simply shown using Pythagorean theorem that the length of vector $\mathbf{x}$ in R^3 is given by:

$$|\mathbf{x}|^2 = x_1^2 + x_2^2 + x_3^2$$

or $$|\mathbf{x}| = (x_1^2 + x_2^2 + x_3^2) = (\mathbf{x} \cdot \mathbf{x})^{1/2}$$

which simply says that the length of a vector can be obtained by computing the dot product of the vector with itself and taking the square root of it. It is also possible to obtain information about the angle between two vectors $\mathbf{x}$ and $\mathbf{y}$ using the concept of dot product. If θ is the angle between $\mathbf{x}$ and $\mathbf{y}$, then the dot product or Euclidean inner product $\mathbf{x} \cdot \mathbf{y}$ is defined by :

$$\mathbf{x} \cdot \mathbf{y} = \begin{cases} |\mathbf{x}|\,|\mathbf{y}| \cos\theta & \text{if } \mathbf{x} \neq 0 \text{ and } \mathbf{y} \neq 0 \\ 0 & \text{if } \mathbf{x} = 0 \text{ and } \mathbf{y} = 0 \end{cases}$$

This relationship simply suggests the following information about θ :

θ	is acute	if and only if	$\mathbf{x}.\mathbf{y}>0$
θ	is obtuse	if and only if	$\mathbf{x}.\mathbf{y}<0$
θ	$=\pi/2$	if and only if	$\mathbf{x}.\mathbf{y}=0$

Based on this information, two vectors **x** and **y** are said to be orthogonal if their dot product is zero. Obviously, two vectors are orthogonal if and only if they are geometrically perpendicular. Thus, the dot product can be very useful in situations where it is desired to decompose a vector into a sum of two perpendicular vectors. For example, for two nonzero vectors such as **x** and **y**, it is always possible to write **y** as :

$$\mathbf{y} = \mathbf{v}_1 + \mathbf{v}_2$$

where $\mathbf{v}_1$ is a scalar multiple of **x** and $\mathbf{v}_2$ is perpendicular to **x** as shown below.

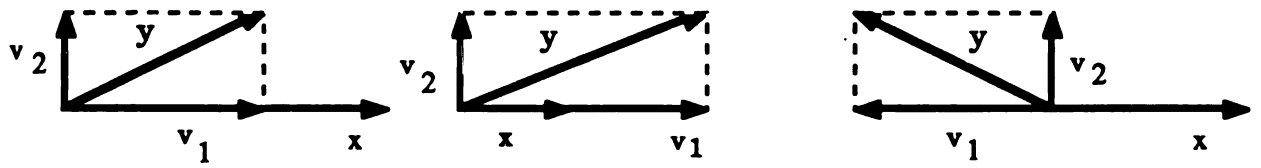

The vector $\mathbf{v}_1$ is called the orthogonal projection of **y** on **x** and $\mathbf{v}_2$ is called the component of **y** orthogonal to **x**. the vectors $\mathbf{v}_1$ and $\mathbf{v}_2$ can be easily obtained. Since $\mathbf{v}_1$ is a scalar multiple of **x**, then:

$$\mathbf{v}_1 = k\mathbf{x}$$

$$\mathbf{y} = \mathbf{v}_1 + \mathbf{v}_2 = k\mathbf{x} + \mathbf{v}_2$$

Taking the dot product of both sides with $\mathbf{x}$,

$$\mathbf{x}.\mathbf{y} = (k\mathbf{x} + \mathbf{v}_2).\mathbf{x} = k|\mathbf{x}|^2 + \mathbf{v}_2.\mathbf{x}$$

Since $\mathbf{v}_2$ is perpendicular to $\mathbf{x}$; $\mathbf{v}_2.\mathbf{x} = 0$ and

$$k = \frac{\mathbf{x}\cdot\mathbf{y}}{|\mathbf{x}|^2}$$

and therefore:

$$\mathbf{v}_1 = \frac{\mathbf{x}\cdot\mathbf{y}}{|\mathbf{x}|^2}\cdot\mathbf{x}$$ is the orthogonal projection of $\mathbf{y}$ on $\mathbf{x}$ and

$$\mathbf{v}_2 = \mathbf{x} - \frac{\mathbf{x}\cdot\mathbf{y}}{|\mathbf{x}|^2}\cdot\mathbf{x}$$ is the component of $\mathbf{y}$ orthogonal to $\mathbf{x}$

The several concepts of vector algebra which have been reviewed so far, can now be used in the construction of an orthonormal basis described next.

CONSTRUCTION OF ORTHONORMAL BASIS

The Gram-Schmidt Process

In the previous section, some basic concepts of vector algebra such as norm, dot product, and linear independency along with a few important characteristics of vector spaces such as spanning set, basis, and dimension were briefly reviewed. A good understanding of these ideas are essential to the comprehension of orthonormal basis discussed here.

As mentioned before, the basis for a given vector space is defined as a set of linearly independent vectors which span the vector space. In many problems which involves the use of vector spaces, the selection of a basis for the space is at the discretion of the problem solver. The best choice is naturally to select a basis which will simplify the solution of the problem at hand. Often times, this best choice is a basis in which all vectors are orthogonal to one another. This means that all pairs of distinct vectors in the set are perpendicular. An orthogonal set in which each vector has a norm of one (unit length) is called orthonormal.

These conditions are very useful and are, in part, the motivation behind finding an orthonormal basis for vector spaces, since it is exceptionally simple to express a vector in terms of an orthonormal basis. For example if a vector space V has an orthonormal basis $\mathbf{v}_1, \mathbf{v}_2, \ldots, \mathbf{v}_n$, then any vector $\mathbf{x}$ in V can be expressed as a linear combinations of basis vectors by :

$$\mathbf{x} = c_1 \mathbf{v}_1 + \ldots\ldots\ldots + c_j \mathbf{v}_j + \ldots\ldots + c_n \mathbf{v}_n$$

Then the coefficients c_j can be computed easily

$$\mathbf{x} \cdot \mathbf{v}_j = c_1 \mathbf{v}_1 \cdot \mathbf{v}_j + \ldots\ldots + c_j \mathbf{v}_j \cdot \mathbf{v}_j + \ldots\ldots\ldots + c_n \mathbf{v}_n \cdot \mathbf{v}_j$$

$$= \quad 0 \quad + \ldots\ldots + \quad c_j \quad + \ldots\ldots\ldots + \quad 0$$

so that

$$c_j = \mathbf{x} \cdot \mathbf{v}_j$$

There is yet another interesting and useful aspect to an orthonormal set. If $\mathbf{v}_1$, $\mathbf{v}_2$,....., $\mathbf{v}_n$ are an orthonormal set of vectors in the vector space V, and Z denotes the space spanned by this orthonormal set, then every vector $\mathbf{x}$ in V can be expressed in the form

$$\mathbf{x} = \mathbf{z}_1 + \mathbf{z}_2$$

where $\mathbf{z}_1$ is in Z and $\mathbf{z}_2$ is orthogonal to Z by letting,

$$\mathbf{z}_1 = (\mathbf{x} \cdot \mathbf{v}_1)\,\mathbf{v}_1 + (\mathbf{x} \cdot \mathbf{v}_2)\,\mathbf{v}_2 + \ldots\ldots + (\mathbf{x} \cdot \mathbf{v}_n)\,\mathbf{v}_n$$

$$\mathbf{z}_2 = \mathbf{x} - (\mathbf{x} \cdot \mathbf{v}_1)\,\mathbf{v}_1 - (\mathbf{x} \cdot \mathbf{v}_2)\,\mathbf{v}_2 - \ldots\ldots - (\mathbf{x} \cdot \mathbf{v}_n)\,\mathbf{v}_n$$

This process is geometrically shown below.

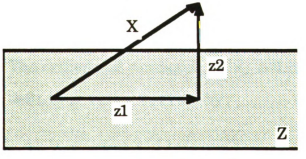

Generally it is possible to construct an orthonormal basis for any finite dimensional vector space. One of the well known ways of constructing such a set is the Gram-Schmidt procedure which is done in the following way. Suppose that V is any nonzero n-dimensional vector space with a spanning

set $S = (\mathbf{x}_1 , \mathbf{x}_2 , ... , \mathbf{x}_n)$. The Gram-Schmidt process for construction of an orthonormal set $O = (\mathbf{o}_1 , \mathbf{o}_2 , ... , \mathbf{o}_n)$ would involve the following steps:

Step 1. Pick any of the $\mathbf{x}$'s, say $\mathbf{x}_1$, and simply normalize it ,

$$\mathbf{o}_1 = \frac{\mathbf{x}_1}{|\mathbf{x}_1|}$$

Notice that

$$|\mathbf{o}_1| = \frac{|\mathbf{x}_1|}{|\mathbf{x}_1|} = 1$$

Step 2. To construct a vector $\mathbf{o}_2$ of norm one that is orthogonal to $\mathbf{o}_1$, one may pick another of the $\mathbf{x}$'s , say $\mathbf{x}_2$, and compute the component of $\mathbf{x}_2$ orthogonal to the space Z_1 spanned by $\mathbf{o}_1$ and then normalize it ; that is,

$$\text{Proj}_{Z1}\mathbf{x}_2 = (\mathbf{x}_2 \cdot \mathbf{o}_1)\,\mathbf{o}_1 \qquad \text{projection of } \mathbf{x}_2 \text{ on } \mathbf{o}_1$$

The orthogonal component of $\mathbf{x}_2$ orthogonal to $\mathbf{o}_1$ can be defined as vector $\mathbf{y}_2$ given by :

$$\mathbf{y}_2 = \mathbf{x}_2 - \text{Proj}_{Z1}\mathbf{x}_2 = \mathbf{x}_2 - (\mathbf{x}_2 \cdot \mathbf{o}_1)\,\mathbf{o}_1$$

Note that $\mathbf{y}_2$ is perpendicular to $\mathbf{o}_1$, for

$$\mathbf{y}_2 \cdot \mathbf{o}_1 = \mathbf{x}_2 \cdot \mathbf{o}_1 - (\mathbf{x}_2 \cdot \mathbf{o}_1)(\mathbf{o}_1 \cdot \mathbf{o}_1)$$
$$= \mathbf{x}_2 \cdot \mathbf{o}_1 - \mathbf{x}_2 \cdot \mathbf{o}_1 = 0$$

To obtain a unit vector o_2 perpendicular to o_1 , we normalize y_2 ,

$$o_2 = \frac{x_2 - (x_2 \cdot o_1)\, o_1}{\left| x_2 - (x_2 \cdot o_1)\, o_1 \right|} = \frac{y_2}{|y_2|}$$

Of course, the vector y_2 cannot be zero because that would imply that x_2 and o_1 are linearly dependent.

Step 3. Having found o_1 and o_2, one chooses x_3 and forms its projection on the space Z_2 spanned by o_1 and o_2 :

$$\text{Proj}_{Z_2} x_3 = (x_3 \cdot o_1)\, o_1 + (x_3 \cdot o_2)\, o_2$$

Similarly, the component of x_3 orthogonal to the space Z_2 shown by vector y_3 , is obtained by subtracting this projection from x_3

$$y_3 = x_3 - (x_3 \cdot o_1)\, o_1 - (x_3 \cdot o_2)\, o_2$$

As before it can be checked that y_3 is perpendicular to both o_1 and o_2 ,

$$y_3 \cdot o_1 = (x_3 \cdot o_1) - (x_3 \cdot o_1) = 0$$
$$y_3 \cdot o_2 = (x_3 \cdot o_2) - (x_3 \cdot o_2) = 0$$

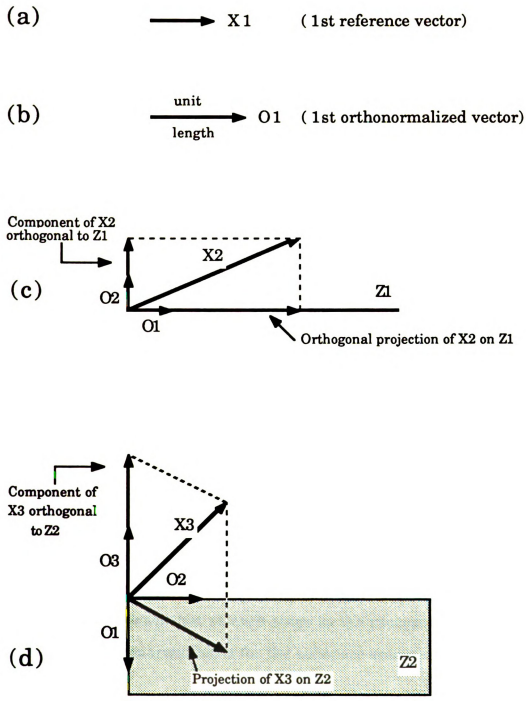

Figure 5.1 The geometric representation of the Gram-Schmidt orthonormalization process.

The orthonormalized vector o_3 is then obtained by normalizing y_3 ,

$$o_3 = \frac{y_3}{|y_3|}$$

The geometrical vector representation of the above three steps is shown in Figure 5.1.

One proceeds in this way , successively computing o_1 , o_2 ,... , o_j . To find o_{i+1} one computes:

$$y_{j+1} = x_{j+1} - (x_{j+1} \cdot o_1)\, o_1 - \ldots\ldots - (x_{j+1} \cdot o_j)\, o_j$$

and $$o_{j+1} = \frac{y_{j+1}}{|y_{j+1}|}$$

It can be continued until one runs out of x's in the independent set. Since the orthonormal set o_1 , o_2 ,....., o_n obtained in this way is linearly independent, it will be an orthonormal basis for the n-dimensional space V. Also, it can be shown that at each stage in the process, the vectors o_1, o_2 , , o_j form an orthonormal basis for the subspace spanned by x_1 , x_2 ,....., x_j .

In the next section the utility of the Gram-Schmidt procedure to Infrared Spectroscopic analysis is discussed.

Application to the Qualitative and Quantitative analysis of Pure and Mixtures using IR Reference Spectra

The theoretical considerations of the application of the Gram-Schmidt procedure to the qualitative and quantitative analyses of pure samples and mixtures using IR spectral data is described here. First, it is important to point out that, in principle, the proposed method is technique independent and is certainly amenable to any spectrometric technique capable of generating compound specific spectra (predictor vectors). However, all the work in this research has been done on an Infrared Spectrometer and, therefore, the discussion below is pertinent only to IR spectroscopy.

To be able to effectively utilize the Gram-Schmidt process, an n-dimensional vector approach must be used. This can be achieved by treating an IR spectrum of a given compound as an n-dimensional (composed of n resolution elements) vector such as

$$S = (I_1 , I_2 , \ldots\ldots\ldots , I_n).$$

Secondly, a set of linearly independent vectors which spans the sample space must be available. This is, in fact, equivalent to the very basic assumption of all spectroscopic techniques (i.e., IR) that a given compound has a unique spectrum different from all other compounds. Thus, the spectra of a set of reference compounds will constitute a set of linearly

vaila

nkno

This

he G

previ

propo

Note

Next

The

Who

independent vectors. Therefore, once a library of IR molecular spectra is available, it can serve as a spanning set for an n-dimensional space of unknown compounds.

$$S = (S_1 , S_2 , ... , S_n); \text{ Spaning set}$$

This spanning set can be transformed into an orthonormalized basis using the Gram-Schmidt procedure. Analogous to the manner explained in the previous section, the first orthonormalized spectrum O_1 is made proportional to the first molecular spectra by a normalization constant :

$$O_1 = T_{11} S_1 \qquad ; T_{11} = (S_1 . S_1)^{1/2}$$

Note that O_1 is normalized

$$(O_1 . O_1) = T_{11}^2 (S_1 . S_1) = 1.0$$

Next O_2 can be computed as

$$O_2 = \frac{[S_2 - (S_2 . O_1) O_1]}{[(S_2 . S_2) - |(S_2 . O_1)|^2]^{1/2}}$$

The denominator assures that $O_2 . O_2 = 1.0$ and also note that O_2 is orthogonal to O_1 since

$$(O_2 . O_1) = \frac{(S_2 . O_1) - (O_1 . O_1)}{[(S_2 . S_2) - |(S_2 . O_1)|^2]^{1/2}} = 0.0$$

The Nth spectrum is orthonormalized to the previous library using

$$O_N = \frac{[S_N - \sum_{i=1}^{N-1} (S_N . O_i) O_i]}{[(S_N . S_N) - \sum_{i=1}^{N-1} |(S_N . O_i)|^2]^{1/2}}$$

The analysis of a sample is then performed by computing the projection of the sample spectrum into this orthonormalized reference space. Since a pure sample can be thought of as a mixture containing only one component, let's consider a more general case of a mixture. A mixture spectrum $M(\lambda)$ is presumed to be a linear combination of the orthonormal spectra which span the reference space represented by th following equation:

$$M_{(\lambda)} = \sum_{i=1}^{N} P_i \, O_i(\lambda) \qquad (1)$$

where $M_{(\lambda)}$ denotes the absorbance of the mixture at the wavelength λ, N is the number of reference spectra and $P_i = (M . O_i)$ are the projections of the mixture in the O_i direction. For a mixture of n components, there are only $n < N$ nonzero projections. The concentrations of the components are obtained from these projections. If a given projection is less than or equal to

zero, the corresponding reference compound is presumed to be not present in the mixture.

Considering that the orthonormal spectrum can be expressed as linear combinations of the molecular spectra

$$O_i = \sum_{j=1}^{i} T_{ij} S_j \qquad (2)$$

then the mixture spectrum can be transformed to the molecular basis using

$$M_{(\lambda)} = \sum_{i=1}^{N} P_i O_i \qquad (3)$$

Substituting for O_i from equation (2) yields

$$M_{(\lambda)} = \sum_{i=1}^{N} P_i \sum_{j=1}^{i} T_{ij} S_j \qquad (4)$$

Rearranging the summation indices one obtains

$$M_{(\lambda)} = \sum_{j=1}^{N} \left(\sum_{i=j}^{N} P_i T_{ij} \right) S_j = \sum_{j=1}^{N} K_j S_j \qquad (5)$$

Assuming that each component in the mixture acts as an independent absorber and the interaction among various components are negligible

(Beer's Law is obeyed), one can then use Beer's Law to evaluate the coefficients K_j . For each of the component spectra $S_j(\lambda)$, Beer's Law for a given pathlength may be written as:

$$S_j = C_j^o \, a_j \qquad (6)$$

Substituting the Beer's Law expression for each S_j into equation (5) for a mixture

$$M_{(\lambda)} = \sum_{j=1}^{n} C_j \, a_j = \sum_{j=1}^{n} \frac{C_j}{C_j^o} \, S_j \qquad (7)$$

Comparison equation (7) with equation (5) yields

$$K_j = \frac{C_j}{C_j^o}$$

where C_j is the concentration of jth component in the mixture and C_j is the concentration of the same component in a standardized reference solution. Note that equation (7) is the sum over the entire library containing all possible components. The coefficients K_j may be interpreted as :

$$K_j = \begin{cases} \dfrac{C_j}{C_j^o} = \text{Positive value} & ; \text{Component j present} \\ \leq 0 & ; \text{Component j absent} \end{cases}$$

Note, that not only positive coefficients for various components would be indicative of their presence in the sample (qualitative analysis), but the magnitude of these coefficients is also directly proportional to their concentrations. Therefore, one is able to obtain both qualitative and quantitative information for both pure samples and mixtures from a single run.

Another important characteristic of the Gram-Schmidt transformation is its lower triangular growth at the time of library inception, that is :

$$O_1 = T_{11}\ S_1$$

$$O_2 = T_{21}\ S_1 + T_{22}\ S_2$$

$$O_3 = T_{31}\ S_1 + T_{32}\ S_2 + T_{33}\ S_3$$

.

.

.

.

$$O_N = T_{N1}\ S_1 + T_{N2}\ S_2 + \ldots\ldots\ldots\ldots\ldots + T_{NN}\ S_N$$

Where T_{ij} are the transformation coefficients and S_1 , ... , S_N are the reference spectra in the library. Figure 5.2 also shows a simplified version of the Gram-Schmidt transformation for ten hypothetical reference spectra A through J .

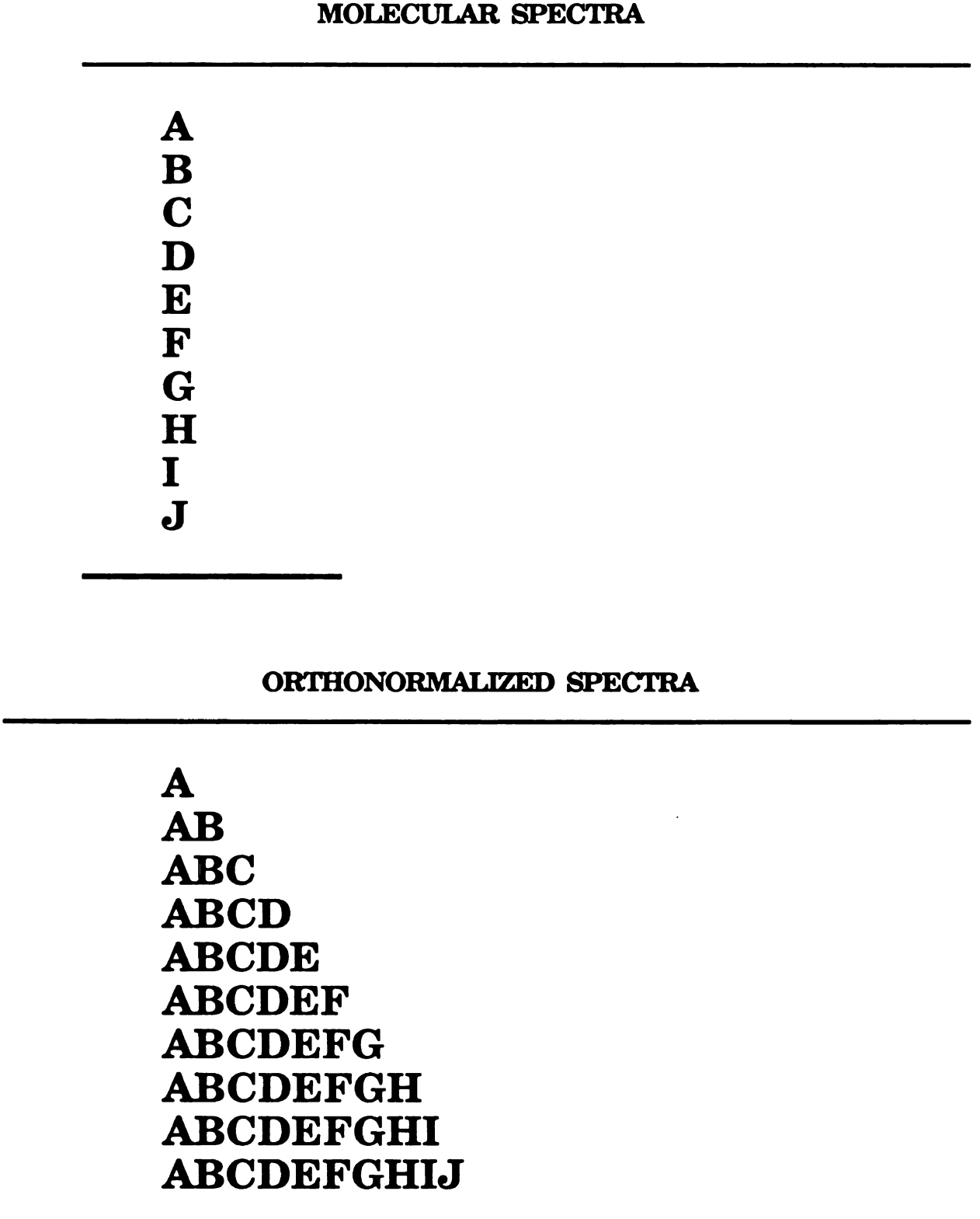

Figure 5.2 Representation of Gram-Schmidt transformation for ten hypothetical compounds.

An important consequence of this triangular growth of the library is that it allows for an efficient partial analysis for a given target compound. As can be seen from the simplified figure 5.2, if one is, for instance, interested in compound I, it appears as a part of only two orthonormalized reference spectra; and thus, the projections in only these two directions has to be computed for its analysis. It may, therefore, be desirable for the compounds that are most frequently analyzed to be placed at the beginning of the library at the time of library inception. This results in tremendous saving in time and computational effort. Most other matching factors used in conventional search routines search the entire library regardless of whether a given compound is at the beginning or the end of the library. This convenient feature of an orthonormalized library can be mathematically expressed in a more general way. To determine the concentration of reference compound N in a given mixture, only one projection need to be computed

$$K_N = \frac{C_N}{C_N^o} = \sum_{i=N}^{N} P_i \, T_{iN} = (M . O_N) \, T_{NN}$$

and similarly for compound N-1, only two projections are to be computed

$$K_{N-1} = \sum_{i=N-1}^{N} P_i \, T_{i,N-1} = (M . O_{N-1}) \, T_{N-1,N-1} + (M . O_N) \, T_{N-1,N}$$

In general, N - j + 1 projections are needed to determine the concentration of the jth reference compound.

Several

assess t

an orth

applica

pure co

orthonc

analysi

then co

convent

Differen

inseparab

All of t

Spectro

a 12 bit

of the in

observed

mixture

of 600 .

acquisit

average

second.

EXPERIMENTAL RESULTS

Several categories of experiments have been designed and carried out to assess the extent to which the theoretical advantages attributed to the use of an orthonormal reference library are realized in its applications. First, the application of the method as a search algorithm for the identification of pure compounds is investigated. Next, the potential advantages of the orthonormal method to the computerized qualitative and quantitative analysis of mixtures is demonstrated. The performance of the method is then compared to two matching algorithms most frequently used in conventional library search, namely, the Dot Product and the Absolute Difference. Finally its utility as a curve resolution technique for resolving unseparated chromatographic peaks is examined.

All of the experimental work has been done on a dispersive Infrared Spectrometer (Beckman Acculab 1) interfaced to a microcomputer through a 12 bit analog to digital converter. The manufacturer specified resolution of the instrument was 4 cm^{-1} , but resolution of 6 - 8 cm^{-1} were practically observed due to the age of the instrument. All reference, unknown, and mixture spectra contain 450 absorbance values over the IR frequency range of 600 - 4000 cm^{-1} . A 0.025 mm NaCl cell was used for all spectral acquisition. Each absorbance value was obtained as the logarithm of an average of 20 data points digitized by the ADC at a rate of 20 conversion per second. All of the chemical reagents were from Fisher Chemical Company

which were used without any further purification. The samples were all prepared by volume; and therefore, the reported results are all in fractional volumes.

Identification of Pure Compounds

To examine the usefulness of the orthonormal method for the identification of pure compounds, a small library containing ten IR reference spectra was compiled. All of the spectra were orthonormalized using the previously described Gram-Schmidt process to obtain an orthonormalized reference library. Independent samples from each of the reference compounds were prepared and labeled as A through J and were treated as unknowns. The IR spectrum of each unknown was acquired, normalized, and subsequently projected into the orthonormalized reference library. The computed coefficients were then used as a match factor. Three independent runs of the above experiment were performed and the computed coefficients were averaged. The results obtained are shown in table 5.2 .

Note that the projection step is actually a fitting process where the unknown spectrum is approximated as a best fit by the linear combinations of the reference spectra in the library. The relative error of the fit is computed from the following formula:

Table 5.2 Analysis of Pure Samples

	Unknowns				
References	A	B	C	D	E
Cyclohexane	**0.986**	0.054	-0.044	-0.220	-0.002
Hexane	-0.0005	**0.922**	0.038	-0.030	-0.035
Toluene	0.010	0.017	**1.00**	0.070	0.016
Methylene chloride	0.006	-0.006	-0.007	**1.15**	0.008
Methyl acetate	0.002	0.006	0.029	0.003	**1.02**
Ethyl acetate	-0.002	-0.005	-0.033	-0.013	0.064
Carbon tetra-Cl	-0.0030	0.003	0.015	0.022	0.008
Propanol	0.004	0.004	-0.003	-0.008	0.007
Acetone	-0.008	0.003	0.002	0.009	-0.094
Acetic acid	0.007	0.0009	0.004	0.013	0.011
Relative Errors ($x10^3$)	4.41	2.23	7.81	5.66	4.41

Table 5.2 continued

	Unknowns				
References	F	G	H	I	J
Cyclohexane	-0.037	-0.002	0.087	-0.022	0.081
Hexane	0.028	-0.015	-0.031	0.027	-0.116
Toluene	0.021	0.030	0.070	0.026	0.067
Methylene chloride	-0.024	-0.042	-0.046	-0.020	-0.027
Methyl acetate	0.073	0.011	-0.006	0.052	0.100
Ethyl acetate	**0.902**	-0.007	0.033	-0.036	-0.074
Carbon t-chloride	0.017	**1.01**	0.028	0.004	0.029
Propanol	-0.002	0.004	**0.873**	-0.008	0.017
Acetone	0.020	0.0007	-0.003	**0.98**	0.002
Acetic acid	0.003	0.0005	-0.004	-0.008	**0.942**
Relative Errors ($x10^3$)	3.40	3.37	4.01	4.16	3.75

$$\delta = \left[\frac{(\frac{1}{449}) \int_{\lambda min}^{\lambda max} (M(\lambda) - M'(\lambda))^2 \, d\lambda}{\int_{\lambda min}^{\lambda max} (M(\lambda))^2 \, d\lambda} \right]^{1/2}$$

Where $M(\lambda)$ is the actual unknown spectrum and $M'(\lambda)$ is the best fit. The computed relative errors for each of the unknowns are also listed in table 5.2. A fairly small magnitudes of the relative errors ($\sim 10^{-3}$) indicates a performance of a good fit in each case.

Table 5.3 shows the results obtained when samples that are not represented in the library are analyzed. These samples include: A, benzonitrile ; B, diethylamine ; C, m-xylene ; D, methyl sulfoxide ; and E, bromopropane. When compared to the results for compounds present in the library (table 5.2) , there are a number of points to be noted. First there is a rather broad distribution of the fractional volumes contributed by various library members. Second, there is at least one large negative contribution to the fit. These are the result of trying to approximate the unknown spectrum as a linear combination of reference spectra which do not contain many features common to it.

Another striking difference is the magnitude of the relative errors for these samples relative to those of table 5.2. Notice that an order of magnitude increase in relative error ($\sim 10^{-2}$) is obtained for all the samples. Similar results have been obtained for numerous other analyses involving compounds that are not included in the library. This certainly indicates

Table 5.3 Analysis of Pure Samples not Present in the Library

	Unknowns				
References	A	B	C	D	E
Cyclohexane	0.099	0,060	0.029	0.630	-0.310
Hexane	-0.260	0.330	0.232	-0.730	0.770
Toluene	0.770	0.310	0.788	1.13	0.270
Methylene chloride	0.016	0.150	-0.320	-0.530	-0.053
Methyl acetate	0.093	-0.110	0.060	-0.320	0.085
Ethyl acetate	-0.068	0.090	-0.012	0.760	0.100
Carbon t-chloride	0.323	0.070	0.244	0.090	0.130
propanol	0.019	0.040	-0.013	0.180	0.001
Acetone	0.016	0.020	-0.005	-0.150	-0.022
Acetic acid	-0.012	0.020	-0.002	-0.070	0.021
Relative Errors ($x10^3$)	27	25	18	35	23

that the magnitude of the relative errors can be effectively used as another dimension of information to indicate the presence or absence of a substance in the library.

The results obtained, clearly demonstrate that the use of orthonormal reference spectra is an effective approach to the identification of pure compounds. The method gave unambiguous identifications in all cases where the unknowns were present in the library. Some small contributions from other components of the library were frequently observed for these samples, such as 5.4% cyclohexane for sample B (Hexane). Often times, this discrepancy can be eliminated through the use of non-negativity constraints (next section). However, errors of this magnitude do not pose a serious problem in applications where the sample is known to be pure.

For those samples not present in the library, the orthonormal method was not only capable of classifying the unknown compound by structural similarities to those of the library, but also the relative error proved to be a reliable indicator of whether or not the substance was represented in the library.

The most notable advantage of the orthonormal method, however, is that it allows for a more general analysis that is capable of identifying the components of the mixture. This feature of the method is demonstrated in the next section.

ANALYSES OF MIXTURES

Most computerized compound identification systems are designed to handle pure samples. Quite often, ambiguous and unreliable results are obtained if the sample happens to be impure or a mixture. Since most analysts frequently encounter samples of a complex mixture, it is certainly advantageous to be able to perform mixture analysis with the same computational efficiency as that of pure samples. The computation mechanism operative in the orthonormal procedure successfully allows for this type of analysis, since it is indifferent to the nature of the sample. the same computation (projection step) is performed regardless of whether the sample is pure or a mixture which accounts for computational efficiency. Moreover, several additional measures have been undertaken in order to improve the quantitative accuracy of the method as applied to mixture analysis. These measures include the following:

1. The imposition of the Non-negativity Constraints (NNC)

2. Analysis over a selected Active Region (AR)

3. Analysis using mixture references

As will be seen from the obtained data, the use of one, two, or all three of the above measures can often result in a significant improvement of

quantitation results. A brief description of each of theses steps is presented at this point.

1. Non-negativity Constraints (NNC)

As was seen from the data for the analysis of pure samples, after the first projection is performed a number of reference spectra receive negative coefficients. Since negative coefficients are physically meaningless, one may impose a non-negativity constraint on the fit by forcing it to have only a positive solution. This may be done simply by removing from consideration those spectra which received negative coefficients in the previous analysis. The process is then repeated in an iterative fashion until all coefficients become positive. As will be seen from the data, for all cases examined this process converges to a non-negative solution with a relative error comparable to those of the unconstrained analysis.

2. Analysis over an Active Region (AR)

After an NNC operation is repeated a number of times, one usually obtains a positive solution consisting of coefficients for the components that are quite possibly present in the mixture. It was found that further improvement in quantitation can be obtained by repeating the analysis over a selected region (active region) of the reference spectra. The criteria for selection of the active region is to find a spectral window within which the most differences in reference spectra occur. Although this process can be placed under computer control, for all the reported data in this work they were determined by displaying the reference spectra on the monitor and

visually searching for areas where they are the most different and at the same time exhibit a good degree of spectral features.

3. Fitting the unknown mixture by a set of reference mixtures

It was pointed out before that the orthonormal method is indifferent to whether the sample is pure or a mixture. The same argument is certainly true for the reference spectra. The reference spectra may well consist of a series of mixtures of known and varying concentrations and of a given set of components. The spectrum of the unknown can then be projected into this mixture space from which the individual component concentrations of the unknown mixture may easily be computed. Note that this is very similar to a typical factor analysis experiment (39). Therefore, the orthonormal method can be complementary to the results obtained by a factor or principal component analysis. The ability to use mixture reference spaces can also be very useful in quality control applications where it may be desired to check a large samples of mixtures containing a defined set of components with known ranges of concentrations.

To assess the utility of the orthonormal method to the qualitative and quantitative analyses of mixtures, a series of experiments with various samples of mixtures have been carried out. A small orthonormal library containing ten reference compounds has been employed. Table 5.4 shows the list of compounds in the library and their corresponding abbreviations used for ease of tabulation. All of the mixtures have been prepared.by volume, and the results are reported as percent fractional volumes.

Table 5.4 List of compounds in the library

Names	Abbreviations
Cyclohexane	(CYC)
Hexane	(HEX)
Toluene	(TOL)
Methylene chloride	(MCL)
Methyl acetate	(MAC)
Ethyl acetate	(EAC)
Carbon tetrachloride	(CTC)
O - Xylene	(OXY)
Acetone	(ACT)
Acetic acid	(ACA)

Table 5.5 shows the results obtained for MIXTURE 1 which was in fact a sample of pure acetone. Although it is evident from the first analysis that the sample is not a mixture and is certainly pure acetone, the application of the NNC operation tow times resulted in higher quantitative accuracy. The analysis on the selected active region in this case does not lead to any further quantitation improvement. In fact, for this sample it might not have been necessary to do this step at all since the quantitative result of the previous step was highly accurate. Also notice that the standard deviations remain relatively constant for all the steps pointing to the performance of a good fit in each case.

The results for MIXTURE 2 which consisted of 50% cyclohexane and 50% hexane is shown in Table 5.6. Again the results from the first run clearly point to cyclohexane and hexane as the only two major components. The application of the NNC three times leads to excellent qualitative analysis, since the list is narrowed down to the only two components present in the mixture. Although somewhat improved by the NNC operations, the quantitative results are still largely at error. Significant improvement in quantitation is realized in this case by repeating the analysis over the selected region of 600 - 1900 cm^{-1}. The standard deviations of the fits remain fairly constant indicating a good fit in each step. Also, an important point that was previously alluded to was the frequent observance of small fractional volumes (~7%) contributed by some library members at the time of the first projection. For instance, looking at the data from the first run, methyl acetate (6.8%) may well be suspected to be present in the sample. This suspicion is soon eliminated after the first NNC application where the coefficient for methyl acetate turns negative. As will be seen from all the

Table 5.5 : Results of the analysis of MIXTURE 1

MIXTURE 1 : ACT (100%)

CYC	HEX	TOL	MCL	MAC	EAC	CTC	0XY	ACT	ACA
1.6	-1.0	0.50	0.70	2.0	-1.4	-1.2	-1.6	105	-0.50

SD = 0.05

NNC (1)

CYC	TOL	MAC	ACT
-0.08	-2.75	0.24	102.5

SD = 0.05

NNC (2)

MAC	ACT
-0.025	100.25

SD = 0.053

A.R (600 - 1000) Cm^{-1}

MAC	ACT
-3.19	103.19

SD = 0.025

Table 5.6 Results of the analysis of MIXTURE 2

MIXTURE 2 : CYC (50%) , HEX (50%)

CYC	HEX	TOL	MCL	MAC	EAC	CTC	0XY	ACT	ACA
32.8	74.6	- 9.4	- 3.5	6.8	- 7.3	1.3	1.4	2.0	1.5

NNC (1) SD = 0.043

CYC	HEX	MAC	CTC	OXY	ACT
32.42	79.14	- 1.43	- 1.52	- 9.13	0.53

SD = 0.055

NNC (2)

CYC	HEX	ACT
33.69	68. 41	- 2.10

SD = 0.061

NNC (3)

CYC	HEX
34.10	65.89

SD = 0.063

A . R (600 - 1900) Cm^{-1}

CYC	HEX
49.88	50.11

SD = 0.062

subsequent data, the small fractional volumes (not present in the mixtures) are consistently eliminated by the successive NNC operations This is very useful for it can provide greater assurance as to whether, for example, methyl acetate is actually present in the sample or the 6.8% coefficient is simply caused by the redundancy of the choices from which the best fit is to be computed.

Table 5.7 shows the results for a ternary mixture (MIXTURE 3) consisting of 30% cyclohexane, 40% ethyl acetate, and 30% acetone. Similar to the previous samples, the method is successful in reducing the list down to the three components actually present in the sample with better than 5% quantitative accuracy.

The next two experiments with MIXTURE 4 and MIXTURE 5 are carried out to compare the improvement in quantitation realized by fitting the unknown mixtures by a reference space of mixture spectra relative to those of a typical analysis performed for previous samples. MIXTURE 4 consisted of 80% cyclohexane and 20% hexane and the results of the first projection along with the subsequent NNC operations for this mixture are shown in Table 5.8. Notice that the two components in the mixture are correctly identified, but the quantitative results are about 9% in error. Using the 88.8% cyclohexane and the 11.11% hexane from table 5.8 as an initial estimate of their concentrations, two independent mixtures of cyclohexane and hexane with concentrations within the above range were prepared. The spectra of the two mixtures were acquired and subsequently orthonormalized. The spectrum of MIXTURE 4 was then projected into this two dimensional mixture space. The results obtained are shown in

Table 5.7 Results of the analysis of MIXTURE 3

MIXTURE 3 : CYC (30%) ; EAC (40%) ; ACT (30%)

CYC	HEX	TOL	MCL	MAC	EAC	CTC	0XY	ACT	ACA
63.1	- 3.27	- 6.43	7.03	- 5.87	59.5	- 5.32	- 18.1	43.4	- 3.55

SD = 0.13

NNC (1)

CYC	MCL	EAC	ACT
35.6	- 3.55	39.0	28.9

SD = 0.15

NNC (2)

CYC	EAC	ACT
34.4	37.1	28.5

SD = 0.15

Table 5.9. The results of table 5.9 clearly show a significant improvement in quantitation compared with the data in table 5.8. In fact, an increase in quantitative accuracy from about 9% to better than 0.5% is achieved.

The analysis of MIXTURE 5 was carried out in a similar manner to that of MIXTURE 4. This mixture was a four component system containing: 30% cyclohexane, 20% methyl acetate, 30% ethyl acetate, and 20% acetone. The results obtained from a typical orthonormal analysis and those of using a mixture space are shown in Table 5.10 and 5.11, respectively. It is again evident from the results in table 5.11 that the accuracy of quantitating individual components in MIXTURE 5 has greatly improved.

The overall results shown and the experience with numerous other samples prove that the orthonormal method is an effective approach to the analysis of mixtures. The method is particularly useful in applications where a list of possibilities either exists or can otherwise be predicted. To this end it is also amenable to those situation where it is of interest to analyze a large number of samples in a relatively short period of time.

As can be seen from all the cases examined, the qualitative and quantitative results obtained from even the first run were quite reliable. The use of non-negativity constraints proved to be a reliable method of not only eliminating the suspected compounds (small positive coefficients), but also of providing greater assurance about the components that are actually present in the unknown mixture. It is also important to point out that mixture analysis with the orthonormal method requires only one run on a single sample.

Table 5.8 Results of the analysis of MIXTURE 4

MIXTURE 4 : CYC (80%) ; HEX (20%)

CYC	HEX	TOL	MCL	MAC	EAC	CTC	0XY	ACT	ACA
79.7	20.6	- 2.68	- 2.04	8.26	- 9.88	1.35	- 5.33	2.95	- 2.44

NNC (1) SD = 0.09

CYC	HEX	MAC	CTC	ACT
93.2	13.9	- 4.20	- 3.27	0.361

NNC (2) SD = 0.10

CYC	HEX	ACT
89.3	14.4	- 3.77

NNC (3) SD = 0.10

CYC	HEX
88.8	11.11

SD = 0.10

Table 5.9 Results of the analysis of MIXTURE 4

MIXTURE 4 : CYC (80%) ; HEX (20%)
(Fitting into Mixtures)

MIXTURES	CYC (%)	HEX (%)	Coeff. (C)
(1)	90	10	48.2
(2)	70	30	51.7

CYC % = 0.9 * C (1) + 0.7 * C (2) = **79.6%**

HEX % = 0.1 * C (1) + 0.3 * C (2) = **20.3%**

Table

CY
71.

Table 5.10 Analysis of MIXTURE 5

MIXTURE 5 : CYC (30%) ; MAC (20%) ; EAC (30%) ; ACT (20%)

CYC	HEX	TOL	MCL	MAC	EAC	CTC	0XY	ACT	ACA
71.1	- 10.5	3.30	2.15	19.0	47.5	1.94	- 25.1	39.0	- 2.90

NNC (1)

SD = 0.13

CYC	TOL	MCL	MAC	EAC	CTC	ACT
39.3	- 19.3	4.89	14.6	32.2	- 0.44	28.8

SD = 0.14

NNC (2)

CYC	MCL	MAC	EAC	ACT
33.1	- 2.71	14.0	31.0	24.5

SD = 0.15

NNC (3)

CYC	MAC	EAC	ACT
32.3	13.7	29.9	24.3

SD = 0.15

Table 5.11 Analysis of MIXTURE 5

MIXTURE 5 : CYC (30%) ; MAC (20%) ; EAC (30%) ; ACT (20%)
(Fitting into Mixtures)

MIXTURES	CYC	MAC	EAC	ACT	C (%)
(1)	30	30	20	20	26.9
(2)	35	15	30	20	14.9
(3)	32	15	28	25	71.3
(4)	30	15	30	25	-13.1

$$\%\,X = \sum_{i=1}^{n} X(n) \times C(n)$$

CYC %	**= 32.5%**	(30)
MAC %	**= 19.3%**	(20)
EAC %	**= 26.2%**	(30)
ACT %	**= 23.2%**	(20)

This

quan

An e

mixt

spac

Oth

com

nam

mix

mix

This is rarely the case with any other method particularly in regard to the quantitative analysis of multicomponent systems.

An exception to this rule is, of course, when the procedure of fitting into mixtures is employed. Therefore, one must only attempt to utilize mixture spaces when it is intended to obtain results of high quantitative accuracy. Otherwise it should be avoided since the use of this step does, in fact, compromise the above mentioned advantage of the orthonormal method, namely that of single shot analysis. However, the potential applications of mixture spaces are limited to circumstances where the components of the mixture are not only known but also available in pure form.

CO

As wa
search
library
algori
of the
either
spect
used
above
are a
root
spect
occu
prod
(ider
one
simi

Whe
as t
that
of e

COMPARISON OF THE ORTHONORMAL METHOD TO OTHER LIBRARY SEARCH MATRICES

As was previously pointed out, the identification of compounds by library search is done by comparison of the unknown spectrum with a digitized library of reference spectra. A variety of matrices have been used as search algorithms (matching factors) to match the unknown spectrum with those of the library. The tow most common matrices are based on computing either the dot products (DT) or the absolute differences (AD) of the unknown spectrum and the spectra of the library compounds. Many other commonly used matching routines are, in fact, based on various derivatives of the above two matrices. With the use of the dot products, the reference spectra are actually normalized to unity by one's dividing through by the square root of the sum of the intensities. The dot products of the unknown spectrum with those of the library members are then computed, and the occurrence of a dot product approaching unity is considered a match. A dot product of exactly one is only possible if the two compounds are identical (identity search). Otherwise, a dot product with closest approximation to one may be obtained for the reference compound with the most structural similarity to that of the unknown (similarity search).

When the absolute differences approach is used, the unknown is identified as the reference spectrum that yields a difference closest to zero. Notice that both procedures fundamentally rely on the uniqueness of the spectrum of every compounds. This is, in fact, an implicit linear independency

assumption in both methods, although no attempt is made by neither of the methods to insure that this assumption is not violated.

In this section the performance of the orthonormal procedure is compared to those of the dot products and the absolute differences methods. In this regard, the results obtained by all three methods for a same set of samples on the same ten member library are compared and evaluated. The dot products were computed from the following formula:

$$(DP)_i = \sum_{j=j_{min}}^{j_{max}} M_j S_{ji} \left[\sum_{j=j_{min}}^{j_{max}} M_j^2 \sum_{j=j_{min}}^{j_{max}} S_{ji}^2 \right]^{1/2}$$

where M_j is the jth data point in the unknown spectrum and S_{ji} is the jth data point in the spectrum of the ith compound in the library. As can be seen from the formula, the reference spectra are normalized in DP but not orthogonalized. The average absolute differences were computed from

$$(AD)_i = \sum_{j=j_{min}}^{j_{max}} \frac{|M_j - S_{ji}|}{450} .$$

A total of six samples (A through F) were examined in this study. Samples A, B, and C were cyclohexane, hexane, and acetone, respectively. Sample D, diethylamine, and sample E, cyclohexene, were not present in the library; and finally sample F was a binary mixture consisting of 20% cyclohexane and 80% hexane. The results of the analyses of these samples

by orthonormal, dot products, and absolute differences are shown in tables 5.12, 5.13, and 4.14, respectively.

As can be seen from the data in these tables, samples A, B, and C are correctly identified as cyclohexane, hexane, and acetone, respectively, by each of the three methods. The results of the analyses of many other samples have shown that all three methods exhibit the same predictive power when the samples are pure. No noticeable advantage is shown by the orthonormal method in regard to pure samples. Examining the results obtained for sample D (not present in the library) indicate that the absence of sample D (diethylamine) from the library may be easily revealed from the magnitude of the relative error in the orthonormal method. To a lesser degree of reliability, one may also arrive at the same conclusion from the DP and AD results for this sample. Notice that all the dot products are considerably less than one, and none of the absolute differences are approaching zero.

Sample E (cyclohexene) was also not present in the library, but its spectrum is very similar to the spectra of library compounds cyclohexane and, to a lesser extent, toluene. The results of the analysis by the orthonormal method is certainly in agreement with these facts. Again, notice that the magnitude of the relative error points to the absence of cyclohexene from the library, while the coefficients of 0.75 for cyclohexane and 0.30 for hexane is indicative of its structural similarity to both compounds.

The results of orthonormal analysis for sample F which was a binary mixture consisting of 20% cyclohexane and 80% hexane show a number of

Table 5.12 Analysis using **orthonormal method**

References	Samples					
	A	B	C	D	E	F
CYC	**1.00** **(0.99)**	0.07 (0.06)	0.02 (0.00)	-0.06 (0.00)	0.75 (0.72)	**0.13** **(0.12)**
HEX	.07 (0.01)	**1.00** **(0.94)**	0.01 (0.00)	0.56 (0.05)	0.14 (0.13)	**0.94** **(0.88)**
TOL	-0.06 (0.00)	-0.05 (0.00)	0.01 (0.00)	0.21 (0.17)	0.30 (0.15)	-0.07 (0.00)
MCL	-0.01 (0.00)	-0.02 (0.00)	-0.01 (0.00)	0.19 (0.19)	-0.02 (0.00)	-0.04 (0.00)
MAC	0.05 (0.00)	0.02 (0.00)	0.02 (0.00)	-0.17 (0.00)	-0.08 (0.00)	0.00 (0.00)
EAC	-0.06 (0.00)	-0.03 (0.00)	-0.01 (0.00)	0.17 (0.00)	0.10 (0.00)	0.00 (0.00)
CTC	0.00 (0.00)	0.01 (0.00)	-0.01 (0.00)	0.01 (0.01)	-0.03 (0.00)	0.00 (0.00)
OXY	-0.01 (0.00)	0.01 (0.00)	-0.02 (0.00)	-0.01 (0.00)	-0.11 (0.00)	0.03 (0.00)
ACT	0.02 (0.00)	0.03 (0.00)	**1.02** **(1.00)**	-0.03 (0.00)	0.03 (0.00)	0.02 (0.00)
ACA	-0.02 (0.00)	-0.02 (0.00)	-0.01 (0.00)	0.04 (0.03)	-0.01 (0.00)	-0.01 (0.00)
Relative Error ($\times 10^3$)	**4.6**	**4.9**	**3.3**	**23**	**17**	**3.6**

Table 5.13 Analysis using the **dot product**

References	Samples					
	A	B	C	D	E	F
CYC	0.99	0.94	0.25	0.69	0.92	0.95
HEX	0.94	0.99	0.30	0.75	0.89	0.99
TOL	0.41	0.48	0.48	0.69	0.54	0.49
MCL	0.07	0.10	0.13	0.48	0.16	0.10
MAC	0.23	0.26	0.75	0.38	0.28	0.27
EAC	0.24	0.29	0.76	0.43	0.31	0.30
CTC	0.00	0.01	0.06	0.30	0.02	0.01
OXY	0.61	0.70	0.44	0.74	0.67	0.70
ACT	0.22	0.28	1.00	0.35	0.26	0.28
ACA	0.36	0.37	0.62	0.54	0.43	0.39

Table

Refer
CY
HE
TC
MC
MA
EA
CT
OX
AC
AC

Table 5.14 Analysis using the **absolute differences**

References	Samples					
	A	B	C	D	E	F
CYC	0.05	0.08	0.34	0.27	0.09	0.07
HEX	0.07	0.04	0.33	0.26	0.10	0.03
TOL	0.20	0.20	0.29	0.30	0.18	0.20
MCL	0.20	0.21	0.37	0.31	0.21	0.22
MAC	0.48	0.47	0.27	0.54	0.47	0.47
EAC	0.46	0.45	0.26	0.50	0.45	0.45
CTC	0.20	0.22	0.38	0.37	0.22	0.22
OXY	0.18	0.16	0.31	0.28	0.15	0.15
ACT	0.33	0.32	0.03	0.44	0.33	0.32
ACA	1.37	1.36	1,17	1.20	1.33	1.34

interesting points when compared to those of the other two methods. The orthonormal method clearly indicates the presence of both components. Notice that cyclohexane and hexane are the only two components that make non-negative contributions. Both DP and AD, on the other hand, predict sample F as being pure hexane.

In general, the successful application of DP and AD relies heavily upon a perfect match between the unknown and a reference compound in the library. This is something which is rarely achieved due to subtle changes in external conditions, the presence of noise in the spectra, and changes in other experimental parameters. As a consequence, the dot products and absolute differences do not always give definitive identifications. Quite often, these methods fail to discriminate between related compounds. In particular, both methods are incapable of differentiating between a pure compound and a mixture with similar spectrum.

In conclusion, the overall results for the six samples examined demonstrate that the orthonormal method shows an equivalent performance to that of the other two methods for identification of pure compounds. However, the orthonormal method is certainly more powerful when it comes to samples not represented in the library or to those of mixtures. This latter consideration is extremely important in those situations where the IR spectra are used in conjunction with separation techniques for peak identifications. This is the subject of the next section.

APPLICATION OF THE ORTHONORMAL METHOD TO THE RESOLUTION OF SEVERLY OVERLAPPING CHROMATOGRAPHIC PEAKS

Introduction

Major activities in the field of chemical analysis today are directed toward the analysis of complex mixtures such as food, biological fluids and environmental samples. The information content of the analytical signal for such systems is multivariate in nature. The analytical chemist is often charged with the task of decomposing this multivariate information into its univariate components to determine the signal due to the analyte of interest in the composite signal. Efforts to achieve this by means of chemical separation are not only time consuming but often unsuccessful. Instrumental approaches in dealing with the problem have been mainly centered around the development of hyphenated instruments capable of providing multivariate data from which univariate information may then be extracted. This has resulted in the emergence of very powerful analytical techniques such as GC/IR, GC/MS, GC/MS/MS and GC/IR/MS which can generate large quantities of multidimensional data on a single chromatographic peak. The major rate limiting step in further expansion of this technology for complete utilization of its power appears to be the maturity gap between the instrumentation on one hand and data processing methodologies on the other.

Among the existing techniques, combined gas chromatography/infrared spectroscopy and gas chromatography/mass spectrometry are thus far the most established and well documented ones in regard to complex mixtures (53-54). The utilization of such techniques, however, does not in any way guarantee complete separation; and their full fruitfulness is not often realized due to overlapping components. This may be considered a serious pitfall in light of the fact that overlapping chromatographic peaks in complex mixtures is a very commonly occurring event as pointed out by Davis and Giddings (55). To this end, many mathematical methodologies have been proposed to decompose an overlapping peak into its constituent components.

O'Haver and Green (56) have shown the usefulness of derivative functions for improving resolution. Application of the method, however, is limited to situations where the experimental S/N is high and also depends upon relative intensities and separations in relation to the half width as demonstrated by the same authors (57).

There have been many curve resolution techniques described for obtaining the response shape where the selection of an appropriate choice depends upon the amount of information available prior to the analysis. Lawton and Sylvestere (58) have described a self modeling curve resolution (SMCR) technique for estimating the component spectra of a series of binary mixtures. This technique was extended by Borgen and Kowalski (59) to resolve three components and by Sharaf (60) to obtain qualitative and quantitative resolution of ternary mixtures using various chromatographic/spectrometric systems. A similar approach was taken by

Vandeginste and coworkers (61) to resolve a three component mixture eluting from an LC/UV-VIS system.

Factor analysis as well as principle component analysis using both IR (62-63) and mass spectral (64-66) data have also been employed to study mixtures of overlapping peaks. Although these latter techniques, contrary to curve resolution, do not assume a predefined peak shape, they do however assume a constant peak shape over a range of relative concentrations. This may not often be a valid assumption as pointed out by Lundeen and Juvet (67).

Another approach within the framework of curve resolution is that of band fitting. These methods assume that the peak shape (either mathematical or empirical) for each of the components of a composite profile is predefined and that it remains constant at various concentrations. These are not only severe assumptions and therefore susceptible to error; but when added with the restriction of needing a considerable amount of advance information about the system, these limitations make this alternative limited in scope. Critical evaluation and the limitation of curve fitting techniques have been the subject of two excellent publications (68-69).

In this section the application of the orthonormal method to the qualitative and quantitative resolution of fused chromatographic peaks is demonstrated. Isenhour and coworkers have also made use the Gram-Schmidt procedure in a different way for gas chromatogram reconstruction (70). In this work, they have employed direct interferograms from a GC/FTIR instrument. Their approach is similar to gas chromatogram

reconstruction from mass spectral total ion currents. After the collection of several background interferograms, they are orthonormalized to represent the background space. Subsequently, the orthogonal components of each successively scanned interferogram to this background space are computed. This orthogonal component will be a measure of the total absorption of an IR active species in the light path.

To examine the utility of the orthonormal method to the resolution of overlapping peaks, samples of pure compounds and mixtures of known composition from structurally related components were prepared to simulate pure and overlapping peaks respectively. Reagent grade compounds from the Fisher company were used without further purification for preparation of all samples. All reference and mixture spectra were collected in a similar manner described before.

The first question to be asked about a given chromatographic peak attributed to a given component is whether it is pure or composite. If composite, the second question might be how many components are there and at what relative concentrations are they coeluting. The proposed method can offer reliable answers to these questions provided that a list of possibilities is available.

Peak purity determination

In this type of application it is often desirable to determine the purity of a peak which is perceived to belong to a given component. A typical example may be regular analyses of a large number of samples for the presence of a

certain component. As mentioned earlier, the best results are obtained when a list of possibilities either exists or can be provided as an output from a larger search. The top twenty candidates containing the analyte of a large search may, for example, be used for this purpose. Once such list is available as a reference, all the reference spectra are orthonormalized using the Gram-Schmidt procedure. Subsequently, the projection of the peak spectrum into this orthonormalized reference space is computed. If the peak is pure, a coefficient approaching unity will be obtained for the peak component in the reference space.

The following experiment has been designed to test the applicability of the proposed method for peak purity determination. A small reference space containing nineteen compounds, many of which are similar, has been selected and their IR spectra have been acquired. An orthonormalized reference space has been constructed based on these IR spectra using the Gram-Schmidt procedure. Pure samples have been prepared and under the same conditions their IR spectra have been collected and subsequently projected into the orthonormalized reference space.

Table 5.15 lists the results obtained for this experiment when sample A (chlorobenzene) and sample B (chloroform) were examined against the reference list. Notice that all components with negative coefficients are assumed to be absent along with those having negligible positive contributions. This non-negativity assumption will be exploited for improvement of quantitative results later in this paper. Data in table 5.15 indicate that in both cases the samples are correctly identified as being pure chlorobenzene with a coefficient of 0.974 (97.4%) and pure chloroform with a

Table 5.15 Peak purity determination

Reference compounds	A		B	
	Coeff.	(%)	Coeff.	(%)
Chlorobenzene	**0.974**	**(97.4)**	- 0.080	(0.00)
Chloroform	- 0.000	(0.00)	**1.002**	**(100)**
Nitrobenzene	0.012	(0.00)	- 0.005	(0.00)
Acetonitrile	0.025	(0.00)	- 0.033	(0.00)
Toluene	0.053	(0.00)	0.101	(10.1)
Hexane	0.000	(0.00)	- 0.017	(0.00)
Acetone	- 0.047	(0.00)	- 0.370	(0.00)
Benzene	0.021	(0.00)	- 0.046	(0.00)
3-Me-3-pentanol	0.007	(0.00)	- 0.004	(0.00)
Methylene chloride	- 0.058	(0.00)	0.077	(0.00)
Methly acetate	- 0.010	(0.00)	0.018	(0.00)
Dimethyl sulfoxide	- 0.031	(0.00)	- 0.012	(0.00)
M-xylene	- 0.019	(0.00)	- 0.013	(0.00)
Anisole	0.022	(0.00)	0.063	(0.00)
Me-benzyl alcohol	0.023	(0.00)	0.000	(0.00)
Aniline	0.034	(0.00)	0.077	(0.00)
Bromobenzene	- 0.089	(0.00)	0.028	(0.00)
Isoamyl alcohol	- 0.008	(0.00)	- 0.004	(0.00)
Dimethyl foramid	0.006	(0.00)	- 0.022	(0.00)
Relative errors ($x10^3$)	6.2		7.5	

coefficient of 1.00 (100%). A good fit is also indicated by the small values for the relative errors of the fit.

Although the coefficient of exactly one (1.00) for chloroform in sample A can be interpreted as clear indication of its purity, a 10% contribution from toluene is nevertheless indicated. This may not be a serious problem in many practical situations and could often times be rejected based on chromatographic retention time consideration. Moreover, experience with running many pure samples has shown that this kind of discrepancy is observed from time to time as the method attempts to achieve a best fit by combining small positive and negative contributions from the rest of the reference space. However a coefficient of greater than 0.95 (95%) has never been obtained except for pure samples.

The results obtained clearly demonstrate the effectiveness of the proposed method for peak purity determination particularly considering the fact that in many practical situations the analyst deals with yet a smaller set of possibilities than the one employed in this experiment. Additionally, since only one spectrum need be collected on a peak profile, this technique may prove to be especially useful in circumstances where a large number of samples are to be processed rapidly for the presence of certain peaks.

Resolution of overlapping peaks

In resolving overlapped peaks, the analyst is typically interested in determining the number of components in a peak where there usually exists a small list of possibilities. To test the applicability of the method to

such situations the following experiment has been designed. A small reference set of four structurally related compounds — benzene, chlorobenzene, bromobenzene and nitrobenzene ——has been selected; and in a similar way as explained in the previous section, their orthonormalized base has been formed. Samples ranging from pure (pure peak) to ternary mixtures (fused peaks) were prepared and their spectra projected into the above reference space. The composition of the samples were as follows: sample A, pure chlorobenzene; sample B, 50% chlorobenzene and 50% bromobenzene; sample C, 30% benzene and 70% nitrobenzene; and finally sample D, 30% chlorobenzene, 20% bromobenzene and 50% nitrobenzene.

Table 5.16 lists the results for this experiment. As evident from the data in table 5.16, sample A is clearly identified as pure and samples B, C and D are all successfully determined as being mixtures. An overall good quantitative accuracy (average of $\pm 3\%$) is obtained with the exception of that for sample B where 15% benzene is erroneously predicted. This may not pose a serious problem if the peak was expected to be, for example, a mixture of halogenated benzenes. In addition to the retention time consideration mentioned before, the prediction of the presence of benzene may be suspect based on the magnitude of the relative error of the fit which is approximately twice as large for sample B than for the others. Moreover, due to domain independency of the method, one can use mass spectral data to more easily distinguish benzene from its halogenated derivatives.

It is important to realize, however, that when applied to peak resolution, there are two unique advantages offered by the proposed method

Table 5.16 Resolution of overlapping peaks

Reference compounds	A	B	C	D
	Coeff. (%)	Coeff. (%)	Coeff. (%)	Coeff. (%)
Benzene	0.03 (0.00)	0.15 (15.0)	0.29 (29.0)	- 0.05 (0.00)
Chlorobenzene	0.96 (96.0)	0.53 (53.0)	- 0.08 (0.00)	0.32 (32.0)
Bromobenzene	- 0.05 (0.00)	0.48 (48.0)	0.08 (0.00)	0.14 (14.0)
Nitrobezene	0.03 (0.00)	- 0.03 (0.00)	0.71 (71.0)	0.51 (51.0)
Relative errors ($x10^3$)	6.5	12	5.6	7.4

particularly in contrast with such techniques as factor analysis (FA) and principle component analysis (PCA). The first and most important advantage is that chromatographic resolving power will not impose a limit on peak resolution. On the other hand, FA and PCA will totally fail if, for example, two components are eluting from the column at exactly the same time with the same peak profile. All mixture spectra are identical in such cases making the resolution impossible by these methods. Secondly, to collect the maximum number of spectra possible during the eluting time of a peak, FA and PCA are influenced by the rate of spectral acquisition eventually determined by the instrumental background. The orthonormalization procedure is not affected by this scanning speed limitation since only one or a few spectra need to be acquired across the peak profile.

Analogous to other curve resolution techniques, however, the accuracy of the proposed method will also suffer if the uniqueness of reference spectra are not realized; in such cases some false positive results such as that observed for sample B may be encountered. Therefore, the spectrometer's resolution and S/N ratio can play an important role in this respect. Higher quantitative accuracy would have definitely been obtained had an FT/IR instrument been employed in place of the dispersive one used in this work. The simultaneous use of complementary mass spectral data, nonetheless, can greatly attenuate this problem.

As was shown in the previous section, a remarkable improvement in quantitation is quite often realized by imposing a non-negativity constraint (NNC) on the fit. Table 5.17 lists the results when a ternary mixture is

Table 15.17 Results of imposing non-negativity constraint; obs. (actual)

Reference compounds	First run	Second run,NNC1	Third Run,NNC2
Hexane	39 (30)	27 (30)	**28** (30)
Acetone	- 0.05 (0.0)	-	-
Acetonitrile	- 0.09 (0.0)	-	-
Methyl acetate	- 0.01 (0.0)	-	-
Methylene chloride	- 0.01 (0.0)	-	-
Chlorobenzene	- 0.14 (0.0)	-	-
Bromobenzene	0.01 (0.0)	- 0.09 (0.0)	-
Nitrobenzene	- 0.00 (0.0)	-	-
Benzene	0.47 (30)	0.35 (30)	**0.32** (30)
Toluene	0.79 (40)	0.47 (40)	**0.40** (40)
Relative errors ($x10^3$)	8.69	9.8	9.8

examined against a set of ten references. The mixture is composed of hexane (30%), benzene (30%), and toluene (40%). Data in table 5.17 indicate that after the first projection (1st run) six components receive negative coefficients. The mixture is identified as containing hexane, benzene and toluene but the quantitative results are not as accurate. In the second run with the NNC imposed, not only a significant quantitative improvement is achieved; but also the last component not in the mixture turns negative leaving exclusively those components that are actually present in the mixture. The application of the NNC in the third run results in yet further quantitative accuracy. Note that the relative error remains fairly constant indicating a performance of a good fit in all three runs.

The results obtained in this section demonstrates that, as applied to the resolution of overlapping peaks, the orthonormal method offers several advantages. The method utilizes the whole multivariate IR spectral information delivered by the instrument. It is an effective curve resolution tool without requiring limiting assumptions on the chromatographic peak profile or resolution. However, an a priori knowledge of a small list of possibilities is required. In cases where a peak component is not represented in the reference list, a relative error of at least an order of magnitude higher is obtained pointing to the absence of the component from the list. Even under these circumstances, the compound in the reference list most similar to the desired compound will be obtained thus providing information about its type. The technique can be used in conjunction with a large reference space arranged in the order of retention times, and a small reference list within a given retention time window may

be examined for a given peak. In fact, it may be possible to adopt this method to operate in real time as data are collected.

CONCLUSION AND FUTURE PROSPECTS

It was shown in the previous sections that the orthonormal method offers several unique advantages for the automated spectroscopic identification of organic compounds. Namely, the method is computationally efficient and allows for the analysis of both pure and mixture samples with the same amount of computational efforts. The effectiveness of the orthonormal procedure in dealing with mixtures appears to be well suited for applications involving various chromatographic-spectrometric regimes. The method is also capable of delivering both qualitative and quantitative information with a single shot analysis of either pure or mixed samples. Moreover, the technique independency aspect of the orthonormal algorithm allows for the synergistic use of spectroscopic data from several techniques to enhance confidence on the final outcome of the analysis.

However, since the primary objective of this research have been to explore the extent to which the theoretical advantages associated with the use of orthonormalized reference spectra can be met in practice, all of the experiments have been carried out based on a small library. Little attention has been given to the size of the library or other parameters such as computational needs or the required computer time which may place a limit upon the successful application of the method to large databases. It is, therefore important to address some of these issues in order to provide some insight into the nature of the factors which might cause the

orthonormal method to collapse. A number of these factors, from a strictly theoretical point of view, are discussed here beginning with the possible application of the orthonormal method as a search algorithm for a large library.

Generally, for a search system to be useful, the results must be reliable for large databases. In other words, it must be possible to distinguish between a large number of library entries many of which are similar. The Gram-Schmidt orthogonalization is essentially a normalized difference operation. Similar components are selectively removed from each subsequent reference vectors (spectra). In principle, the successive difference method works as long as the number of vectors, that is reference spectra, is less than the number of dimensions which is the number of data points in the spectrum. Problems can arise when there are too few dimension for doing large data sets. By analogy, one should consider a three-dimensional vector. If the Gram-Schmidt operation is performed on a one-dimensional vector, the basis set is then a line. If two vectors are used to form the basis, the basis is then a plane. The Gram-Schmidt then measures three-dimensional vectors that lie perpendicular to that plane. Only the third dimension is measured. If a three-dimensional vector is used for the basis set, the basis is a volume. If one has only three dimension, there in no orthogonal component to that volume. By analogy the same is true for 100 or 1000 dimensions. Therefore, the major question may be at this point whether it is profitable to have 1000 dimensions for each, for example, infrared spectrum.

Another issue of concern may be the computational efforts demanded by the orthonormal method. Note that this concern only applies to the orthonormalization step at the time of library inception which is done only once for a given library. The analysis step is, in fact, more efficient than other methods such as absolute differences and dot products. Once a library is orthonormalized, the method allows for a more general analysis without an additional sacrifice in computational efficiency. The generality of the analysis is achieved by treating each sample as if it were a mixture which also makes the method capable of dealing with the overlapped peaks in GC-IR applications.

However, there are several points that are debatable with regard to the concerned expressed earlier. One important point is that the computation in the orthonormal method is kept at a minimum by partitioning the overall procedure into a one-time only orthonormalization step and an identification step which is repeated for every sample. This is a favorable division of labor because the orthonormalization requires ~ (NPTS)3 floating point operations (FLOPS), whereas ~ (NPTS)2 FLOPS are required in the identification step.

Secondly, the concern with spectrum dimensionality in the orthonormal method is to insure that the linear independency assumption is not violated. Under these circumstances, however, the method yields accurate qualitative and quantitative information as opposed to typical search systems which only produce some list of possible candidates. It was pointed out in an earlier section that methods such as dot products and absolute differences make no attempt to insure that their reference library is

linearly independent. Thus, it is not uncommon for these procedures to be applied in cases where the number of points in the reference spectra are considerably less than the number of compounds in the library. Such applications are bound to fail in cases where two or more compounds have similar spectra, regardless of which identification algorithm is employed.

It is also important to point out that there are a number of steps which may be taken to reduce the severity of the problem of computational demand for the orthonormalization part of the method. For instance, a library can be built gradually; that is, each additional spectrum can be orthonormalized to an existing library. In this way, the calculations can be spread out over time. Of course, the computational efforts involved in orthonormalizing each spectrum increases with the size of the library and may have to eventually be done on a Mainframe. Furthermore, the use of prefilters and specialized sublibraries will allow for a significant reduction in the size of any one library without a sacrifice in information content. Also notice that with regard to the analysis of mixtures resulting from incomplete separation, the size limitation is not a critical factor. Small libraries based on retention index windows which are likely to include a small subset of the compounds from the library may be selected and subsequently orthonormalized.

Finally an important factor for the evaluation of any search system is the amount of computer time necessary for a typical analysis. Since the algorithm was originally written in BASIC to run on an Apple microcomputer, the analysis times were fairly long. A better estimate of the required computer time may be made from the results of an experiment

performed recently. The algorithm was coded in C language to run on a VAX-station 3200. A data set containing 108 primary mass spectra acquired on a Finnigan TSQ-70 triple quadruple mass spectrometer was orthonormalized. Every compound in the data set was then used as an unknown and was subsequently analyzed using the orthonormal method. The total CPU elapsed time for the analysis of all 108 compounds was 13.54 minutes. This amounts to approximately 7.7 seconds per analysis . Therefore, the analysis time for a library of 1000 compounds would be on the order of a few minutes. However, the real answer to many of the concerns discussed above can only be obtained through experimental investigation of the performance of the orthonormal method for large data bases in the future.

REFERENCES

1. Clerc, J. T., in "Computer Enhanced Analytical Spectroscopy", edited by: Henk, L. C. Meuzelaar and Thomas, L. Isenhour, **1987**, chapter 7, p. 145.

2. Clerc, J. T., Koenitzer, H., in "Data Processing in Chemistry" (Z. Hippe, ed.), Elsevier, Amsterdam, **1981**, p. 151.

3. Cooper, J. R.; Bowter, Ian, C.; and Wilkins, C. L. Analy. Chem., **1986**, 58, 2791.

4. Laude, Jr., D. A.; Wilkins, C.L., in "Computer Enhanced Analytical Spectroscopy", **1987**, ch. 12, p. 239.

5. Sasaki, S.; Kudo, Y.; J. Chem. Inf. Comput. Sci., **1985**, 25, 252.

6. McLafferty, F. W.; Stauffer, D.B. J. Chem. Inf. Comput. Sci., **1985**, 25, 252.

7. Trulson, M. O.; and Munk, M. E. Anal. Chem., **1983**, 55, 2137.

8. Zupan, J.; Munk, M. E. Anal. Chem., **1985**, 57, 1609.

9. Woodruff, H. B.; Smith, G. M. Anal. Chem. **1980**, 52, 2321.

10. Tomellini, S.A.; Saperstein, D. D.; Stevenson, J. M.; Smith, J. M. ; Woodruff, H. B.; and Seelig, P. F. Anal. Chem., **1981**, 53, 2367.

11. Woodruff, H. B.; Smith, G. M. Anal Chim. Acta **1981**, 133, 545.

12. Tomellini, S. A.; Stevenson, J. M.; Woodruff, H. B.; Hartwick, R. A. Anal. Chim. Acta **1984**, 162, 227.

13. Tomellini, S. A.; Hartwick, R. A.; Woodruff, H. B. Appl. Spectrosc. **1985**, 39, 331.

14. Tomellini, S. A.; Stevenson, J. M.; and Woodruff, H. B. Anal. Chem. **1984**, 56, 67.

15. Puskar, M. A.; Levine, S. P.; and Lowry, S. R. Anal. Chem. **1986**, 58, 1156.

16. de Haseth, J. A.; and Mir, K. A., Pittsburgh Conference, **1985**, paper No. 216.

17. Saperstein, D. D. Appli. Spectrosc. **1986**, 40, 344.

18. Gribov, L. A.; Elyashberg, M.E. CRC Crit. Rev. Anal. Chem. **1979**, 8, 111.

19. Woodruff, H. B. in "Computer Enhanced Analytical Spectroscopy" Edited by: Henk L. C. Meuzelaar and Thomas L. Isenhour, Elsevier, Amsterdam, **1987**, ch. 10, p. 201.

20. Palmer, P. T., Ph.D. thesis, Michigan State University, **1988**.

21. McLafferty, F. W.; and Stuffer, B. D., J. Chem. Inf. Comput. Sci. **1985**, 25, 245.

22. McLafferty, F. W.; Hertel, R. H.; Willwock, R.D., Org. Mass Spectrom. **1974**, 9, 690.

23. Pesyna, G. M.; Venkataraghavan, R.; Dayringer, H. G.; McLafferty, F. W. Anal. Chem. 1976, 48, 1362.

24. Kwok, K. S.; Venkataraghavan, R.; McLafferty, F. W. J. Am. Chem. Soc. **1973**, 95, 4185.

25. Kuentzel, L.E. Anal. Chem. **1951**, 23, 1413.

26. Baker, A. W.; Wright, N.; and Opler, A. Anal. Chem. **1953**, 25, 1460.

27. Sparks, R. A.; American Society of Testing and Materials, Philadelphia, Pennsylvania, **1964**.

28. Anderson, D. H. and Covert, G. L. anal. Chem. **1967**, 39, 1288.

29. Erley, D. S. Anal. Chem. **1968**, 40, 894.

30. Lytle, F. E.; Brazie, T. L.; Anal. Chem. **1970**, 42, 1532.

31. Erley, D. S. Appl. Spectrosc. **1971**, 25, 200.

32. Jurs, P. C. Anal. Chem. **1971**, 43, 364.

33. Lytle, F. E. Anal. Chem. **1970**, 42, 355.

34. Lowry, S. R.; Huppler, D. A.; and Anderson, C. R. J. Chem. Inf. Comput. Sci. **1985**, 24, 235.

35. Divis, R. A.; White, R. L. Anal. Chem. **1989**, 61, 33.

36. Azarraga, L. V.; Hanna, D. A. "ERL GC-FTIR software and user guide (USEPA/ERL)": GIFTS: Athens, GA, **1979**.

37. Hanna, A.; Marshall, J. C.; Isenhour, T. L. J. Chromatogr. Sci. **1979**, 17, 434.

38. Erickson, M. D. Appl. Spectrosc. **1981**, 35, 181.

39. Delaney, M. F.; Uden, P. C. Anal Chem. **1979**, 51, 1242.

40. de Haseth, J. A.; Azarraga, L. V. Anal. Chem. **1981**, 53, 2292.

41. Milne, G. W.; Heller, S. L. J. Inf. Comput. Sci. **1980**, 20, 204.

42. Lowry, S. R.; Huppler, D. A. Anal. Chem. **1981**, 53, 889.

43. Lowry, S. R.; Huppler, D. A. Anal. Chem. **1983**, 55, 1288

44. Lowry, S. R.; Huppler, D. A.; and Anderson, C. R. J. Chem. Inf. Comput. Sce. **1985**, 25, 235.

45. Ruprecht, M.; Clerc, J. T. J. Chem. Inf. Comput. Sci. **1985**, 25, 241.

46. Hippe, Z.; and Hippe, R. Appl. Spectrosc. Rev. **1980**, 16, 135.

47. Zupan, J. Anal Chem. **1982**.

48. Milne, G. W. A.; Budde, W. L.; Heller, S. R.; Martinsen, D. P.; and Oldham, R. G. Org. Mass Spectrom. **1982**, 17, 547.

49. de Haseth, J. Chemistry Department, University of Georgia, Athens, GA 30602 (404-542-2626, ext. 50).

50. Sadtler Research Laboratories, 3316 Spring Garden Street, Philadelphia, Pennsylvania, PA 19104 (215-382-7800).

51. Pouchert, C. J. "The Library of FT-IR Spectra", (No. 212, 700-0), Aldrich Chemical Company, 940 W. St. Paul Avenue, Milwaukee, WI 53233.

52. Nicolet Instruments, IR Library Department, 5225-1 Verona Road, Madison, Wisconsin 53711.

53. Williamson, R. E.; Crowell, R. A.; and Trotter, H. F. Calculus of Vector Functions, **1972**, Prentice-Hall Inc., New Jersey.

54. Anton, H. Elementary Linear Algebra, **1981**, Wiley, New York.

55. Malinowski, E. R.; Howery, D. G. Factor Analysis in Chemistry, **1980**, Wiley, New York.

56. White, R. L. Appl. Spectrosc. **1987**, 23, 165.

57. Brooks, J. W.; Middleditch, B.S. Mass Spectrom. **1979**, 5, 142.

58. Davis, J. M.; Giddings, J. C. Anal. Chem. **1983**, 55, 418.

59. O'Haver, T. C.; Green, U. G. L. Intern. Lab. **1975**, 5, 611.

60. O'Haver, T. C.; Green, U. G. L. Anal. Chem. **1976**, 48, 312.

61. Lawton, W. H.; Sylvester, E. A. Technometrics **1971**, 13, 617.

62. Borgen, O. S.; Kowalski, B. R. Anal. Chim. Acta **1985**, 174, 1-26.

63. Sharaf, M. A. Anal. Chem. **1986**, 58, 3084.

64. Vandeginste, B.; Essers, R.; Bosman, T.; Reijnen, J.; Kateman, G. Anal. Chem. **1985**, 57, 971.

65. Gillette, P. C.; Lando, J. B.; Koenig, J. L. Anal. Chem. **1983**, 55, 630.

66. Fredericks, P. M.; Lee, J. B.; Osborn, P. R.; Swinkels, D. A. J. Appl. Spectrosc. **1985**, 39, 303.

67. Ritter, J. L.; Lowry, S. R.; Isenhour, T. L.; Wilkins, C. L. Anal. Chem. **1976**, 48, 591.

68. Sharaf, M. A. Kowalski, B. R. Anal. Chem. **1981**, 53, 518.

69. Sharaf, M. A.; Kowalski, B. R. anal Chem. **1982**, 54, 1291.

70. Lundeen, J. T.; Juvet, Jr., R. S. Anal. Chem. **1981**, 53, 1369.

71. Vandeginste, B. G. M.; De Galan, L. Anal Chem. **1975**, 47, 2124.

72. Maddams, W. F. Appl. Spectrosc. **1980**, 34, No. 3, 245.

73. de Haseth, J. A.; Isenhour, T. L. Anal. Chem. **1977**, 49, 1977.